Microtubule Interactions and Regulation of the Mitotic-Kinesin Like Protein-1 and Kinesin-Like Calmodulin-Binding Protein

Bettina Edith Deavours

Dissertation submitted to the faculty of Virginia Polytechnic Institute
and State University in partial fulfillment of the
requirements for the degree of

Doctor of Philosophy
in
Biology

Dr. Richard Walker, chair
Dr. Charles Rutherford
Dr. Brian Storrie
Dr. Brenda Winkel
Dr. Eric Wong

December 4, 2001
Blacksburg, VA

Keywords: microtubule, kinesin, mitosis, ATPase

Microtubule Interactions and Regulation of the Mitotic-Kinesin Like Protein-1 and Kinesin-Like Calmodulin-Binding Protein

Bettina Edith Deavours

(ABSTRACT)

Microtubules are essential for many dynamic processes occurring within eukaryotic cells including organelle and vesicular trafficking, motility of cilia and flagella, and mitosis. Microtubules operate in conjunction with the kinesin superfamily of microtubule-dependent motor proteins, which use the energy from ATP hydrolysis to "walk" along microtubule tracks, and in doing so generate force for the transport of cellular cargo and mitosis. The goal of this project was to define the microtubule interactions and regulation of two kinesin-like proteins (KLPs), the *Homo sapiens* mitotic kinesin-like protein-1 (HsMKLP-1) and the *Arabidopsis thaliana* kinesin-like calmodulin-binding protein (KCBP). Functional domains of HsMKLP-1 and KCBP were heterogeneously expressed in insect cells (HsMKLP-1) and/or *E. coli* (HsMKLP-1, KCBP) and used to examine the microtubule binding and ATPase activity of HsMKLP-1 and KCBP catalytic domains.

Overall, the HsMKLP-1 catalytic domain was found to operate in a similar fashion to other KLPs with respect to microtubule binding and ATP hydrolysis, but HsMKLP-1 exhibited enhanced microtubule binding of the dimer and weaker affinity for ATP that functionally distinguishes it from other KLPs. HsMKLP-1 proteins were also used to generate HsMKLP-1 specific antibodies to be used as a tool for characterizing native HsMKLP-1. To define the role of nuclear localization in regulating the activity of HsMKLP-1 during interphase, sequences directing nuclear localization of HsMKLP-1 were identified. Mutation of the nuclear localization sequence ^{799}PNGSRKRR^{806} to ^{799}PNGSRTSR^{806} or removal of AA's 830-856 of HsMKLP-1, which contains the nuclear localization sequence ^{851}PKRKKP^{856}, were sufficient to abolish nuclear localization. In the absence of a functional nuclear localization sequence HsMKLP-1 localized to microtubule plus ends, suggesting that nuclear localization serves to limit the interaction of HsMKLP-1 with the interphase microtubule array.

The KCBP catalytic domain, which contains a calmodulin-binding site, was used to determine the effect of Ca^{2+}/calmodulin on the microtubule binding and ATPase activity of KCBP. Ca^{2+}/calmodulin was found to inhibit the binding of KCBP to microtubules and reduced the motor's microtubule-stimulated ATPase activity, which suggests that Ca^{2+}/calmodulin may modulate the activity of KCBP *in vivo* by regulating the motor's association with microtubules.

GRANT INFORMATION

This work was supported by NIH grant GM52340 as well as grants from the Virginia Tech Graduate Research and Development Project (totaling $1000) and Sigma Xi (totaling $1047).

ACKNOWLEDGMENTS

I would like to express my sincere appreciation and gratitude to Dr. Richard Walker for giving me the opportunity to work in his lab. Dr. Walker first introduced me to motor proteins during an undergraduate Cell Biology lecture course and is directly responsible for developing my interest in motor proteins into a Ph.D. education. I am grateful to Dr. Walker for giving me the freedom to independently develop my research, while serving as a valuable source of information and advice. I am truly grateful for all of his friendship and guidance over the past 6 years and will leave Virginia Tech with very fond memories of being in his lab. I would also like to thank the members of my graduate advisory committee: Dr. Charles Rutherford, Dr. Brian Storrie, Dr. Brenda Winkel, and Dr. Eric Wong for their support and valuable suggestions concerning my research. I would especially like to thank Dr. Winkel and Dr. John McDowell for all of their advice, support, encouragement, and efforts on my behalf concerning my post-doctoral pursuits.

I would like to thank Dr. Joe Cowles for all of his support as Department Head of Biology and for giving me the opportunity to teach the next generation of Biology students. I am also grateful to Mary Schaeffer, Judy Alls, and Cathy Light for all of their uncompromising support and assistance in teaching the Biology labs. Also within the Biology department, I wish to thank Melanie Huffman, Michelle Wooddall, and Karen Boone in bookkeeping for all of their assistance with financial matters, Sue Rasmussen for her help and assistance with graduate school affairs and for making sure that all of my paperwork is in order, and all of the other members of the Biology staff that work behind-the-scenes to ensure that the department runs smoothly.

My time in the Biology department would not have been as enjoyable without the numerous friendships and interactions with fellow Biology graduate students. I would especially like to acknowledge my colleagues on the "5th floor" for making Derring Hall an enjoyable place to work, and all past and present graduate and undergraduate students in Dr. Walker's lab.

Outside of Virginia Tech, I would like to thank Andy Mackey for all of his help with kinesin kinetics and for diligently responding to my endless questions and emails without complaint. I would also like to thank Dr. Mark Mooseker, Dr. Kerry Bloom, Dr. Edward Taylor, the Marine Biological Lab, and the members of Physiology 98 for making the summer of 1998 such a memorable experience and for renewing my sense of excitement and wonder about science.

Most importantly, I would to thank my parents Victor and Lorraine Randecker and sister Carrie Deavours for all of their love, support, and encouragement that have made this Ph.D.

possible. They are responsible in one way or another for all of my accomplishments and I can not express the sincere love, appreciation, and gratitude I have for them. I would also like to thank Corey Broeckling for his companionship and endless encouragement and support, especially during the last couple of months. I would also like to thank my two cats Kiwi and Nerkie, for putting up with my long hours and for always putting a smile on my face at the end of the day.

TABLE OF CONTENTS

LIST OF TABLES

LIST OF FIGURES

LIST OF ABBREVIATIONS

The abbreviations used are:

AMP-PNP: adenosine 5'-(β,γ-imino)-triphosphate

BSA: bovine serum albumin

DTT: dithiothreitol

HsMKLP-1: *Homo sapiens* mitotic kinesin-like protein 1

IPTG: isopropylthio-β-D-galactoside

KCBP: kinesin-like calmodulin-binding protein

KHC: kinesin heavy chain

KLP: kinesin-like protein

MT: microtubule

MTOC: microtubule organizing center

MKLP-1: mitotic kinesin-like protein-1

PIPES: Piperazine-N,N'-bis-(2-ethanesulfonic acid)

PMSF: phenylmethylsulfonyl fluoride

SDS-PAGE: sodium dodecyl sulfate polyacrylamide gel electrophoresis

Trx-KCBP: thioredoxin-KCBP fusion protein

CHAPTER 1: INTRODUCTION

LITERATURE REVIEW

Microtubules (MTs) are indispensable for the proper functioning of eukaryotic cells. In non-dividing cells, MTs form a network throughout the cytoplasm that underlies and helps maintain the structure of organelles such as the Golgi and ER. In addition, MTs serve as the tracks for organelle and vesicle movement. As the major component of axonemes and the mitotic spindle, MTs also play fundamental roles in motility and cell division. During mitosis, MTs form the mitotic spindle to which chromosomes attach and which ultimately is responsible for the migration of the duplicated chromosomes to each spindle pole (Brinkley, 1997).

Because of the fundamental role that MTs and associated proteins play in cells, disruption of MT functioning often has detrimental effects. Severe perturbation of MT processes may hamper normal growth and development and result in the death of the organism. Impairment of cell motility and division may manifest in conditions such as infertility, Down's Syndrome and the development of some cancers. In order to understand how disruption of MT functioning can have such a detrimental impact on cells, it is important to understand how MT processes are controlled. Insight into the regulation of MT-associated processes will not only help elucidate the mechanisms that lead to a disease state, but may also impact the diagnosis and treatment of such devastating diseases.

Microtubules are polymers of tubulin heterodimers (Downing and Nogales, 1998). Each ~100 kDa tubulin dimer is composed of the closely related α and β tubulin polypeptides. Because of the heterogeneity of the tubulin subunits, the organization of tubulin dimers within a MT has important consequences for its structure and function. During assembly, tubulin dimers stack head-to-tail to form a long rod or protofilament. The lateral association of protofilaments (typically 13 protofilaments) forms the hollow cylinder characteristic of MT structure (Mandelkow and Mandelkow, 1984). The orientation of the tubulin dimers results in an intrinsic polarity of the MT, with the α subunit exposed at one end of the MT (termed the minus-end) and the β subunit at the other (termed the plus-end) (Fan et al., 1996).

The two ends of a MT are also distinguished by the dynamics of their assembly (Mitchison and Kirschner, 1984). MTs are dynamic structures that continuously add and disassociate tubulin subunits from their ends. This growth and shortening of MTs, termed dynamic instability, results from the heterogeneous nature of each MT end. Consequently, one

end (designated as the plus end) is characterized by the rapid addition of tubulin subunits and rapid growth, while the other end (termed the minus end) grows more slowly.

MT structures commonly found within cells are often characterized by having a distinct organization with respect to plus and minus ends. MTs are not randomly polymerized within the cytosol, but are typically nucleated from a structure known as a MT organizing center (MTOC), or centrosome. MT minus ends are generally associated with the MTOC so that the MT extends by the addition of tubulin subunits to the unencumbered plus ends. During interphase in animal cells, MTs typically form a radial array that extends throughout the cytoplasm. However, at the onset of mitosis MTs undergo a dramatic reorganization to form the mitotic spindle. The spindle is formed by the association of two half-spindles, each of which is nucleated from a MTOC. The MT minus-ends are located within the spindle poles, while the plus ends from each half-spindle extend toward the opposite pole. MTs also form highly organized structures such as cilia, flagella, axons, and dendrites that are restricted to particular animal cell types. During plant cell division, MTs form two unique structures not present in animal cells: the pre-prophase band and the phragmoplast. The pre-prophase band is a circular ring of MTs that forms during early prophase and serves to "mark" the position of the future cell wall. The phragmoplast is a bipolar array of MTs that forms later in the cell cycle and is associated with the deposition of new cell wall materials.

The particular organization of MTs within a cell has important considerations for a group of MT-associated proteins called MT-dependent motor proteins, which operate in conjunction with MTs to drive many different MT-dependent processes. MT-dependent motor proteins are force-generating enzymes that use the energy of ATP hydrolysis to "walk" along MT tracks. In so doing, MT-dependent motor proteins transport a wide variety of cargo (organelles, vesicles, MTs) within cells. MT-dependent motor proteins can be classified into two superfamilies: the dynein superfamily and the kinesin superfamily. Dyneins are characterized by being minus-end directed motors, i.e., these proteins "walk" toward the minus-ends of MTs. Dyneins are large molecules typically composed of two or more heavy chains (each heavy chain ~500 kDa) and multiple intermediate and light chains (Porter and Johnson, 1989). Dyneins play fundamental roles in cellular organization and motility, most notably in the movement of cilia and flagella (Holzbaur and Vallee, 1994). In addition, dyneins are involved in chromosome attachment to MTs during mitosis (Echeverii et al., 1996; Vaisberg et al., 1993).

In contrast to the dyneins, the kinesin superfamily represents a large and complex group of motor proteins with diverse structural features and roles. Conventional kinesin (Greek for "to move"), the family namesake, was originally isolated from squid axons as one of the proteins responsible for MT-dependent transport of vesicles and organelles from the cell body to the synapse (Vale et al., 1985a). Because conventional kinesin was the first kinesin family member identified and is the most extensively studied, it has served as a prototype for all subsequently-identified kinesin family members (termed KIFs or kinesin-like proteins (KLPs)), although it is now clear that not all kinesin family members share the same structural organization or functional role as conventional kinesin. Structurally, conventional kinesin (also referred to as simply "kinesin") is a heterotetramer ($\alpha_2\beta_2$) composed of two heavy chains and two light chains (Kuznetsov et al., 1988) (Fig. 1.1). The heavy chains are characterized by having a three domain structure: a head or motor domain, a stalk or rod domain, and a tail domain (Yang et al., 1989). As the name suggests, the motor domain (~340 AA) is the site of ATP hydrolysis and MT binding and is generally well conserved among KLPs (KLPs typically share 30-45% homology in this region with little sequence homology extending outside of the motor domain) (Vale and Goldstein, 1990). Crystal structures of the motor domains of kinesin and several KLPs have been solved (Gulick et al., 1998; Kikkawa et al., 2000; Kozielski et al., 1997; Kull et al., 1996; Sablin et al., 1998; Sablin et al., 1996; Sack et al., 1997; Turner et al., 2001) and demonstrate a remarkable conservation of structural elements among kinesin family members that can be extended to include elements common to the catalytic domain of another force-generating enzyme myosin, as well as adenylate kinase and monomeric G-proteins such as ras and EF-Tu (Vale, 1996). Adjacent to the motor domain of kinesin is the stalk domain (~500 AA), a region characterized by a high propensity to form α-helices, that is responsible for the dimerization of two heavy chains (de Cuevas et al., 1992). Heavy chains dimerize in a parallel fashion such that the motor domains of each heavy chain are present at one end of the molecule. In comparison to the motor domain, the tail domain of conventional kinesin (~150 AA) is not well characterized although it is proposed to be the site of cargo interaction. The tail domain is also the site at which the light chains interact with the heavy chains. The light chains of kinesin are not essential for kinesin function *in vitro* and may serve to regulate cargo binding and the overall activity of the motor protein *in vivo* (Hackney et al., 1991).

Since the identification of conventional kinesin, over 250 proteins sharing significant homology to the kinesin motor domain have been identified from a wide variety of eukaryotic organisms including insects, plants, fungi, and humans (Greene et al., 1996). Genome sequencing efforts have facilitated identification of all KLPs genes in individual organisms

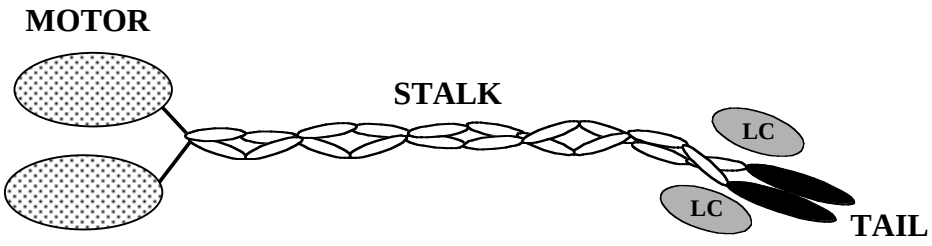

Figure 1.1. Structural representation of conventional kinesin
Kinesin is a heterotetramer composed of two heavy chains and two light chains (LC). Each heavy chain is composed of a globular N-terminal motor domain, followed by a stalk domain, and C-terminal tail domain.

including mouse (45 KLPs), humans (45 KLPs), *Arabidopsis thaliana* (38 KLPs), *Drosophila melanogaster* (23 KLPs), *Caenorhabditis elegans* (21 KLPs), and *Saccharomyces cerevisiae* (9 KLPs) (Greene et al., 1996; Miki et al., 2001). Many KLPs exhibit unique structural and functional characteristics that have greatly expanded the repertoire of cellular roles for KLPs to include mitosis, cytokinesis, and cellular morphogenesis as well as vesicle and organelle transport. KLPs can be catagorized into eight families based on their structural organization and sequence homology outside of the conserved motor domain (Kim and Endow, 2000).

The *kinesin heavy chain*, *unc-104/KIF1*, and *KRP85/95* kinesin families are involved in vesicle and organelle transport (Hall and Hedgecock, 1991; Hirokawa et al., 1991; Okada et al., 1995). Several members of these families were identified from neuronal tissues, which due to their particular cellular structure and need to transport cargo over long distances may require the activity of several KLPs. Although members of these three kinesin families share similar cellular roles, structurally they are quite distinct. As discussed above, members of the *kinesin heavy chain* family, which includes conventional kinesin, are heterotetramers, composed of two heavy chains and two light chains, while members of the *KRP85/95* family are heterotrimeric, composed of two closely-related heavy chains and an additional non-KLP subunit (Cole et al., 1993; Yamazaki et al., 1995). Most unusual is the *unc-104/KIF1*family, whose members are composed of a single polypeptide (Nangaku et al., 1994; Okada et al., 1995). Although monomeric, members of the *unc-104/KIF1* family are capable of processive movement along a MT similar to kinesin (Okada and Hirokawa, 1999). While kinesin's processivity is believed to stem from the alternation of binding of its two motor domains, KIF1A has evolved an unique mechanism that allows it to remain tethered to the MT while moving along it (Okada and Hirokawa, 2000).

Although conventional kinesin was originally identified in non-dividing neuronal tissue, the majority of KLPs, belonging to the remaining five kinesin families, are believed to orchestrate events during cell division based on immunolocalization data, mutant analysis, and antibody inhibition experiments (McIntosh and Pfarr, 1991). KLPs operating at discrete locations in the MT-based mitotic spindle have been implicated in the separation of spindle poles during prophase, organization and stabilization of the fully-formed spindle, movement of chromosomes during metaphase and anaphase, spindle elongation during anaphase B, regulation of MT dynamics contributing to the process of chromosome separation, and cytokinesis (Barton and Goldstein, 1996). The *C-terminal* kinesins are distinguished by having their motor domain at the C-terminus of the protein as opposed to the N-terminus as is generally the case for most

KLPs, and by moving towards minus, rather than plus ends of MTs. Members of this family, including Ncd and Kar3, contribute to chromosome-to-pole movements and spindle stabilization during meiosis and/or mitosis (Endow, 1993). The *bimC* family of KLPs are plus-end directed motors that include Eg5 from *Xenopus laevis* and BimC from *Aspergillus nidulans*. These motors are thought to contribute to spindle pole separation during prophase and spindle elongation during anaphase (Walczak and Mitchison, 1996). Consistent with their role in bundling and sliding antiparallel MTs, members of the *bimC* family form homotetramers, composed of two antiparallel heavy chain dimers. The *chromokinesins* are an unusual family of KLPs that are believed to participate in chromosome movement due to their ability to bind both DNA and MTs (Wang and Alder, 1995). *MCAK/Kif2* family members all have their motor domains situated in the middle of the heavy chain, although their functional roles range from vesicle transport to mitosis (Noda et al., 1995; Walczak et al., 1996).

Members of the *MKLP-1* family are implicated in driving MT-dependent processes during mitosis and cytokinesis. This family includes HsMKLP-1 (*Homo sapiens* mitotic kinesin-like protein-1) and members from *Cricetulus griseus* (CHO1), *Danio rerio* (ZfMKLP-1), *Drosophila melanogaster* (Pav-MKLP-1/DmMKLP-1), and *Caenorhabditis elegans* (Zen-4/CeMKLP-1) (Greene et al., 1996). HsMKLP-1 was originally isolated from a HeLa cDNA library using an antibody directed against CHO1 (Nislow et al., 1992). HsMKLP-1 localizes to nuclei during interphase, the equatorial region of the spindle during mitosis where it remains through anaphase, and the midbody during cytokinesis (Nislow et al., 1992).

The localization of HsMKLP-1 in dividing cells suggested a role for the MKLP-1 family in mitosis and initial experiments demonstrated that injection of a CHO1 antibody into dividing mammalian cells prior to anaphase resulted in a significant proportion (70-75%) of cells arresting in a metaphase-like state (Nislow et al., 1990). This result, coupled with the ability of bacterially-expressed HsMKLP-1 to bundle and slide MTs past each other *in vitro*, suggested that HsMKLP-1 may function analogously *in vivo* to drive spindle pole separation during anaphase B (Nislow et al., 1992). However, this model of HsMKLP-1 function has come under scrutiny in light of recent reports which document a role for the MKLP-1 family in cytokinesis rather than mitosis. *Drosophila* embryos harboring mutations in the *pavarotti* gene, which encodes Pav-MKLP-1, show defects in the organization of the central spindle at telophase and fail to complete cytokinesis (Adams et al., 1998). Zen-4/CeMKLPL-1 is also required for the completion of cytokinesis in embryos of *C. elegans* as demonstrated by *zen-4* mutants and RNA-mediated interference of CeMKLP-1 (Powers et al., 1998; Raich et al., 1998). In contrast to

results from mammalian cells, no mitotic defect was observed in *Drosophila* or *C. elegans* cells lacking MKLP-1, and specifically no alteration in the separation of spindle poles during anaphase B was observed (Adams et al., 1998; Raich et al., 1998).

Consistent with the observation that HsMKLP-1 bundles and slides MTs *in vitro*, the phenotype of *Drosophila* and *C. elegans* cells lacking MKLP-1 suggests that this protein functions to bundle and organize MTs in the central spindle and that loss of central spindle organization contributes to a failure of cytokinesis. The central spindle consists of overlapping antiparallel MTs that become tightly focused following anaphase to form the midbody, which is later discarded after completion of cell division. In *pavarotti* mutants, fewer MT bundles were present at telophase and mild to severe disorganization of midzone MTs were also noted in *C. elegans* cells lacking CeMKLP-1 (Adams et al., 1998; Powers et al., 1998; Raich et al., 1998). Additional experiments in which CHO1 was overexpressed in insect cells also indicates a role for MKLP-1 in MT-organization. The overexpression of the motor domain of CHO1 caused a dramatic reorganization of the cortical MT array in these cells to form processes similar with respect to MT polarity and structure to dendrites (Sharp et al., 1996a), suggesting that MKLP-1 or a similar protein in neurons may contribute to dendrite formation in developing neurons.

The majority of KLPs have been characterized from animals and fungi, and although several KLPs have been identified from higher plants, the roles and functions of these motors have not been as well characterized as they have been in other cell types. Genome sequencing of *Arabidopsis thaliana* has identified 38 KLPs (Greene et al., 1996); only a few of these KLPs (termed Kat for kinesin *Arabidopsis thaliana*) were previously known. The roles of these Kat motors have not been examined in detail, although work on Kat a, b, and c indicates that these Kat proteins are involved in mitosis (Liu et al., 1996; Liu and Palevitz, 1996; Mitsui et al., 1996). Of the Kat proteins, only Kat c has been reported to have properties characteristic of a MT motor protein including ATP-dependent binding to MTs and MT-stimulated ATPase activity (Mitsui et al., 1994). In addition, a 100 kDa polypeptide from tobacco pollen tubes and 120/125 kDa polypeptides from tobacco phragmoplasts have been shown to possess properties similar to KLPs including ATP-sensitive binding to MTs and MT-stimulated ATPase activity (Asada and Shibaoka, 1994; Cai et al., 1993).

Although there is an astonishing variety of KLPs, one distinguishing feature of kinesin superfamily members is their ability to convert the energy of ATP hydrolysis to mechanical movement. The mechanism by which this energy transduction occurs is still not completely

understood, but is believed to occur via a series of conformational changes resulting from changes in the nucleotide state of the motor that serve to propel the molecule in the direction of movement. Initial work on purified bovine conventional kinesin demonstrated that the intrinsic ATPase activity of the protein is low and that MTs stimulate this activity ~1000-fold over basal rates of hydrolysis (Kuznetsov and Gelfand, 1986). It was further established that in the absence of MTs, release of P_i preceded ADP release which was rate-limiting (Hackney, 1988; Sadhu and Taylor, 1992).

Further characterization of kinesin was facilitated by the ability to express and purify truncated kinesin polypeptides from bacteria (Gilbert and Johnson, 1993). Expressing kinesin proteins in bacteria eliminated heterogeneity seen in kinesin preparations from native sources (which were mostly due to heterogeneity in light chain content), provided sufficient quantities of protein for kinetic studies, and allowed the motor domain of kinesin to be characterized independently of the stalk and tail domains that were previously shown to influence the ATPase activity of the motor domain (Kuznetsov et al., 1989). In addition, bacteria lack KLPs, which can contaminate preparations from eukaryotic sources. The utility of this approach was first demonstrated using a bacterially-expressed motor domain construct of *Drosophila* kinesin, which exhibited MT-stimulated ATPase activity and rate-limiting ADP release in the absence of MTs, similar to bovine kinesin (Gilbert and Johnson, 1993).

The current "hand-over-hand" model of kinesin motility was first proposed based on the observation that single kinesin molecules were able to translocate MTs for several microns in a MT gliding assay, which suggested that kinesin motility results from individual motor domains stepping along a MT in a hand-over-hand fashion (Howard et al., 1989). This ability to move for long distances along a MT without detachment is termed processivity. In this model, each motor domain would alternate between strong and weak binding states, which would allow the kinesin molecule to translocate along a MT while maintaining continuous attachment. The correlation between weak and strong MT binding states with the nucleotide state of the motor has been examined using nucleotides and nucleotide analogs to prolong the known nucleotide intermediates in the ATP hydrolysis cycle (no nucleotide, ATP, ADP•Pi, ADP). The tight binding of kinesin to MTs in the presence of the non-hydrolyzable ATP analog AMP-PNP was exploited in the initial purification of kinesin from bovine brain and suggested that the ATP state binds tightly to MTs (Vale et al., 1985a). In a MT gliding assay, depletion of ATP or addition of the slowly hydrolyzable ATP analog, ATP-γS, prolonged attachment of MTs to squid kinesin while ADP promoted dissociation, suggesting that the no nucleotide and ATP states were strong

binding while the ADP state was weak (Romberg and Vale, 1993). Equilibrium binding studies with kinesin constructs have now confirmed these findings and shown that the ADP•Pi state is also a weak binding state (Crevel et al., 1996; Lockhart and Cross, 1996; Rosenfeld et al., 1996). Furthermore, equilibrium binding studies as well as biochemical, structural, and biophysical approaches have established that isolated motor domains of kinesin bind MTs with a stoichiometry of one motor domain:tubulin dimer and that the motor domain contacts both α and β subunits of the tubulin dimer, with β tubulin as the predominant contact (Harrison et al., 1993; Huang and Hackney, 1994; Walker, 1995).

A pathway for how kinesin couples ATP hydrolysis to movement along a MT has been proposed based on extensive kinetic analysis of kinesin coupled with structural and biophysical studies (Fig. 1.2, numbers refer to steps in the mechanism) (Gilbert and Johnson, 1993; Gilbert et al., 1998; Gilbert et al., 1995; Hancock and Howard, 1999; Kawaguchi and Ishiwata, 2001; Ma and Taylor, 1995a; Ma and Taylor, 1995b; Moyer et al., 1996; Moyer et al., 1998). In the absence of MTs, kinesin has a low steady state rate of ATP hydrolysis; ATP binds and is rapidly hydrolyzed to ADP and P_i. Following hydrolysis, P_i is released while ADP remains tightly bound. Because ADP release is rate-limiting, in the absence of MTs, kinesin motor domains have ADP bound (1). MTs stimulate the ATPase activity of kinesin primarily by stimulating the rate of ADP release (MTs also stimulate the rate of hydrolysis, which alone, is not sufficient to account for the ~1000-fold increase in hydrolysis rate in the presence of MTs) (Ma and Taylor, 1995b). In the presence of MTs, kinesin binds the MT with one motor domain (2) which stimulates the release of ADP from the bound head (3). ATP binding to the bound head induces a conformational change in the bound head which directs the free head towards the MT plus end (4). Hydrolysis of ATP by the bound head induces the binding of the second motor domain to the MT (5) which subsequently releases its ADP (6). The first head then detaches from the MT in the ADP•Pi state (7) and Pi is then released (8). In this mechanism, the kinesin dimer has taken one "step" along the MT with the hydrolysis of one ATP.

Although studies of conventional kinesin have provided much of the framework for understanding how KLPs function, a major challenge for future research is to determine whether all KLPs have the same properties as conventional kinesin. Several groups have begun to address this issue by characterizing additional KLPs, most notably Ncd (Non-claret disjunctional). Ncd, named after a well-known *Drosophila* mutation identified ~90 years ago, the first minus-end directed KLP identified, spurred a plethora of studies that were undertaken to determine if this protein functioned like kinesin and if any differences between the two could

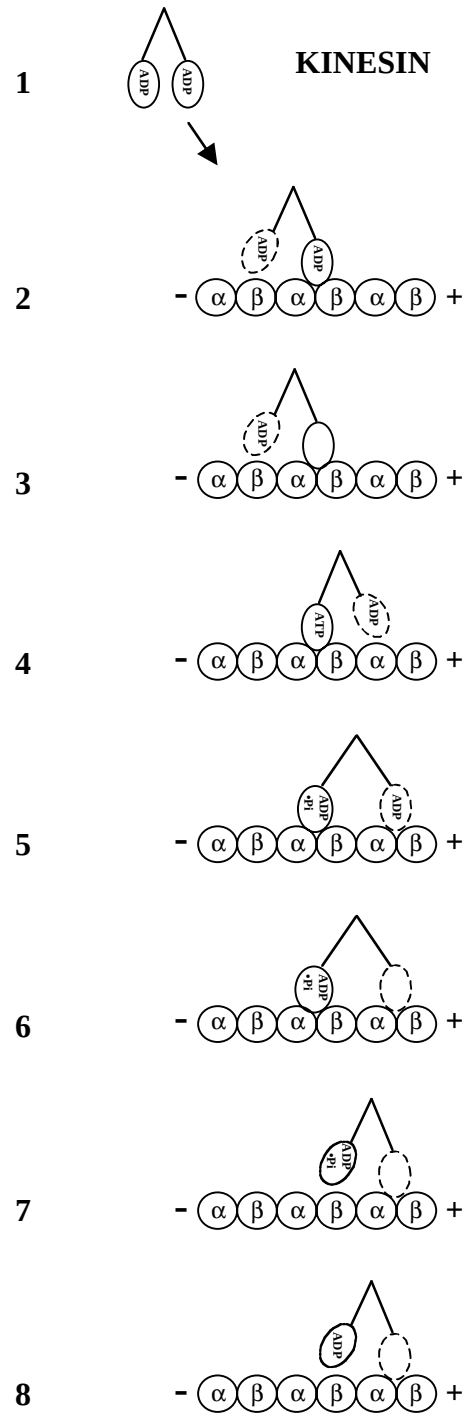

Figure 1.2. Schematic representation of the kinesin MT-ATPase
For clarity, MTs are represented as a single protofilament with alternating α and β tubulin subunits. The plus (+) and minus ends (-) are designated. The nucleotide state of each kinesin motor domain is indicated. See text for details. Modified from Hancock and Howard (1999).

account for its reversed directionality (Lockhart and Cross, 1994). Initial studies of the Ncd motor domain established that both Ncd and kinesin bound to the same site on a MT and that ADP release was the rate-limiting step of the Ncd ATPase (Lockhart et al., 1995a; Lockhart et al., 1995b; Ma and Taylor, 1995b). The crystal structure of the motor domain of Ncd (Sablin et al., 1996), which is nearly identical to the kinesin motor domain structure, coupled with extensive biochemical and biophysical studies (Foster and Gilbert, 2000; Foster et al., 1998; Mackey and Gilbert, 2000; Pechatnikova and Taylor, 1999; Pechnatnikova and Taylor, 1997) have further established that overall, the motor domains of kinesin and Ncd operate in a similar fashion and that unique motor characteristics (such as directionality) are determined primarily by sequences outside of the motor domain. For example, although the motor domains of kinesin and Ncd are superimposable, the region immediately adjacent to the motor domain (termed the "neck") of kinesin and Ncd differs dramatically in structure (Kozielski et al., 1997; Sablin et al., 1998) and this region has been implicated in controlling the directionality of kinesin and Ncd as well as explaining why kinesin, but not Ncd, is capable of processive movement along a MT (Endow and Waligora, 1998; Sablin et al., 1998). These studies of conventional kinesin and Ncd indicate that observed differences between KLPs are the result of specific adaptations that functionally distinguish the different kinesin families. For example, processivity is an important characteristic for motors such as conventional kinesin that transport small vesicles over large distances, but may not be required for spindle-associated KLPs such as Ncd that function in MT arrays. Limited kinetic information for other KLPs has made it difficult to extend this comparison to other kinesin family members and a major goal for future research is to determine how members of other kinesin families functionally compare to kinesin and Ncd.

Although kinesin and KLPs have been an area of active research since the discovery of kinesin in 1985, several questions remain to be addressed. These include: 1) How do the different KLP families functionally compare? Since almost all of the present knowledge of how motors operate is derived from work on only four of the eight KLP families, it is still unclear how closely members of the other four families conform to the current models of KLP force generation. 2) How are the activities of KLPs regulated? The majority of KLPs, including five of the eight KLP families are involved in some aspect of mitosis and, although some progress has been made in this area, how specific KLPs are regulated with respect to the cell cycle remains to be addressed.

Cell division is fundamental to the survival of an organism and must be stringently controlled in order to ensure the proper inheritance of chromosomes and the survival of the

organism. Consequently, proteins involved in the process of cell division are often subject to considerable regulation (Nigg et al., 1996). Because the activity of these proteins is limited to a discrete phase of the cell cycle (M-phase), it must be tightly regulated both temporally with respect to the phase of the cell cycle and spatially within the cell. Although specific roles for KLPs in mitosis have been defined, we are just beginning to understand how their activity is regulated.

Evidence from *in vitro* and *in vivo* studies indicate that at least two mammalian KLPs with roles in mitosis, CENP-E and HsEg5, are regulated by phosphorylation (Blangy et al., 1995; Liao et al., 1994). Studies with wild-type and mutant HsEg5 indicate that phosphorylation regulates the localization of HsEg5 to the mitotic spindle (Sawin and Mitchison, 1995). HsEg5 is phosphorylated *in vitro* and *in vivo* by the cell cycle kinase p34cdc2 and mutation of the phosphorylation site abolishes the localization of HsEg5 to centrosomes (Blangy et al., 1995; Sawin and Mitchison, 1995). HsEg5 is also phosphorylated by the mitotic aurora-related protein kinase pEg2 (Giet et al., 1999), although the role of pEg2 phosphorylation of HsEg5 is not known. CENP-E functions in chromosome attachment to kinetochores and alignment on the spindle equator (Yen et al., 1992). Phosphorylation of CENP-E by a p34cdc2 kinase inhibits the ability of the tail domain to bind to MTs, suggesting that the localization and/or activity of CENP-E during mitosis is controlled by cell-cycle dependent phosphorylation (Liao et al., 1994).

The second mechanism of regulation exhibited by mitotic KLPs that may serve to limit the activity of these proteins during interphase is sequestration in interphase nuclei. Of the five KLP families that contain mitotic KLPs, members of four of these families localize to nuclei. No functional role for KLPs in the nucleus has been discovered, which suggests that nuclear localization may serve to regulate the activity of KLPs by controlling their interaction with MTs. Sequestration of KLPs in the nucleus is also predicted to prevent inappropriate interactions with the interphase MT array, although this hypothesis has not been tested.

The third type of regulation exhibited by mitotic KLPs is cell-cycle dependent control over protein abundance, which serves to restrict protein accumulation to M-phase. Both CENP-E and HsEg5 protein levels appear to undergo cell-cycle dependent accumulation similar to that of the mitotic cyclin B (Sawin and Mitchison, 1995; Yen et al., 1992). In addition, Kat b and c protein levels have been shown to undergo cell-cycle accumulation in synchronized tobacco cell cultures (Mitsui et al., 1996). Regulation of KLPs may not be limited to these three mechanisms

and furthermore, different mechanisms of regulation may exist for a single KLP, which may serve to enhance the level of control over the activity of individual types of proteins.

A novel type of regulation for a KLP, involving calcium and calmodulin, was suggested by the identification of a kinesin-like calmodulin binding protein (KCBP) from *A. thaliana* (Reddy et al., 1996b). KCBP, a minus-end directed *C-terminal* KLP, was identified by its ability to bind to calmodulin (CaM) in a calcium-dependent manner (Reddy et al., 1996b; Song et al., 1997). KCBP was the first KLP identified to have a CaM-binding site, and although initially thought to be unique to plants, a KLP with a CaM-binding site has since been identified in sea urchin (Rogers et al., 1999). The CaM-binding site of KCBP is localized to a 23 AA sequence adjacent to the motor domain that is predicted to form a basic amphihelix similar to CaM-binding domains of other proteins (Reddy et al., 1996b). KCBP localizes to the preprophase band, mitotic spindle, and phragmoplast in dividing cells (Bowser and Reddy, 1997), and antibody injection experiments indicate a role for KCBP in cell division (Vos et al., 2000). An additional role for KCBP in trichome (plant hair) morphogenesis was revealed when *Arabidopsis zwichel* mutants, impaired in trichome development, were found to harbor mutations in the gene for KCBP (Oppenheimer et al., 1997).

Although KCBP was the first KLP demonstrated to have a CaM-binding site, CaM regulation of motor proteins is not unprecedented. In particular, regulation of the actin-based myosins by calcium and CaM has been well established (Wolenski, 1995). In addition to regulation of myosin light chain kinase activity in smooth muscle, CaM and CaM-like proteins function to regulate the activity of several unconventional myosins. CaM binding to these myosins may be calcium-dependent or independent, and typically more than one CaM may bind a given molecule. The effects of calcium and CaM on these myosins is often quite complex. For example, brush border myosin I binds CaM in the absence of calcium. In the presence of calcium, CaM dissociation from brush border myosin activates the basal rate of ATP hydrolysis, yet inhibits the actin-stimulated rate of ATP hydrolysis and motility *in vitro*. In contrast to brush border myosin I, brain myosin V binds CaM only in the presence of calcium. The binding of calcium/CaM to brain myosin V increases its actin-stimulated rate of ATP hydrolysis (Wolenski, 1995).

The presence of a CaM-binding site, coupled with the role of calcium and CaM in various signaling pathways within plant cells (Pooviah and Reddy, 1993), suggested a possible regulatory mechanism for KCBP *in vivo*. Stimuli such as temperature, light, mechanical

stimulation, and certain plant hormones have been shown to increase the concentration of cytosolic calcium in plants (Bush, 1993) and plant hormones such as gibberellic acid and abscisic acid are known to operate via calcium/CaM dependent pathways (Gilroy, 1996). In *Haemanthus* endosperm cells, calcium and CaM localization to the kinetochore MTs and spindle poles suggests a role for CaM in the depolymerization of MTs during chromosome separation (Vantard et al., 1985). In *Tradescantia* stem hair cells, calcium is suggested to stimulate the metaphase to anaphase transition (Helper, 1987). The role of calcium and CaM in plants is quite complex, and it is not clear how calcium and CaM may regulate the activity of KCBP *in vivo*.

OBJECTIVES

One of the primary goals of the present study is to extend work on the kinetic mechanism of kinesin and Ncd to the MKLP-1 family of KLPs. Specifically, my objectives are to:

i) develop a heterologous protein expression system for expressing and purifying HsMKLP-1 proteins

ii) determine how the HsMKLP-1 motor domain functionally compares to kinesin and Ncd in order to address how differences within the conserved catalytic domain of KLPs correlate to differences in function

The second goal of this project is to define factors that contribute to the regulation of mitotic KLPs. Specifically, my objectives are to:

i) identify sequences directing nuclear localization of HsMKLP-1 in order to establish the role of subcellular localization in regulating the activity of HsMKLP-1 during interphase

ii) determine how calcium and calmodulin regulate the activity of the kinesin-like calmodulin binding protein (KCBP) from *Arabidopsis thaliana*

CHAPTER 2: HETEROLOGOUS EXPRESSION OF THE MITOTIC KINESIN-LIKE PROTEIN-1 IN BACTERIAL AND INSECT CELL EXPRESSION SYSTEMS

(Portions published as: Deavours, B.E. and Walker, R.A. (1999) *Biochem. Biophys. Res. Comm*. 260: 605-608.)

Introduction

Kinesin-like proteins (KLPs) use the energy from ATP hydrolysis to drive organelle and vesicle transport and orchestrate events during mitosis and cytokinesis. Kinesin was first identified in squid axons as the protein responsible for MT-based movement of vesicles and organelles (Vale et al., 1985b) and since then over 250+ KLPs sharing homology to kinesin have been identified from a wide range of eukaryotic organisms (Greene et al., 1996). The ability of kinesin to translocate MTs on a glass coverslip facilitated its initial purification from squid axoplasm, squid optic lobes, and bovine brain (Vale et al., 1985a). Initial characterization of bovine brain kinesin demonstrated that the kinesin ATPase was similar to, yet distinct from the well characterized myosin ATPase. Both myosin and kinesin exhibited polymer-stimulated ATPase activity (actin for myosin and MTs for kinesin) as well as rate-limiting product release (Kuznetsov and Gelfand, 1986; Hackney, 1988; Sadhu and Taylor, 1992). However, in contrast to myosin, release of Pi by kinesin preceded the rate limiting step (Hackney, 1988).

The extent of similarity between the kinesin and myosin ATPases suggested that kinesin and myosin coupled ATP hydrolysis to force production in a similar fashion. Comparison of the kinesin and myosin ATPases required a detailed kinetic investigation of the kinesin ATPase, which was complicated by the heterogeneity of native kinesin preparations, as well as limited by the amount of protein obtained from native sources. Further characterization of kinesin was facilitated by the ability to express and purify truncated kinesin polypeptides from bacteria (Gilbert and Johnson, 1993). Expressing kinesin proteins in bacteria eliminated heterogeneity seen in kinesin preparations from native sources, provided sufficient quantities of protein for kinetic studies, and allowed the motor domain of kinesin to be characterized independently of the stalk and tail domains, which were previously shown to influence the ATPase activity of the motor domain (Kuznetsov et al., 1989). The utility of this approach was first demonstrated using a bacterially-expressed motor domain construct of *Drosophila* kinesin which exhibited MT-stimulated ATPase activity and rate-limiting ADP release in the absence of MTs, similar to bovine kinesin (Gilbert and Johnson, 1993). Since then, extensive biochemical, biophysical, and structural analysis of kinesin proteins prepared from bacteria has provided the majority of what we know about how kinesin operates and has allowed a detailed model for kinesin function to be

developed (Gilbert and Johnson, 1993; Gilbert et al., 1998; Gilbert et al., 1995; Hancock and Howard, 1999; Kawaguchi and Ishiwata, 2001; Kozielski et al., 1997; Kull et al., 1996; Ma and Taylor, 1995a; Ma and Taylor, 1995b; Moyer et al., 1996; Moyer et al., 1998; Sack et al., 1997). The ease and reproducibility of expressing kinesin proteins in bacteria has also greatly facilitated characterization of additional KLPs such as Ncd (Non-claret disjunctional), and has allowed direct comparisons to be made among kinesin family members (Foster et al., 2001; Gulick et al., 1998; Kikkawa et al., 2000; Lockhart and Cross, 1996; Okada and Hirokawa, 2000; Sablin et al., 1998; Sablin et al., 1996; Turner et al., 2001).

Expression of kinesin proteins in bacteria has several additional advantages over purification from native sources. Recombinant KLPs often accumulate to levels representing a significant fraction of total bacterial protein, which allows milligram quantities of protein to be purified from a few grams of bacteria as well as facilitating purification away from bacterial proteins. Proteins can also be expressed with affinity tags such as glutathione S-transferase (GST) or a stretch of histidines (His tag) to provide straightforward affinity purification, or modified by site-directed mutagenesis for structure-function studies. In comparison to eukaryotic expression systems, bacteria lack MTs and MT-associated proteins which can contaminate preparations of kinesin proteins purified from eukaryotic sources. However, eukaryotic expression systems may be necessary if the target protein requires post-translational modifications or if expression of the protein in bacteria is poor.

Although kinesin was originally characterized from native sources, purification of most KLPs is not feasible due to their low abundance in native tissues or difficulties associated with purifying proteins from particular cell types or organisms. In contrast to kinesin, the majority of KLPs have been identified by molecular and genetic approaches and several of these proteins are present at levels too low for conventional biochemical purification procedures. In addition, purification from native sources often requires the development of specific antibodies for identifying fractions containing the KLP of interest. For several mitotic KLPs, purification is further complicated by the fact that their synthesis is subject to cell cycle regulation which often limits protein abundance to particular stages of the cell cycle. Moreover, some organisms such as *D. melanogaster* or *C. elegans*, which have provided a wealth of genetic information about select KLPs, are not directly amenable to large scale biochemical procedures.

I chose to examine the expression of the *Homo sapiens* Mitotic Kinesin-Like Protein 1 (HsMKLP-1) in bacterial and eukaryotic systems in order to develop a heterologous protein

expression system for HsMKLP-1 that would provide sufficient quantities of purified protein for detailed characterization. HsMKLP-1 is a member of the MKLP-1 family of KLPs demonstrated to be involved in mitosis and cytokinesis and in the generation of MT-based structures (Adams et al., 1998; Powers et al., 1998; Raich et al., 1998; Sharp et al., 1996b). Unlike kinesin, which functions in membrane transport, HsMKLP-1 operates in the mitotic spindle, which suggests that functionally, HsMKLP-1 may exhibit properties distinct from kinesin. In support of this hypothesis, HsMKLP-1 has been demonstrated to bundle and slide antiparallel MTs *in vitro* (Nislow et al., 1992), although how HsMKLP-1 bundles MTs and generates sliding forces is unknown. Recombinant proteins will be used to characterize the structural and functional domains of HsMKLP-1. In particular, expression of the motor domain of HsMKLP-1 will allow a detailed analysis of the HsMKLP-1 ATPase relative to kinesin, while expression of the putative cargo-binding domain of HsMKLP-1 will aid in the identification of proteins that functionally interact with HsMKLP-1. Finally, expressed proteins will be used to generate antibodies against HsMKLP-1 in order to facilitate purification of native HsMKLP-1 to compare the properties of native and recombinant HsMKLP-1 proteins. I show here that expression of HsMKLP-1 proteins in *E. coli* is enhanced in mammalian codon-optimized bacterial strains and is sufficient for purification of reasonable quantities of protein, suggesting that poor expression in a standard bacterial expression strain is due to differences in codon usage between *E. coli* and *H. sapiens*. HsMKLP-1 proteins were also expressed in insect cells using the baculovirus expression system, although bacterial expression of HsMKLP-1 proteins is advantageous due to the ease and lower expense associated with culturing *E. coli* relative to insect cells, shorter timeframe for protein expression in *E. coli*, and more straightforward purification procedures.

Materials and Methods

Cloning of the cDNA encoding HsMKLP-1 into pET32a bacterial expression vector

cDNAs encoding AAs 1-461, 641-856 and 411-856 of HsMKLP-1 were amplified from a HeLa quick clone cDNA library (Clontech) using Pfu polymerase (Stratagene) and the following primers which contain restriction enzyme sites for Nco I (single underline), Hind III (dotted underline), or Not I (double underline):

5’-GAAAAAAAAGCCATGGTGTCAGCGAGAGC-3’ (0 forward),

5’-CAATGGTTCATTTCAAGCTTAACCTCGAGGCTG-3’ (461 reverse),

5’- GAAGGAAAAGTGCCCATGGTCGTGTGTGTGAACCCC-3’ (411 forward),

5’-GCCAAACAGCTGGCCATGGAGAATAAACTCTGG-3’ (641 forward), and

5’-ATCTAAGACAAACACTGCGGCCGCTTAGTTTATAAGTATACA-3’ (856 reverse).

PCR products from reactions containing 0 forward/461 reverse, 411 forward/856 reverse, and 641 forward/856 reverse primers were digested with Nco I/Hind III or Nco I/Not I and ligated into appropriately digested pET32a vector (Novagen) to create p32a-461Δ, p32a-Δ411, and p32a-Δ641. The insertion of a Nco I restriction site in the 0 forward primer resulted in a Lys to Val change in the second amino acid of HsMKLP-1. The Xho I/Not I fragment from p32a-Δ411 was ligated into Xho I/Not I digested p32a-461Δ to obtain a full length HsMKLP-1 cDNA in pET32a (p32a-MKLP-1). The p32a-MKLP-1 plasmid was sequenced and several discrepancies to the published sequence of HsMKLP-1 were noted (Fig. 2.1) (Nislow et al., 1992). These nucleotide differences not only resulted in the addition of 2 AA's and reassignment of 44 AA of HsMKLP-1, but truncated the protein 105 AA as compared to the published sequence (Fig. 2.2). With the exception of the nucleotides encoding the second AA of HsMKLP-1, our nucleotide sequence of HsMKLP-1 corresponds to the mRNA sequence of HsMKLP-1 in GenBank (accession number X67155) with the exception of one nucleotide difference 170 nucleotides after the stop codon. Our nucleotide sequence is identical to the HsMKLP-1 mRNA sequence NM004856 and differs in only 4 nucleotides from the mRNA sequence XM015567 deposited into GenBank by the NCBI. The deduced protein sequence of HsMKLP-1 we obtained is identical to the protein sequences for X67155, NM004856, and XM015567.

Baculovirus construction

PCR products from reactions containing 411 forward/856 reverse, 641 forward/856 reserve, and 0 forward/461 reverse primers were digested with Nco I/Not I (411/856, 641/856) or Nco I/Hind III (0/461) and ligated into appropriately digested pFastBac Hta plasmid (Gibco, Life Technologies) creating Hta-Δ411, Hta-Δ641, and Hta-461Δ. Recombinant baculoviruses encoding AAs 641-856, 411-856, and 1-461 of HsMKLP-1 (Fig. 5b) were generated using the Bac-to-Bac baculovirus expression system (Gibco, Life Technologies) according to the manufacturer's instructions.

Expression of subdomains of HsMKLP-1 in insect cells

Spodoptera frugiperda (Sf9) cells were purchased from the ATCC and maintained as suspension cultures in Grace's media supplemented with yeastolate, lactalbumin hydrolysate, 0.1% Pluronic F-68, 10% FBS, and antibiotics. Cells (100-200 ml suspension cultures at 1-3 X 10^6 cells/ml) were routinely infected with recombinant baculoviruses at a multiplicity of infection (MOI) of 0.1-1 as described (O'Reilly et al., 1994). To determine the timecourse of expression, cells were infected with recombinant baculoviruses at a MOI of 0-2. Cells were collected 0-144 hours post-infection and lysed in sample buffer (0.125 M Tris-HCl, pH 6.8, 4% SDS, 20% glycerol, 10% β-

Nislow *et.al.* atg**tt**gtcagcgagagctaagacaccccggaaacctaccgtgaaaaa-gggtcccaaacgaaccttaaagacccagttggg
Deavours & Walker atg**gt**gtcagcgagagctaagacaccccggaaacctaccgtgaaaaa**a**gggtcccaaacgaaccttaaagacccagttggg

Nislow *et.al.* --atactgtagggtgcg---actgggctttcctgatcaagagtgttgcatagaagtgatcaataatacaactgttcagctt
Deavours & Walker **gt**atactgtagggtgcg**ccc**actgggctttcctgatcaagagtgttgcatagaagtgatcaataatacaactgttcagctt

Nislow *et.al.* catactcctgagggctacagactcaaccgaaatggagactataaggagactcagtattcatttaaacaagtatttggcact
Deavours & Walker catactcctgagggctacagactcaaccgaaatggagactataaggagactcagtattcatttaaacaagtatttggcact

Nislow *et.al.* cacaccacccagaaggaactctttgatgttgtggctaatcccttggtcaatgacctcattcatggcaaaaatggtcttctt
Deavours & Walker cacaccacccagaaggaactctttgatgttgtggctaatcccttggtcaatgacctcattcatggcaaaaatggtcttctt

Nislow *et.al.* tttacatatggtgtgacgggaagtggaaaaactcacacaatgactggttctccaggggaaggagggctgcttcctcgttgt
Deavours & Walker tttacatatggtgtgacgggaagtggaaaaactcacacaatgactggttctccaggggaaggagggctgcttcctcgttgt

Nislow *et.al.* ttggacatgatctttaacagtatagggtcatttcaagctaaacgatatgttttcaaatctaatgataggaatagtatggat
Deavours & Walker ttggacatgatctttaacagtatagggtcatttcaagctaaacgatatgttttcaaatctaatgataggaatagtatggat

Nislow *et.al.* atacagtgtgaggttgatgccttattagaacgtcagaaaagagaagctatgcccaatccaaagacttcttctagcaaacga
Deavours & Walker atacagtgtgaggttgatgccttattagaacgtcagaaaagagaagctatgcccaatccaaagacttcttctagcaaacga

Nislow *et.al.* caagtagatccagagtttgcagatatgataactgtacaagaattctgcaaagcagaagaggttgatgaagatagtgtctat
Deavours & Walker caagtagatccagagtttgcagatatgataactgtacaagaattctgcaaagcagaagaggttgatgaagatagtgtctat

Nislow *et.al.* ggtgtatttgtctcttatattgaaatatataataattacatatatgatctattggaagaggtgccgtttgatcccataaa-
Deavours & Walker ggtgtatttgtctcttatattgaaatatataataattacatatatgatctattggaagaggtgccgtttgatcccataaa**a**

Nislow *et.al.* cccaaacctccacaatctaaattgcttcgtgaagat**t**aagaaccataacatgtatgttgcaggatgtacagaagttgaagt
Deavours & Walker cccaaacctccacaatctaaattgcttcgtgaagat-aagaaccataacatgtatgttgcaggatgtacagaagttgaagt

Nislow *et.al.* gaaatctactgaggaggcttttgaagttttctggagaggccagaaaaagagacgtattgctaatacccatttgaatcgtga
Deavours & Walker gaaatctactgaggaggcttttgaagttttctggagaggccagaaaaagagacgtattgctaatacccatttgaatcgtga

Nislow *et.al.* gtccagccgttcccatagcgtgttcaacattaaattagttcaggctcccttggatgcagatggagacaatgtcttacagga
Deavours & Walker gtccagccgttcccatagcgtgttcaacattaaattagttcaggctcccttggatgcagatggagacaatgtcttacagga

Nislow *et.al.* aaaagaacaaatcactataagtcagttgtccttggtagatcttgctggaagtgaaagaactaaccggaccagagcagaagg
Deavours & Walker aaaagaacaaatcactataagtcagttgtccttggtagatcttgctggaagtgaaagaactaaccggaccagagcagaagg

Nislow *et.al.* gaacagattacgtgaagctggtaatattaatcagtcactaatgacgctaagaacatgtatggatgtcctaagagagaacca
Deavours & Walker gaacagattacgtgaagctggtaatattaatcagtcactaatgacgctaagaacatgtatggatgtcctaagagagaacca

Nislow *et.al.* aatgtatggaactaacaagatggttccatatcgagattcaaagttaacccatctgttcaagaactactttgatggggaagg
Deavours & Walker aatgtatggaactaacaagatggttccatatcgagattcaaagttaacccatctgttcaagaactactttgatggggaagg

Nislow *et.al.* aaaagtgcggatgatcgtgtgtgtgaaccccaaggctgaagattatgaagaaaacttgcaagtcatgagatttgcggaagt
Deavours & Walker aaaagtgcggatgatcgtgtgtgtgaaccccaaggctgaagattatgaagaaaacttgcaagtcatgagatttgcggaagt

Nislow *et.al.* gactcaagaagttgaagtagcaagacctgtagacaaggcaatatgtggtttaacgcctgggaggagatacagaaaccagcc
Deavours & Walker gactcaagaagttgaagtagcaagacctgtagacaaggcaatatgtggtttaacgcctgggaggagatacagaaaccagcc

Nislow *et.al.* tcgaggtccagttggaaatgaaccattggttactgacgtggttttgcagagttttccacctttgccgtcatgcgaaatttt
Deavours & Walker tcgaggtccagttggaaatgaaccattggttactgacgtggttttgcagagttttccacctttgccgtcatgcgaaatttt

Nislow *et.al.* ggatatcaacgatgagcagacacttccaaggctgattgaagccttagagaaacgacataacttacgacaaatgatgattga
Deavours & Walker ggatatcaacgatgagcagacacttccaaggctgattgaagccttagagaaacgacataacttacgacaaatgatgattga

Nislow *et.al.* tgagtttaacaaacaatctaatgcttttaaagctttgttacaagaatttgacaatgctgttttaagtaaagaaaaccacat
Deavours & Walker tgagtttaacaaacaatctaatgcttttaaagctttgttacaagaatttgacaatgctgttttaagtaaagaaaaccacat

Nislow *et.al.* gcaagggaaactaaatgaaaaggagaagatgatctcaggacagaaattggaaatagaacgactggaaaagaaaaacaaaac
Deavours & Walker gcaagggaaactaaatgaaaaggagaagatgatctcaggacagaaattggaaatagaacgactggaaaagaaaaacaaaac

Nislow *et.al.* tttagaatataagattgagattttagagaaaacaactactatctatgaggaagataaacgcaatttgcaacaggaacttga
Deavours & Walker tttagaatataagattgagattttagagaaaacaactactatctatgaggaagataaacgcaatttgcaacaggaacttga

Nislow *et.al.* aactcagaaccagaaacttcagcgacagttttctga**g**aaacgcagattagaagccaggttgcaaggcatggtgacagaaac
Deavours & Walker aactcagaaccagaaacttcagcgacagttttctga**c**aaacgcagattagaagccaggttgcaaggcatggtgacagaaac

Nislow *et.al.* gacaatgaagtgggagaaagaatgtgagcgtagagtggcagccaaacagctggagatgcagaataaactctgggttaaaga
Deavours & Walker gacaatgaagtgggagaaagaatgtgagcgtagagtggcagccaaacagctggagatgcagaataaactctgggttaaaga

Nislow *et.al.* tgaaaagctgaaacaactgaaggctattgttactgaacctaaaactgagaagccagagagaccctctcgggagcgagatcg
Deavours & Walker tgaaaagctgaaacaactgaaggctattgttactgaacctaaaactgagaagccagagagaccctctcgggagcgagatcg

Nislow *et.al.* agaaaaagttactcaaagatctgtttctccatcacctgtgcctttactctttcaacctgatcagaacgcaccaccaattcg
Deavours & Walker agaaaaagttactcaaagatctgtttctccatcacctgtgcctttactctttcaacctgatcagaacgcaccaccaattcg

Nislow *et.al.* tctccgacacagacgatcacgctctgcaggagacagatgggtagatcataagcccgcctctaacatgcaaactgaaacagt
Deavours & Walker tctccgacacagacgatcacgctctgcaggagacagatgggtagatcataagcccgcctctaacatgcaaactgaaacagt

Nislow *et.al.* catgcagccacatgtccctcatgccatcacagtatctgttgcaaatgaaaaggcactagctaagtgtgagaagtacatgct
Deavours & Walker catgcagccacatgtccctcatgccatcacagtatctgttgcaaatgaaaaggcactagctaagtgtgagaagtacatgct

Nislow *et.al.* gacccaccaggaactagcctccgatggggagattgaaactaaactaattaagggtgatatttataaaacaaggggtggtgg
Deavours & Walker gacccaccaggaactagcctccgatggggagattgaaactaaactaattaagggtgatatttataaaacaaggggtggtgg

Nislow *et.al.* acaatctgttcagtttactgatattgagactttaaagcaagaatcaccaaatggtagtcgaaaacgaagatcttccacagt
Deavours & Walker acaatctgttcagtttactgatattgagactttaaagcaagaatcaccaaatggtagtcgaaaacgaagatcttccacagt

Nislow *et.al.* agcacctgcccaaccagatggtgcagagtctgaatggac**g**cgatgtagaaacaaggtgttctgtggctgtg-agatgagag
Deavours & Walker agcacctgcccaaccagatggtgcagagtctgaatggac-cgatgtagaaacaaggtgttctgtggctgt**g**agatgagag

Nislow *et.al.* caggatcccagctgg-acctg-atatcagcatcacg**g**cacaacccaagcgcaaaaagccatg**a**aactgacagtcccagtac
Deavours & Walker caggatcccagctg**g**acctg**g**atatcagcatcacg-cacaacccaagcgcaaaaagccatg-aactgacagtcccagtac

Nislow *et.al.* tgaaagaacattttcatttgtgtggatgatttctcgaaagccatgccagaagcagtcttccaggtcatcttgtagaactcc
Deavours & Walker tgaaagaacattttcatttgtgtggatgatttctcgaaagccatgccagaagcagtcttccaggtcatcttgtagaactcc

Nislow *et.al.* agctttg**g**ttgaaaatcacggacctcagctacatcatacactgacccaga**at**aaagctttccctatggttccaaagacaac
Deavours & Walker agctttg-ttgaaaatcacggacctcagctacatcatacactgacccaga**gc**aaagctttccctatggttccaaagacaac

Nislow *et.al.* tagtattcaacaaaccttgtatagtgtatgttttgccatatttaatattaatagcagaggaagactccttttttcatcact
Deavours & Walker tagtattcaacaaaccttgtatagtgtatgttttgccatatttaatattaatagcagaggaagactccttttttcatcact

Nislow *et.al.* gtatgaatttttttataatgttttttt**t**aaaatatatttcatgtatacttataaac<u>taa</u>
Deavours & Walker gtatgaatttttttataatgttttttt-aaaatatatttcatgtatacttataaactaa

Figure 2.1. Comparison of the cDNA sequence of HsMKLP-1 amplified from a HeLa cell cDNA library (Deavours & Walker, unpublished) with the published sequence of HsMKLP-1 (Nislow et al., 1992). Deviations in the sequence are underlined in bold face. The sequence we obtained has 10 nucleotide insertions, 6 deletions, and 4 changes as compared to the published sequence (Nislow et al., 1992).

X67155.2 MKSARAKTPRKPTVKKGSQTNLKDPVGVYCRVRPLGFPDQECCIEVINNTTVQLHTPEGYRLNR
X67155.1 MLSARAKTPRKPTVKKGPKRTLKTQLG-YCRVR-LGFPDQECCIEVINNTTVQLHTPEGYRLNR

X67155.2 NGDYKETQYSFKQVFGTHTTQKELFDVVANPLVNDLIHGKNGLLFTYGVTGSGKTHTMTGSPGEG
X67155.1 NGDYKETQYSFKQVFGTHTTQKELFDVVANPLVNDLIHGKNGLLFTYGVTGSGKTHTMTGSPGEG

X67155.2 GLLPRCLDMIFNSIGSFQAKRYVFKSNDRNSMDIQCEVDALLERQKREAMPNPKTSSSKRQVDPE
X67155.1 GLLPRCLDMIFNSIGSFQAKRYVFKSNDRNSMDIQCEVDALLERQKREAMPNPKTSSSKRQVDPE

X67155.2 FADMITVQEFCKAEEVDEDSVYGVFVSYIEIYNNYIYDLLEEVPFDPIKPKPPQSKLLREDKN
X67155.1 FADMITVQEFCKAEEVDEDSVYGVFVSYIEIYNNYIYDLLEEVPFDPINPNLHNLNCFVKIKN

X67155.2 HNMYVAGCTEVEVKSTEEAFEVFWRGQKKRRIANTHLNRESSRSHSVFNIKLVQAPLDADGDNVL
X67155.1 HNMYVAGCTEVEVKSTEEAFEVFWRGQKKRRIANTHLNRESSRSHSVFNIKLVQAPLDADGDNVL

X67155.2 QEKEQITISQLSLVDLAGSERTNRTRAEGNRLREAGNINQSLMTLRTCMDVLRENQMYGTNKMVP
X67155.1 QEKEQITISQLSLVDLAGSERTNRTRAEGNRLREAGNINQSLMTLRTCMDVLRENQMYGTNKMVP

X67155.2 YRDSKLTHLFKNYFDGEGKVRMIVCVNPKAEDYEENLQVMRFAEVTQEVEVARPVDKAICGLTPG
X67155.1 YRDSKLTHLFKNYFDGEGKVRMIVCVNPKAEDYEENLQVMRFAEVTQEVEVARPVDKAICGLTPG

X67155.2 RRYRNQPRGPVGNEPLVTDVVLQSFPPLPSCEILDINDEQTLPRLIEALEKRHNLRQMMIDEFNK
X67155.1 RRYRNQPRGPVGNEPLVTDVVLQSFPPLPSCEILDINDEQTLPRLIEALEKRHNLRQMMIDEFNK

X67155.2 QSNAFKALLQEFDNAVLSKENHMQGKLNEKEKMISGQKLEIERLEKKNKTLEYKIEILEKTTTIY
X67155.1 QSNAFKALLQEFDNAVLSKENHMQGKLNEKEKMISGQKLEIERLEKKNKTLEYKIEILEKTTTIY

X67155.2 EEDKRNLQQELETQNQKLQRQFSDKRRLEARLQGMVTETTMKWEKECERRVAAKQLEMQNKLWVK
X67155.1 EEDKRNLQQELETQNQKLQRQFSEKRRLEARLQGMVTETTMKWEKECERRVAAKQLEMQNKLWVK

X67155.2 DE KLKQLKAIVTEPKTEKPERPSRERDREKVTQRSVSPSPVPLLFQPDQNAPPIRLRHRRSRSA
X67155.1 DE KLKQLKAIVTEPKTEKPERPSRERDREKVTQRSVSPSPVPLLFQPDQNAPPIRLRHRRSRSA

X67155.2 GDRWVDHKPASNMQTETVMQPHVPHAITVSVANEKALAKCEKYMLTHQELASDGEIETKLIKGDI
X67155.1 GDRWVDHKPASNMQTETVMQPHVPHAITVSVANEKALAKCEKYMLTHQELASDGEIETKLIKGDI

X67155.2 YKTRGGGQSVQFTDIETLKQESPNGSRKRRSSTVAPAQPDGAESEWTDVETRCSVAVEMRAGS
X67155.1 YKTRGGGQSVQFTDIETLKQESPNGSRKRRSSTVAPAQPDGAESEWTRCRNKVFCGCEMRAGS

X67155.2 QLGPGYQHHAQPKRKKP
X67155.1 QLDLISASRHNPSAKSHETDSPSTERTFSFVWMISRKPCQKQSSRSSCRTPALVENHGPQLHH

X67155.2
X67155.1 TLTQNKAFPMVPKTTSIQQTLYSVCFAIFNINSRGRLLFSSLYEFFIMFFLKYISCILIN

Figure 2.2. Comparison of the deduced amino acid sequence of the HsMKLP-1 cDNA amplified from a HeLa cell cDNA library (X67155.2) with the published sequence of HsMKLP-1 (X67155.1) (Nislow et. al., 1992). Deviations in the sequence are underlined in bold face.

mercaptoethanol). Samples were separated by SDS-PAGE and transferred to nitrocellulose. Western blotting was performed using a monoclonal anti-6X His antibody (Clontech) and HRP-conjugated 2° antibodies (Pierce). Western blots were developed by ECL using Super Signal Ultra chemiluminescent substrate (Pierce).

Nuclear fractionation of insect cells

Sf9 cells harvested 72 hours post-infection were fractionated essentially as described previously (Miyamoto et al., 1985). Briefly, cells were swelled in hypotonic buffer (10 mM Tris-HCl, pH 7.5, 10 mM NaCl, 1.5 mM $MgCl_2$) supplemented with protease inhibitors for 30 minutes on ice and lysed by Dounce homogenization. Nuclei were pelleted (1,000 xg, 10 minutes) and incubated in hypotonic buffer containing 1% NP-40 and 0.5% deoxycholate for 30 minutes on ice. Stripped nuclei were pelleted as above, lysed in buffer containing 0.1% SDS, 1% Triton X-100, 1% deoxycholate, and 0.15 M NaCl, and then spun at 13,000 xg. Supernatant and pellet fractions were resuspended in sample buffer, separated using SDS-PAGE, and transferred to nitrocellulose. Western blotting was performed as described above.

Purification of 461Δ_{bev} and Δ641$_{bev}$ from insect cells

Cells (100-200 ml culture at 2-3 X 10^6 cells/ml) infected at an MOI of 0.1 with recombinant baculovirus encoding either AA 641-856 (641Δ_{bev}) or AA 1-461 (461Δ_{bev}) of HsMKLP-1 were collected 72 hours after infection and washed twice in buffer. Cells expressing Δ641$_{bev}$ were fractionated as described above. The cytoplasmic and detergent-extracted fractions were combined and the concentrations of Tris-HCl and NaCl adjusted to 20 mM and 0.1 M, respectively. The extract was then clarified at 20,000 xg for 15 minutes at 4°C before being incubated with Talon resin (Clontech) according to the manufacturer's protocol. Bound protein was eluted from the column with 20 mM Tris-HCl pH 8.0, 0.1 M NaCl, and 100 mM imidazole. The binding of 461Δ_{bev} to endogenous Sf9 MTs was used as an initial step in the purification of this construct. Cells expressing 461Δ_{bev} were resuspended in 2 volumes of AB buffer (20 mM PIPES, pH 6.9, 1 mM $MgCl_2$, 1 mM DTT) plus protease inhibitors, lysed by sonication (3 x 6s), and spun at 20,000 xg for 15 minutes at 4°C. The majority of 461Δ_{bev} was extracted from the pellet fraction after centrifugation as described below. The supernatant was additionally clarified at 100,000 xg for 15 minutes at 4°C and endogenous MTs were allowed to polymerize for 30 minutes at 22°C following the addition of 2 mM GTP and 20 μM taxol. MTs were pelleted at 100,000 xg for 15 minutes at 25°C, resuspended in AB buffer supplemented with 10 mM MgATP, 0.1 mM GTP, 5 μM taxol, and 0.5 M NaCl, and pelleted as before. To extract 461Δ_{bev}, the pellet fraction following sonication was resuspended in AB buffer supplemented with

protease inhibitors and 0.5 M NaCl and incubated on ice for 30 minutes before being spun at 100,000 xg for 15 minutes. The supernatant was then desalted using a PD-10 column equilibrated in AB buffer. The Sf9 MT pellet was resuspended in the desalted extract supplemented with 0.1 mM MgGTP, 40 μM taxol, and 2 mM MgAMP-PNP and incubated for 30 minutes at 22°C. MTs were pelleted as before and resuspended in AB buffer plus 10 mM MgATP, 0.1 mM MgGTP, 5 μM taxol, and 0.5 M NaCl for 30 minutes at 22°C. MTs were pelleted as before and the supernatant was incubated with Talon resin as described for $\Delta 641_{bev}$.

Plasmid construction for expression in bacteria

Additional constructs of HsMKLP-1 were cloned into pET32a for expression in bacteria (Fig. 2.3c). cDNA encoding AA 1-524 of HsMKLP-1 was obtained by excising the 1563 bp Nco I/Hind III fragment from p32a-MKLP-1 and ligating it into Nco I/Hind III digested p32a. cDNA encoding AA 1-619 of HsMKLP-1 was amplified from p32a-MKLP-1 using Pfu polymerase (Stratagene), T7 promoter primer, and the following primer which contains a restriction enzyme site for BamHI site (underlined): CTGGATCCTCGTTTATGTCACCATGCC. The PCR product was digested with Nco I and Bam HI and ligated into appropriately digested pET32a to create p32a-619Δ. For cloning into pET21d, the fragments released from digestion of p32a-Δ641 (973 bp), p32a-Δ411 (1689 bp), and p32a-MKLP-1 (2899 bp) with Nco I and Not I and digestion of p32a-461Δ (1397 bp) with Nco I and Hind III were cloned into appropriately digested pET21d creating p21d-Δ641, p21d-Δ411, p21d-MKLP-1, and p21d-461Δ.

Expression and solubility of HsMKLP-1 proteins in bacteria

Plasmids p32a-MKLP-1, p32a-461Δ, p32a-524Δ, p32a-619Δ, p32a-Δ641, and p32a-Δ411 were transformed into BL21 (DE3) pLys S cells or BL21 Codon-plus (DE3)-RIL cells (Stratagene) and cells were grown at 37°C until A_{550} = 0.5-0.7. Protein expression was induced with 0.25 mM IPTG and proceeded at 22°C for 4-6 hours. Cells were pelleted, washed once with 20 mM Tris-HCl pH 8.0, 100 mM NaCl and frozen at -70°C. To test the solubility of HsMKLP-1 proteins, cell pellets were thawed and resuspended in 20 mM Tris-HCl, pH 8.0, 100 mM NaCl, 0.1 mg/ml lysozyme, 0.5 mM MgATP, 10 mM $MgCl_2$ and 40 μg/ml DNase I plus protease inhibitors and briefly sonicated. Cell lysates were spun at 20,000 x g for 15 minutes and the resulting supernatant was spun at 100,000 xg for 15 minutes. Gel samples of the lysate, low speed supernatant, low speed pellet, high speed supernatant, and high speed pellet were resolved by SDS-PAGE and proteins were visualized by Coomassie Blue staining of gels.

Purification of 461Δ, 524Δ, 619Δ, and Δ641 from bacterial cells

461Δ and 524Δ were purified from BL21 Codon-plus (DE3)-RIL cells as follows. Cell pellets were thawed and resuspended in 20 mM Tris-HCl pH 8.0, 100 mM NaCl, 0.5 mM ß-mercaptoethanol, 0.5 mM MgATP, 10 mM $MgCl_2$, 40 μg/ml DNase I, 1 mM PMSF or Complete protease inhibitor tablet (Boehringer Mannheim), and lysed by sonication (3 X 30s pulses). Cell lysates were spun at 20,000 xg for 15 minutes and the resulting supernatant was incubated with Talon metal affinity resin (Clontech) according to the manufacturer's protocol. Bound protein was eluted from the column with buffer containing 100 mM imidazole and then dialyzed against 20 mM PIPES pH 6.9, 100 mM NaCl, 1 mM $MgCl_2$, and 1 mM DTT. The N-terminal 127 AA tag including thioredoxin was removed from the fusion protein following digestion with thrombin protease (1U/mg fusion protein) for 2-3 hours at 22°C. Reactions were stopped by the addition of PMSF to 2 mM and the thioredoxin tag was separated from HsMKLP-1 proteins by FPLC on a HiTrap SP ion-exchange column equilibrated with AB buffer (20 mM PIPES pH 6.9, 1 mM EGTA, 1 mM $MgCl_2$, 1 mM DTT) plus 1 mM PMSF. Proteins were eluted from the column using a gradient of 100-600 mM NaCl. Fractions containing 461Δ were dialyzed against AB buffer containing 100 mM NaCl, snap frozen in liquid N_2, and stored at -80°C. Eluate fractions containing 524Δ were additionally passed over a 350 ml S300 column equilibrated in AB buffer plus 100 mM NaCl and 10 μM ATP and further purified by FPLC on a HiTrap Q column equilibrated as described above for HiTrap SP. Eluate fractions containing 524Δ were snap frozen in liquid N_2 and stored at -80°C. BL21 Codon-plus (DE3)-RIL cells expressing 619Δ were lysed and fractionated as described above for 461Δ and 524Δ except that 0.1 mg/ml lysozyme was added to the lysis buffer. The 619Δ containing pellet after centrifugation was resuspended in Tris buffer (20 mM Tris-HCl, pH 8.0, 500 mM NaCl, 0.5 mM ß-mercaptoethanol) plus 0.5 mM MgATP and protease inhibitors and incubated for 30 minutes on ice before centrifugation at 20,000 xg for 15 minutes. The resulting supernatant was passed over a Ni-NTA column (Qiagen) and the column was extensively washed in Tris buffer plus 0.1% Triton-X. Bound protein was eluted from the column with Tris buffer plus 250 mM imidazole and then dialyzed against Tris buffer before digestion with thrombin protease (5 hours, on ice). Digested proteins were then passed over Ni-NTA resin to remove the thioredoxin tag. The flow-through from the Ni-NTA column was collected, dialyzed against AB buffer plus 100 mM NaCl and 10% sucrose, and passed over a HiTrap SP column as described above. Fractions containing 619Δ were concentrated by centrifugation using a Centricon 30 device (Amicon), snap frozen in liquid N_2 and stored at -80°C. Several additional proteins generated by thrombin digestion consistently co-purified with 461Δ, 524Δ, and 619Δ. Purity of protein preparations was estimated by densitometry of SDS-PAGE gels to be 70-75%. BL21 Codon-plus (DE3)-RIL cells

expressing Δ641 were thawed and resuspended in AB buffer plus 0.1 mg/ml lysozyme, 0.5 mM MgATP, 10 mM $MgCl_2$, 40 μg/ml DNase I, and 1 mM PMSF, and lysed by sonication (3 X 30s pulses). Cell lysates were spun at 20,000 xg for 15 minutes and the resulting supernatant was passed over a HiTrap SP column as described above. Fractions containing Δ641 were diluted 5-fold with AB buffer and passed over a HiTrap Q column as described above. Under these conditions, Δ641 was not retained on the Q column and was collected in the flow-through fraction. The flow-through fraction from the Q column was then passed over an S-Sepharose column and Δ641 was eluted from the column with 0.5 M NaCl. Peak fractions were combined, dialyzed against AB plus 0.1 M NaCl, snap frozen in liquid N_2, and stored at -80°C.

Results:

Baculovirus-mediated expression of HsMKLP-1 proteins in insect cells

In order to identify structural and functional domains of HsMKLP-1, subdomains of HsMKLP-1 were initially tested for expression using the bacterial pET Expression System. In this system, transcription from the strong T7 promoter is regulated by the inducible synthesis of T7 RNA polymerase which allows expression of heterologous proteins to be tightly controlled. Sequences encoding AA 1-461 (Trx-461Δ), 641-856 (Trx-Δ641), and 411-856 (Trx-Δ411) of HsMKLP-1 were initially cloned into the pET32a vector downstream from the T7 promoter (Fig. 2.3c). Proteins were expressed as C-terminal fusions to thioredoxin and a 56 AA leader sequence including a 6-Histidine tag (His tag). Fusion of proteins to thioredoxin has been demonstrated to increase their solubility in bacterial systems (LaVallie et al., 1993) while inclusion of a His tag allowed proteins to be purified using metal affinity chromatography. Expression of HsMKLP-1 proteins in the high-stringency BL21(DE3)pLys cells was either not detectable (Trx-Δ411) or detectable only after immunoblotting (Trx-461Δ, Trx-Δ641). One possibility for the poor expression of HsMKLP-1 proteins in this system is the low frequency of certain tRNAs in *E. coli* that limit translation of human proteins (discussed below, see Table 2.3). As an alternate approach, HsMKLP-1 proteins were tested for expression in insect cells using the baculovirus expression system. Insect cells infected with baculovirus have been shown to express many human proteins that were difficult to express in bacteria (Luckow, 1991). Advantages of an insect-based expression system include post-translational modifications of proteins and codon usage similar to that found in mammalian cells (O'Reilly et al., 1994). Recombinant baculoviruses encoding N- and C-terminal portions of HsMKLP-1 were generated using the Bac-to-Bac expression system (Fig. 2.3a, b). In this system proteins are expressed under the control of the strong polyhedrin promoter, which is responsible for the high level expression (>1 mg/ml of cell culture) of polyhedrin during the later stages of baculovirus

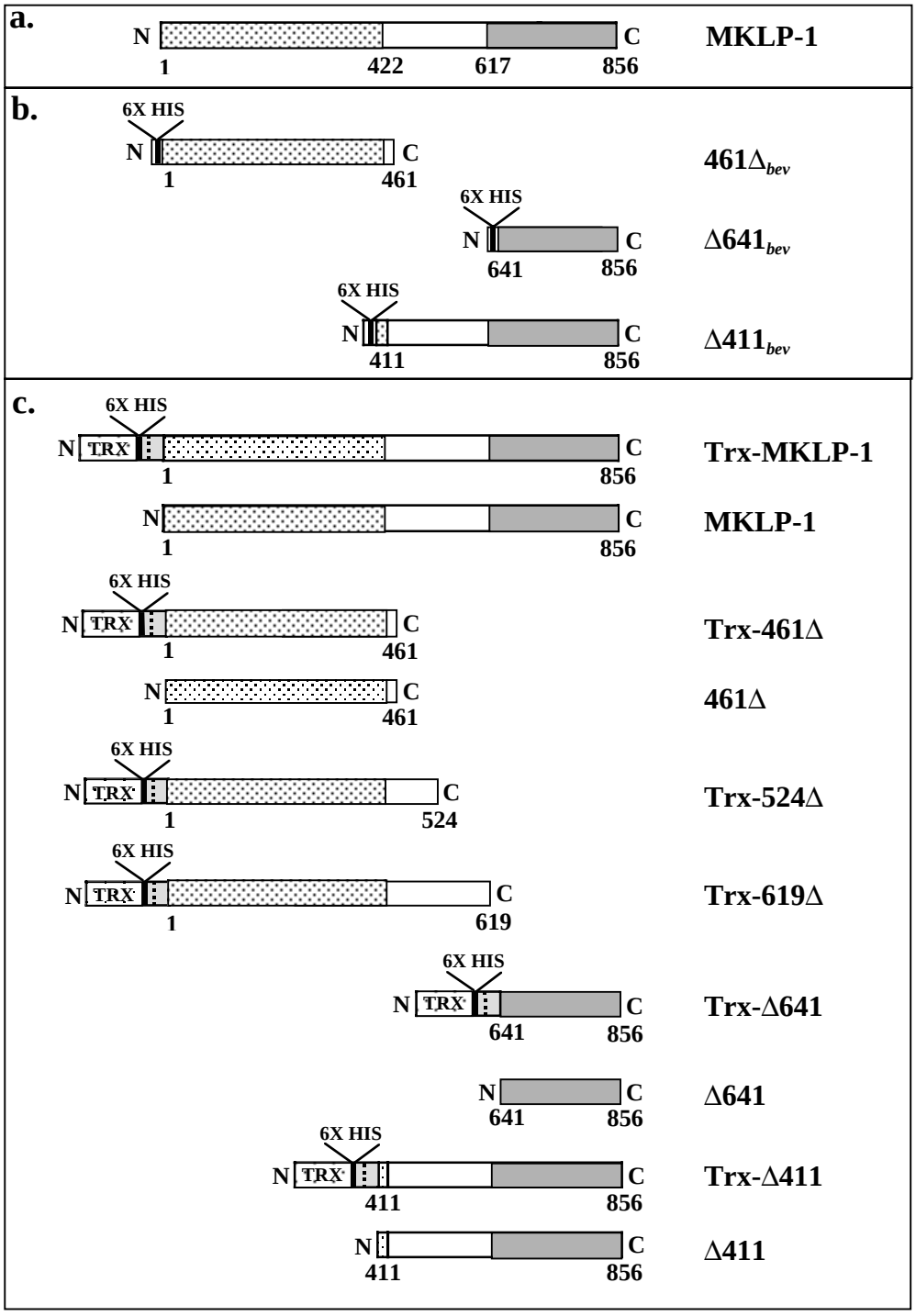

Figure 2.3. Full-length HsMKLP-1 and HsMKLP-1 constructs expressed in insect and bacterial cells. a.) Domain organization of the HsMKLP-1 polypeptide. The motor domain of HsMKLP-1, which shares sequence similarity to the motor domain of kinesin is shown as a stippled box. The stalk domain, which includes sequences predicted to form coiled coils by the program

PAIRCOILS (http://nightingale.lcs.mit.edu/cgi-bin/score) (AA 537-617) (Berger et al., 1995) is in white. The 239 AA tail domain is shown in gray. b.) Schematic representation of HsMKLP-1 constructs expressed in insect cells. Constructs $461\Delta_{bev}$, $\Delta641_{bev}$ and $\Delta411_{bev}$ encode AAs 1-461, 641-856 and 411-856, respectively of HsMKLP-1 in addition to an N-terminal 6-Histidine (6X HIS) tag. c.) Schematic representation of HsMKLP-1 constructs expressed in bacterial cells. Full-length HsMKLP-1 (MKLP-1, Trx-MKLP-1) in addition to AA 1-461 (461Δ, Trx-461Δ), 641-856 (Δ641, Trx-Δ641), and 411-856 (Δ411, Trx-Δ411) were expressed either alone or as C-terminal fusions to thioredoxin (Trx) and a 56 AA linker containing a 6-Histidine (6X HIS) tag. Constructs encoding HsMKLP-1 AA 1-524 (Trx-524Δ) and 1-619 (Trx-619Δ) were only expressed with the N-terminal thioredoxin/His fusion tag. The thrombin protease cleavage site is 30 AA N-terminal to the start codon of each HsMKLP-1 construct and is indicated by the dashed line.

infection when occluded virus is formed. Proteins were expressed with an N-terminal His tag to facilitate purification using metal-affinity chromatography. Construct 461Δ_{bev} (AA 1-461; baculovirus expression vector ($_{bev}$) to distinguish from bacterially-expressed 461Δ) encodes the motor domain of HsMKLP-1 while constructs $\Delta411_{bev}$ (AA 411-856) and $\Delta641_{bev}$ (AA 641-856) encode portions of the stalk and tail domains of HsMKLP-1. To analyze expression of HsMKLP-1 proteins in insect cells, cells were infected with a range of virus concentrations and protein expression was monitored by Western blotting using an antibody recognizing the His tag (Fig. 2.4). Figure 2.4 shows the timecourse of expression of $\Delta641_{bev}$ in insect cells; similar expression profiles were obtained for 461Δ_{bev} and $\Delta411_{bev}$. No expression was detected in the absence of virus and only weak expression was observed at a MOI of 0.001. At higher MOI's expression was detected 48 hours after infection; in all cases expression appeared to peak 72 hours after infection. Expression was maximal 72 hours after infection at a MOI of 0.1 and these parameters were chosen for expressing HsMKLP-1 proteins in subsequent experiments.

Subcellular fractionation of insects cells expressing 461Δ_{bev}, $\Delta411_{bev}$, and $\Delta641_{bev}$

As an initial step in developing a purification strategy for the baculovirus-expressed proteins, insect cells expressing HsMKLP-1 proteins were fractionated and monitored for protein by Western blotting (Fig. 2.5). Fractionation of cells expressing C-terminal constructs of HsMKLP-1 ($\Delta641_{bev}$ and $\Delta411_{bev}$) was consistent with nuclear localization of these proteins. Nuclei isolated following hypotonic lysis of cells expressing $\Delta641_{bev}$, $\Delta411_{bev}$, or $\Delta461_{bev}$ of HsMKLP-1 were treated with NP-40/deoxycholate to remove the outer membrane and lysed using a combination of salt and both ionic and non-ionic detergents. The majority of $\Delta411_{bev}$ and $\Delta641_{bev}$ was present in the final pellet obtained after nuclear lysis, consistent with nuclear localization. Western blotting indicates that $\Delta411_{bev}$ is absent from the cytoplasmic fraction, detergent-extracted fraction, and nuclear extract, suggesting that it is tightly associated with some component of the nuclear matrix. In comparison, $\Delta641_{bev}$ is distributed in both the cytoplasmic and detergent-extracted fractions, indicating that a fraction of $\Delta641_{bev}$ is not contained within the nucleus. Only a small fraction of 461Δ_{bev} was present in the nuclear extract, with the majority of the protein present in the detergent-extracted fraction. Attempts to solubilize $\Delta411_{bev}$ were not successful and further characterization of this construct was not pursued. However, both 461Δ_{bev} and $\Delta641_{bev}$ could be purified from Sf9 cells by metal affinity chromatography (Fig. 2.6, lanes 2 and 3). Purity of these proteins is estimated to be ~65% (461Δ_{bev}) and ~75% ($\Delta641_{bev}$) based on densitometry of Coomassie-blue stained protein gels.

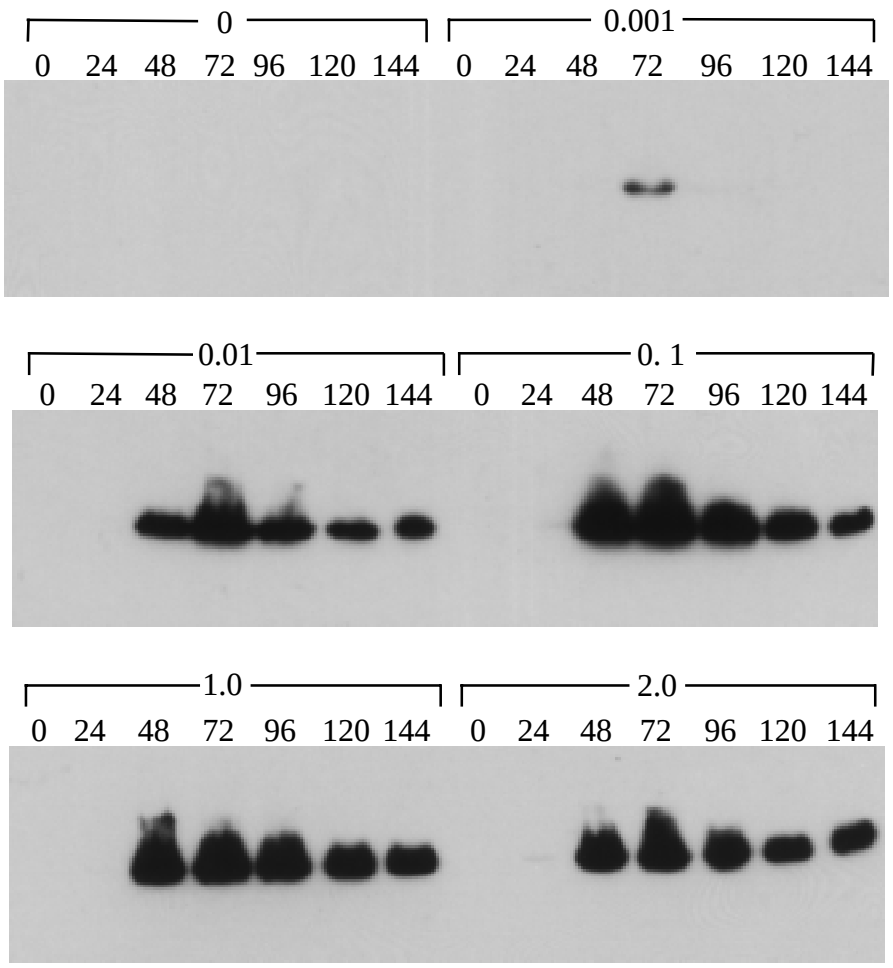

Figure 2.4. Time course of expression of $\Delta 641_{bev}$ in insect cells. Insect cells were infected with recombinant baculovirus encoding AA 641-856 of HsMKLP-1 at a multiplicity of infection (MOI) from 0-2. Cells were harvested 0, 24, 48, 72, 96, 120, and 144 hours after infection and analyzed for $\Delta 641_{bev}$ expression by Western blotting using an antibody recognizing the His tag.

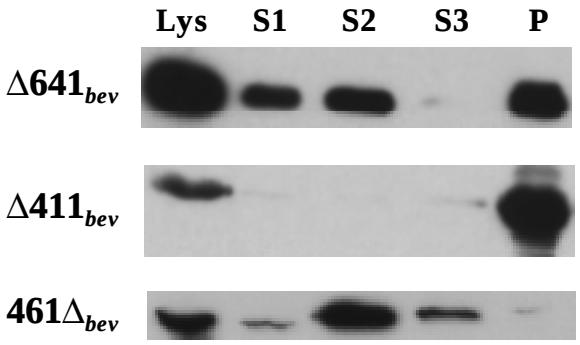

Figure 2.5. Fractionation of insect cells expressing $461\Delta_{bev}$, $\Delta641_{bev}$, and $\Delta411_{bev}$.
Insect cells expressing $\Delta641_{bev}$, $\Delta411_{bev}$ or $461\Delta_{bev}$ were fractionated into cytoplasmic (S1) and nuclear fractions following hypotonic lysis (Lys). Nuclear pellet was treated with NP-40 and deoxycholate to release associated membranes and proteins and separated into supernatant (S2) and pellet fractions following centrifugation. The pellet fraction (stripped nuclei) was resuspended in buffer containing SDS, deoxycholate, Triton X-100 and NaCl and fractionated into supernatant (S3) and pellet (P) fractions following centrifugation. Fractions were analyzed by Western blotting as described in Materials and Methods.

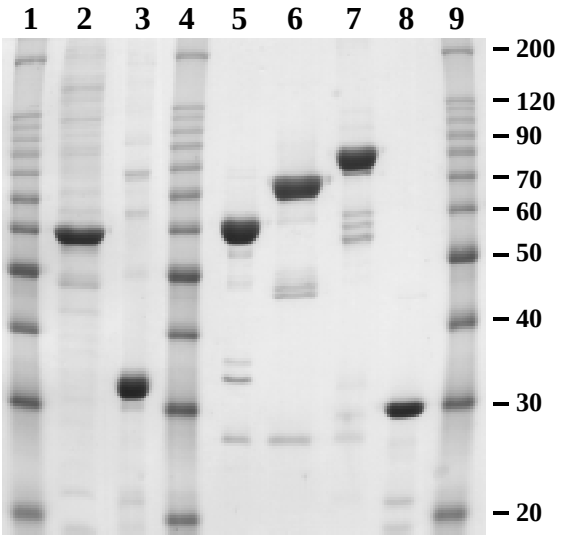

Figure 2.6. Purification of HsMKLP-1 proteins from insect and bacterial cells
Coomassie Blue-stained gel of HsMKLP-1 proteins purified from insect cells (lanes 2 and 3) and bacteria (lanes 5-8). $461\Delta_{bev}$ and $\Delta641_{bev}$ were purified from insect cells by metal affinity chromatography and the eluates from the column are shown in lanes 2 and 3, respectively. Trx-461Δ, Trx-524Δ, and Trx-619Δ were purified from bacterial cells by metal affinity chromatography, digested with thrombin to remove the N-terminal 127 AA tag, and further purified using ion-exchange chromatography, eluates of which are shown in lanes 5 (461Δ), 6 (524Δ), and 7 (619Δ). Several higher mobility bands generated by thrombin cleavage consistently co-purified with each protein and were estimated to represent 25-30% of protein preparations. Δ641 was purified from bacterial cell lysates using ion-exchange chromatography (lane 8). Locations of molecular mass markers (lanes 1, 4 and 9) are indicated. The calculated molecular mass of HsMKLP-1 proteins based on amino acid sequence are 55,637 ($461\Delta_{bev}$), 27,596 ($\Delta641_{bev}$), 55,752 (461Δ), 64,586 (524Δ), 74,359 (619Δ) and 24,502 (Δ641).

Expression of HsMKLP-1 proteins in bacteria

Although HsMKLP-1 proteins were successfully expressed in insect cells, the baculovirus expression system did not yield the expected expression levels and yields after purification sufficient for in depth *in vitro* characterization of these proteins (Table 2.1). In addition, because of issues surrounding the solubility of expressed proteins (notably $\Delta 411_{bev}$), the high cost associated with maintaining Sf9 cultures, limitations associated with scaling up of cell cultures for large scale expression, and the amount of time required for expression of proteins, an alternate system for expressing HsMKLP-1 proteins was sought. Prior to initiation of the baculovirus expression system, expression of HsMKLP-1 proteins was tested in the BL21(DE3)pLys bacterial expression strain and poor expression of HsMKLP-1 proteins was attributed to differences in codon usage between human and bacterial proteins. To test this hypothesis, expression of HsMKLP-1 proteins was tested in the codon-optimized BL21-CodonPlus-RIL bacterial strain. BL21-CodonPlus-RIL cells are engineered to express additional copies of tRNAs that recognize the arginine codons AGA and AGG, the isoleucine codon AUA, and the leucine codon CUA that have been shown to limit the translation of proteins derived from AT-rich genomes. HsMKLP-1 constructs Trx-461Δ, Trx-Δ641, and Trx-Δ411 were all highly expressed in this cell line (Table 2.2). Additionally, sequences encoding HsMKLP-1 AA 1- 524 (Trx-524), 1-619 (Trx-619), and full-length HsMKLP-1 (Trx-MKLP-1) cloned into the pET32a vector as fusions to thioredoxin were highly expressed as well (Table 2.2). To determine the effect of the thioredoxin tag on the expression of HsMKLP-1 proteins, sequences encoding full-length HsMKLP-1, 461Δ, Δ641, and Δ411 were cloned into the pET21d vector for expression without the thioredoxin tag. While Δ641 and Δ411 were expressed at comparable levels with and without the thioredoxin fusion partner, expression of full-length and 461Δ was dramatically reduced in comparison to expression of Trx-MKLP-1 and Trx-461Δ (Table 2.2). Because expression of full-length HsMKLP-1 and 461Δ was minimal in comparison to Trx-MKLP-1 and Trx-461Δ, these constructs were not pursued further.

To examine the solubility of HsMKLP-1 proteins expressed in BL21-CodonPlus-RIL cells, cells were lysed in Tris buffer containing 100 mM NaCl and separated into soluble (supernatant) and insoluble (pellet) fractions by centrifugation (Table 2.2). Some of the Trx-461Δ, Trx-521Δ, Trx-619Δ, Trx-Δ641, and Δ641 protein was present in the soluble fraction after centrifugation, although in each case the majority of expressed protein remained associated with the pellet fraction. In contrast, Δ411, Trx-Δ411, and Trx-MKLP-1 were not detected in the supernatant fraction after centrifugation, although Trx-MKLP-1, as well as Trx-619Δ, could be

Table 2.1. Summary of expression, solubility, and purification of HsMKLP-1 proteins from insect cells[1]

Construct	Expression	Solubility	Yield from purification
$461\Delta_{bev}$	+/-	+	0.3 μg/ml
$\Delta411_{bev}$	++	-	ND
$\Delta641_{bev}$	+	+	3.75 μg/ml

[1]Expression is designated as - (no expression detectable), +/- (protein detectable by immunoblot), + (protein visible by SDS-PAGE), or ++ (protein represents the major band in cell lysates visible by SDS-PAGE). Solubility is designated as either soluble (+) or not (-) based on cell fractionation studies. Yield is expressed per ml of cell culture.

Table 2.2. Summary of expression, solubility, and purification of HsMKLP-1 proteins from BL21-CodonPlus bacterial cells[1]

Plasmid	Construct	Expression	Solubility	Yield from purification
p21d-MKLP-1	MKLP-1	+/-	ND	ND
p32a-MKLP-1	Trx-MKLP-1	+	-[2]	ND
p21d-461Δ	461Δ	-	ND	ND
p32a-461Δ	Trx-461Δ	++	+	17 μg/ml
p32a-524Δ	Trx-524Δ	++	+	4.6 μg/ml
p32a-619Δ	Trx-619Δ	++	+	5 μg/ml
p21d-Δ641	Δ641	++	+	1.2 μg/ml
p32a-Δ641	Trx-Δ641	++	+	8 μg/ml
p21d-Δ411	Δ411	++	-	ND
p32a-Δ411	Trx-Δ411	++	-	ND

[1]See Table 2.1 legend for explanation of symbols. Solubility is based on cell fractionation under standard conditions (Tris buffer, 100 mM NaCl). [2]Trx-MKLP-1 was not soluble under standard conditions, but could be extracted from the insoluble fraction using 0.5 M NaCl.

partially extracted from the pellet fraction with buffer containing 0.5 M NaCl. HsMKLP-1 proteins present in the soluble fraction could be purified by metal-affinity chromatography (Trx-461Δ, Trx-521Δ, Trx-619Δ, Trx-Δ641) or by ion-exchange chromatography (Δ641, Fig. 2.6, lane 8) in the absence of the 6-histidine tag. To avoid potential interference of the thioredoxin tag with the activity of the HsMKLP-1 proteins, the thioredoxin fusion protein was removed from Trx-461Δ, Trx-521Δ, and Trx-619Δ by thrombin digestion and the proteins were further purified by ion-exchange chromatography (Fig. 2.6, lanes 5-7). Purity of these proteins was estimated to be 74% (461Δ), 71% (524Δ), 70% (619Δ), and 73% (Δ641) based on densitometry of Coomassie-blue stained protein gels.

Discussion:

The goal of this work was to develop a reproducible, heterologous protein expression system for expressing and purifying HsMKLP-1 proteins in order to characterize the structural and functional domains of HsMKLP-1. In this regard, a bacterial protein expression system has several advantages over eukaryotic systems. Enzymatic characterization of KLPs requires milligram quantities of protein and bacterial expression systems are cheaper and easier to scale-up for large scale expression and purification. Relative to baculovirus-based expression systems, proteins can be expressed in hours rather than days and without the need for viruses. Purification of proteins from *E. coli* is straightforward and not complicated by partitioning of proteins in subcellular compartments. In addition, expressing and purifying bacterially-expressed kinesin proteins is now standard with the majority of kinesin research being performed with bacterially-synthesized proteins. For these reasons, expression of HsMKLP-1 proteins was initially tested in a standard T7 promoter-based bacterial-expression strain (BL21(DE3)pLys). Poor expression of HsMKLP-1 proteins in this strain is most likely due to differences in codon use between bacterial and human proteins, since high levels of expression were obtained in a mammalian codon-optimized expression strain (BL21-CodonPlus-RIL). A comparison of the frequency of codon use between *H. sapiens* and *E. coli* proteins shows that there are 16 codons represented in *E. coli* proteins at frequencies less than 60% of the frequency observed in *H. sapiens* proteins (Table 2.3). Also included in Table 2.3 is the frequency of each codon within the HsMKLP-1 cDNA sequence. In particular, a dramatic difference in codon use is seen with arginine codons AGA and AGG (frequencies of ~2-3 in *E. coli* proteins compared to ~11 in human proteins). BL21-CodonPlus-RIL cells contain additional copies of tRNAs recognizing these arginine codons as well as tRNAs that recognize the isoleucine codon AUA, and the leucine codon CUA. Although these codons represent ~5% of the total number of codons for HsMKLP-1, the tRNAs

Table 2.3. Comparison of codon frequency in *H. sapiens* and *E. coli* for select codons and frequency in HsMKLP-1 cDNA sequence[1]

Codon	Frequency in *H. sapiens*	Frequency in *E. coli*	Number in HsMKLP-1
AUA (Ile)*	7.2	5.6	10
CUA (Leu)*	7	4	8
AGA (Arg)*	11.5	2.8	22
AGG (Arg)*	11.3	1.7	7
CGA (Arg)	6.3	3.5	15
CGG (Arg)	11.6	5.4	4
CUC (Leu)	19.3	10.3	6
UCC (Ser)	17.5	9.1	7
CCU (Pro)	17.3	7.2	16
CCC (Pro)	20.0	5.1	10
CCA (Pro)	16.7	8.6	19
ACA (Thr)	14.9	8.2	15
AAG (Lys)	32.6	11.5	28
GAG (Glu)	40.2	18.2	29
UGU (Cys)	10	5.1	11
UGC (Cys)	12.3	6.2	3
GGA (Gly)	16.4	8.7	16

[1]Frequencies of codon usage (per thousand) were obtained from http://www.kazusa.or.jp/codon/. Codons listed in Table 2.3 are represented in *E. coli* proteins at frequencies <60% of the frequency the codons are represented in proteins from *H. sapiens*. *BL21-CodonPlus-RIL cells contain additional copies of tRNAs recognizing these codons.

recognizing these codons could becoming limiting during high expression. The greater expression of HsMKLP-1 proteins in insect cells relative to expression in BL21(DE3)pLys S cells may also stem from similar codon use in insect and human proteins (O'Reilly et al., 1994).

N-terminal (461Δ, 461Δ_{bev}) and C-terminal (Δ411, Δ411$_{bev}$, Δ641, Δ641$_{bev}$) constructs of HsMKLP-1 were expressed in both insect and bacterial cells. Although highly expressed in both cell types, Δ411$_{bev}$/Δ411 was totally insoluble and could not be purified from either insect or bacterial cells, which suggests that the behavior of Δ411$_{bev}$/Δ411 is specific to this construct rather than the expression host (Tables 2.1 and 2.2). Full-length HsMKLP-1 expressed in bacteria as a thioredoxin fusion was expressed at much lower levels than Δ411, and although present in the insoluble fraction after cell lysis, could be partially extracted with 0.5 M NaCl (Table 2.2). This suggests that the insolubility of Δ411 may be due to improper folding and aggregation of Δ411 induced by high expression levels. In contrast, both 461Δ/461Δ_{bev} and Δ641/Δ641$_{bev}$ were extracted from insect and bacterial cells under relatively mild conditions and could be purified using metal affinity and/or ion exchange chromatography (Tables 2.2 and 2.3, Fig. 2.6). Although Δ411 and Δ641 were expressed equally well in bacteria with and without the thioredoxin tag, neither 461Δ or full-length HsMKLP-1 were appreciably expressed in the absence of an N-terminal tag (Table 2.2). This suggests that N-terminal sequences of HsMKLP-1 are not optimal for protein expression in bacteria. Expression of HsMKLP-1 proteins with minimal additional sequences is advantageous, and although Δ641 could be expressed and purified without additional sequences (Table 2.2), proteins expressed as thioredoxin fusions could be liberated from thioredoxin by digestion with thrombin protease as demonstrated for Trx-461Δ, Trx-524Δ, and Trx-619Δ (Fig. 2.6). Future work will address the structural and functional properties of these bacterially-expressed HsMKLP-1 proteins.

CHAPTER 3: GENERATION OF ANTIBODIES AGAINST THE MITOTIC KINESIN-LIKE PROTEIN-1

Introduction:

Kinesin-like proteins (KLPs) constitute a large and diverse group of proteins with functions ranging from vesicle and organelle transport to force generation during mitosis and cytokinesis (Greene et al., 1996). Conventional kinesin was first identified as a microtubule (MT) dependent translocator in squid axons (Vale et al., 1985a), and subsequently purified and characterized from bovine brain as a heterotetramer ($\alpha_2\beta_2$), consisting of two motor subunits (heavy chains) and two non-motor subunits (light chains) (Kuznetsov and Gelfand, 1986). Since then, the majority of KLPs have been identified using molecular and genetic approaches and studied using bacterially-expressed proteins. Because only a few KLPs have been purified from native sources and characterized to any extent (Cole et al., 1994; DeLuca et al., 2001; Kashina et al., 1996), it is not clear how the activity of recombinant KLPs compares to that of the native protein. For example, different KLPs may have associated subunits, modifications, or unique structures essential to their function *in vivo*.

An invaluable tool in probing the function of KLPs *in vivo* and in characterizing the activities of native motors is antibodies that recognize specific KLPs. Unlike conventional kinesin, which is highly enriched in neuronal tissue, most KLPs are present at low concentrations and this often limits their detection in cellular extracts by nonimmunological methods. Second, most cells contain a plethora of KLPs, which are not easily distinguished by their biochemical properties (ATPase activity, MT-binding), but can be studied individually using specific antibodies. Third, antibodies have been used to examine the subcellular localization of KLPs (Bowser and Reddy, 1997; Hatsumi and Endow, 1992; Henson et al., 1995; Kuriyama et al., 1995; Liu et al., 1996; Liu and Palevitz, 1996; Nislow et al., 1992; Wordeman and Mitchison, 1995; Yen et al., 1991), which is often suggestive of their function. Fourth, microinjection of antibodies (Nislow et al., 1990; Rogers et al., 2000; Vos et al., 2000) and immunodepletion of KLPs from cell extracts (Boleti et al., 1996; Vernos et al., 1995; Walczak et al., 1996; Walczak et al., 1997; Wein et al., 1996) have offered insight into the roles of KLPs in organisms not amenable to genetic knock-outs. Finally, selective purification of antibody-bound KLPs from native sources has been used to confirm interactions between KLPs and specific proteins (Adams et al., 1998; Lee et al., 1995).

HsMKLP-1 is a member of the MKLP-1 family of KLPs, whose members localize to the mitotic spindle interzone during anaphase and midbody during telophase where they are thought to participate in the bundling and organization of spindle MTs (Adams et al., 1998; Nislow et al., 1992; Nislow et al., 1990; Powers et al., 1998; Raich et al., 1998). Although a role for the MKLP-1 family in mitosis and cytokinesis has been clearly demonstrated, limited biochemical characterization of MKLP-1 family members has precluded the development of a detailed model for MKLP-1 function. The observation that recombinant HsMKLP-1 is able to bundle and slide MTs *in vitro* (Nislow et al., 1992) suggests that it is capable of crosslinking individual MTs, a property that is shared by members of the BimC family. Relative to the other KLP families, members of the BimC family have a unique structure, consisting of 4 motor subunits (homotetramer) assembled into a bipolar structure with motor domains at opposite ends of the protein (Kashina et al., 1996). As illustrated by the BimC family as well as other KLP families, the structural organization of KLPs may reflect specialization for specific functions. The structural organization of the MKLP-1 family is not known; although the molecular mass of full-length CHO1 expressed in insect cells is consistent with a dimer, HsMKLP-1 extracted from HeLa cells has a molecular mass (362 kDa) larger than expected for a dimer (200 kDa), suggesting the presence of additional subunits (Kuriyama et al., 1994). However, this work is complicated by the fact that the molecular mass of HsMKLP-1 was determined from cell extracts rather than purified protein, and may not reflect the molecular mass of the native protein.

In addition to providing information about subunit composition and structural organization, purification of HsMKLP-1 would allow a detailed characterization of the motor properties of the native protein. Recombinant HsMKLP-1 did not support MT translocation in a standard MT gliding assay, although it was demonstrated to bundle and slide MTs *in vitro* at a rate of 4 μm/min (Nislow et al., 1992). The motility of native HsMKLP-1 has not been examined, and it is not clear whether the motility of the recombinant protein is representative of the native protein. Factors that may affect the motility of the native protein include regulatory non-motor subunits and/or post-translational modifications. MKLP-1 family members have been shown to interact with several proteins including the mitotic kinases polo-like kinase (Adams et al., 1998; Lee et al., 1995) and the aurora/Ipl1p-related kinase Air2 (Severson et al., 2000), which suggests that MKLP-1 may be a target of protein kinases *in vivo*. In support of this hypothesis, HsMKLP-1 was phosphorylated by polo-like kinase *in vitro* (Lee et al., 1995), although it is not known whether MKLP-1 is phosphorylated *in vivo*. In addition to regulating the motor activity of HsMKLP-1, phosphorylation may serve to regulate the mitotic localization of HsMKLP-1, as has been demonstrated for the BimC family member Eg5 (Blangy et al., 1995;

Sawin and Mitchison, 1995), and/or the interaction of HsMKLP-1 with cellular components *in vivo*.

Here I report the generation and characterization of MKLP-1 specific polyclonal antibodies. These antibodies were able to specifically recognize native HsMKLP-1 using a variety of approaches including immunoblotting, immunoprecipitation, and immunofluorescence, which suggests they will be useful for characterizing the structural and functional properties of native HsMKLP-1. Specifically, these antibodies could be used to: 1) compare the motility and MT-binding activity of native HsMKLP-1 with that of recombinant HsMKLP-1 proteins, and 2) facilitate purification of HsMKLP-1 from HeLa cells in order to address the subunit composition and phosphorylation status of native HsMKLP-1. In support of this, these antibodies were used to monitor the fractionation of HsMKLP-1 in HeLa cell extracts and throughout several chromatography procedures designed to evaluate strategies for purification of native HsMKLP-1.

Materials and Methods:

Generation and purification of MKLP-1 antibodies

Baculovirus-expressed C-terminal peptides of HsMKLP-1 ($\Delta641_{bev}$ and $\Delta411_{bev}$) were sent to Cocalico Biologicals, Inc (CBI, Reamstown, PA) for immunization of rabbits. $\Delta641_{bev}$ was purified from insect cells as detailed in Chapter 2 and 1 mg was used to immunize 2 rabbits (VP116 and VP117). Because $\Delta411_{bev}$ was not soluble from insect cells, the band corresponding to this peptide was excised from a Coomassie-blue stained SDS-PAGE gel of nuclear pellets from $\Delta411_{bev}$ expressing insect cells (detailed in Chapter 2) and used to immunize one rabbit (VP115). Serum from immunized rabbits was obtained following CBI's standard antibody protocol. IgG was purified from serum using a HiTrap rProtein A column (Pharmacia Biotech). Serum was supplemented with 1 M Tris-HCl pH 8.0 to 100 mM and clarified by centrifugation at 20,000 xg for 15 minutes at 4°C before application to the column. The column was washed with 100 mM Tris-HCl pH 8.0 and IgG was eluted from the column with 100 mM glycine pH 3.0 and immediately neutralized with $1/10^{th}$ volume 1 M Tris-HCl pH 8.0. Fractions were pooled, supplemented with sodium azide to 0.02%, and stored at -20°C.

Western blotting

HeLa cells arrested in mitosis by treatment with 0.15 ug/ml nocodazole for 26 hours or insect cells infected with recombinant baculoviruses (Chapter 2) expressing $461\Delta_{bev}$, $\Delta411_{bev}$, and $\Delta641_{bev}$ (MOI=0.1, harvested at 72 hours) were lysed in sample buffer (0.125 M Tris-Cl, pH 6.8,

4% SDS, 20% glycerol, 10% β-mercaptoethanol), and proteins were resolved by SDS-PAGE and transferred to nitrocellulose. Western blotting was performed using preimmune, anti-$\Delta 641_{bev}$ or anti-$\Delta 411_{bev}$ serum at a 1:2000 dilution and HRP-conjugated 2° antibodies (Pierce) at a 1:50,000 dilution. Western blots were developed by enhanced chemiluminescence (ECL) using Super Signal Ultra chemiluminescent substrate (Pierce).

Immunoprecipitation from HeLa cells

HeLa cells arrested in mitosis as described above were lysed in 20 mM Tris-HCl pH 8.0, 150 mM NaCl, 0.5% NP-40, 5 mM EDTA, and 1.5 mM EDTA supplemented with Complete Protease Inhibitor (Boehringer Mannaheim) for 20 minutes on ice. Cell lysates were spun at 20,000 xg for 20 minutes at 4°C and the resulting supernatant was spun at 100,000 xg for 20 minutes at 4°C. The supernatant following the high speed spin was removed and 200 µl was supplemented with 2.4 µg of VP116 or preimmune IgG for one hour at 4°C. Protein A sepharose (40 µl of a 50% slurry washed extensively in dilution buffer: 10 mM Tris-HCl pH 8.0, 150 mM NaCl, 0.1% Triton X-100, 0.025% sodium azide) was added and the incubation continued for 1 hour. Immunocomplexes were washed twice with dilution buffer supplemented with 0.5 mM MgATP, followed by washes in 10 mM Tris-HCl pH 8.0, 150 mM NaCl, 0.025% sodium azide, and 0.5 mM MgATP, and 50 mM Tris-HCl pH 6.8 plus 0.5 mM MgATP. Proteins bound to protein A beads were eluted by boiling in 20 µl of sample buffer, resolved by SDS-PAGE, and transferred to nitrocellulose. Western blotting was performed as described above using anti-$\Delta 641_{bev}$ antibody (VP116).

Immunofluorescence of HeLa cells

HeLa cells grown on glass coverslips were fixed in methanol (10 minutes at -20°C) and processed for immunofluorescence essentially as described in Spector et al. (1998). In order to better visualize spindle localization by reducing the pool of cytoplasmic HsMKLP-1, in some experiments cells were extracted in 100 mM PIPES pH 6.9, 2 mM EGTA, 1 mM $MgSO_4$, and 0.5% Triton-X for 30 seconds prior to fixation. After fixation, all manipulations were performed at 22°C. Briefly, cells were blocked in 10% BSA in PBS (137 mM NaCl, 2.7 mM KCl, 4.3 mM Na_2HPO_4, 1.4 mM KH_2PO_4) for 10 minutes and incubated with VP116 IgG (1:200) followed by DM1α (1:500, Sigma) for one hour. Coverslips were washed extensively in PBS supplemented with 0.1% Tween-20 and incubated with Oregon Green conjugated anti-rabbit and Texas Red conjugated anti-mouse secondary antibodies (10 µg/ml, Molecular Probes) plus 1 µg/ml DAPI for 30 minutes. Coverslips were washed as before, mounted on glass slides, and observed using

a Nikon Microphot SA microscope equipped with an appropriate multipass dichroic mirror/barrier filter and filter-wheel mounted excitation filters.

Fractionation of HeLa cells

HeLa cells were fractionated essentially as described by Miyamoto et al. (1985) (Chapter 2). Briefly, cells were swelled in hypotonic buffer (10 mM Tris-HCl, pH 7.5, 10 mM NaCl, 1.5 mM $MgCl_2$) supplemented with protease inhibitors for 30 minutes on ice and lysed by Dounce homogenization after addition of 0.5% NP-40. Nuclei were pelleted (1,000 xg, 10 minutes) and incubated in hypotonic buffer containing 1% NP-40 and 0.5% deoxycholate for 30 minutes on ice. Stripped nuclei were pelleted as above, lysed in 50 mM Tris-HCl pH 7.5 containing 0.1% SDS, 1% Triton X-100, 1% deoxycholate, and 0.15 M NaCl, and then spun at 13,000 xg. Supernatant and pellet fractions were resuspended in sample buffer, separated using SDS-PAGE, and transferred to nitrocellulose. Western blotting was performed as described above using anti-$\Delta 641_{bev}$ antibody (VP116).

Partial purification of HsMKLP-1 from HeLa cells

Nocodazole-arrested HeLa cells were obtained from the National Cell Culture Center. Cells (~20 g) were resuspended in 20 mls AB buffer (20 mM PIPES, pH 6.9, 1 mM $MgCl_2$, 1 mM DTT) plus protease inhibitors and 0.1 mM MgATP and lysed by sonication (5 x 10 s) on ice. The lysate was spun at 20,000 xg for 15 minutes at 4˚C and the resulting supernatant was additionally clarified at 100,000 xg for 15 minutes before loading on a HiTrap SP column previously equilibrated in AB buffer plus 0.1 mM MgATP. Fractions containing HsMKLP-1 were identified by Western blotting using VP116 antibodies as described above. To concentrate fractions containing HsMKLP-1, eluates from the HiTrap SP column were diluted 3-fold with AB buffer to lower the NaCl concentration to ~0.1 M, passed over a 1 ml S-Sepharose column, and eluted with 5 mls of AB buffer containing 0.5 M NaCl and ATP. This eluate was loaded on a S-300 Sephacryl column equilibrated in AB buffer plus 0.1 M NaCl and ATP. HsMKLP-1 containing fractions were pooled and loaded on a HiTrap Q column equilibrated as described above for the HiTrap SP column. HsMKLP-1 was eluted from the column with 0.2-0.3 M NaCl.

Results:

Generation and characterization of MKLP-1 antibodies

In order to produce MKLP-1 specific antibodies, polyclonal antibodies were generated against the unique C-terminus of HsMKLP-1 using baculovirus-expressed proteins encoding AA 411-856 ($\Delta 411_{bev}$) and 641-856 ($\Delta 641_{bev}$) of HsMKLP-1 (Chapter 2). These proteins encompass

the stalk and tail ($\Delta411_{bev}$) and tail ($\Delta641_{bev}$) domains of HsMKLP-1, which have little sequence homology with KLPs outside of the MKLP-1 family. Antibodies were generated against both $\Delta411_{bev}$ and $\Delta641_{bev}$ in order to account for any possible differences in antigenicity. Anti-$\Delta411_{bev}$ (VP115) and anti-$\Delta641_{bev}$ (VP116 and VP117) antibodies recognized both $\Delta411_{bev}$ and $\Delta641_{bev}$ on immunoblots, but did not recognize $461\Delta_{bev}$, which encompasses the N-terminal motor domain of HsMKLP-1 (Fig. 3.1). VP116 and VP117 also recognized a ~80 kDa protein present in cell lysates prepared from the *Spodoptera frugiperda* insect cell line (Fig. 3.1, VP116; faint bands can be seen on VP117 blot), which may represent a *S. frugiperda* homolog of MKLP-1. MKLP-1 has been identified from *Drosophila melanogaster*, although the molecular mass of DmMKLP-1 is ~100 kDa (Adams et al., 1998; Schmid and Tautz, 1998). The immunoreactivity of VP115 was much lower than VP116 and VP117 (exposure times for blots in Fig. 3.1 are not equivalent; VP115 blot was exposed 4-fold longer than VP116 and VP117 blots). It is not clear why VP115 exhibited lower immunoreactivity, although it may relate to differences in how the antigens were prepared ($\Delta411_{bev}$ was excised from an SDS-PAGE gel while $\Delta641_{bev}$ was purified in solution). In comparison to VP117, VP116 exhibited greater reactivity on immunoblots and this antibody was chosen for further analysis.

VP116 recognized a protein at ~100 kDa in lysates of unsynchronized HeLa cells (Fig. 3.4, Lys), which is close to the predicted molecular mass of HsMKLP-1 (98 kDa) and consistent with previous reports that have identified proteins at ~100 kDa (Nislow et al., 1992) and ~115/100 kDa (Nislow et al., 1990) in HeLa cell lysates. In lysates of nocodazole-arrested HeLa cells, VP116 recognized a protein with a slightly higher molecular mass (~110 kDa) on immunoblots, with an additional faint band observed at 95 kDa (Fig. 3.2a). In addition, a ~110 kDa protein was immunoprecipitated from mitotic HeLa cell lysates using VP116, but not preimmune antibodies (Fig. 3.2b).

Immunolocalization of HsMKLP-1 in HeLa cells using VP116 was nearly identical to the previously reported localization of MKLP-1 in PtK1 cells (Nislow et al., 1992). In interphase cells, VP116 staining colocalized with nuclei (Fig. 3.3, top row), although the intensity of nuclear staining was variable from cell to cell, suggesting that HsMKLP-1 protein levels are not constant throughout the cell cycle. In metaphase cells, a large pool of HsMKLP-1 was present in the cytoplasm (Fig. 3.3, metaphase, second row) with additional localization to spindle fibers that is more clearly seen in cells extracted with Triton-X prior to fixation (metaphase extracted, third row). In contrast to a previous report (Nislow et al., 1992), no staining was observed at spindle poles during metaphase. In metaphase as well as early anaphase (Fig. 3.3, early

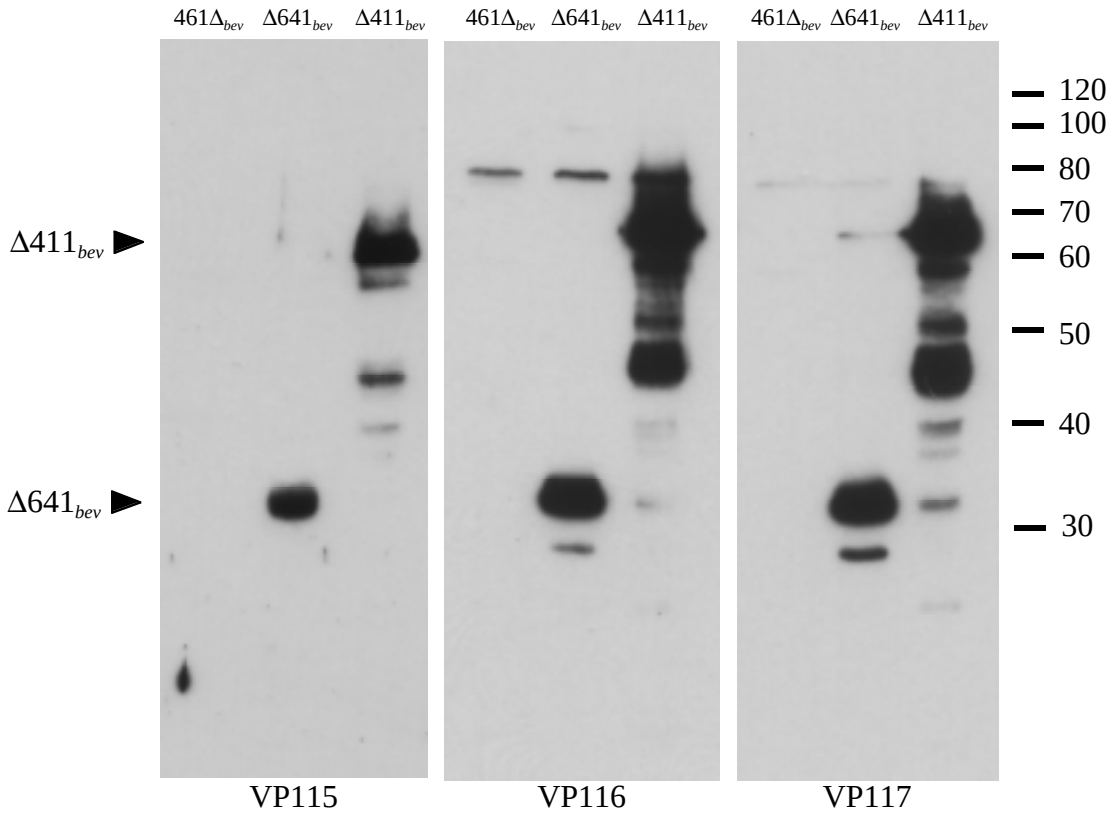

Figure 3.1. Western blots of Sf9 cell lysates expressing $461\Delta_{bev}$, $\Delta641_{bev}$, and $\Delta411_{bev}$ probed with VP115, VP116, and VP117 antiserum. VP115 was generated against HsMKLP-1 AA's 411-856 ($\Delta411_{bev}$), while VP116 and VP117 were generated against HsMKLP-1 AA's 641-856 ($\Delta641_{bev}$). The locations of $\Delta411_{bev}$, $\Delta641_{bev}$, and MW markers are indicated. Blots were developed using ECL and exposed for 1 minute (VP115) or 15 seconds (VP116 and VP117) to autoradiography film.

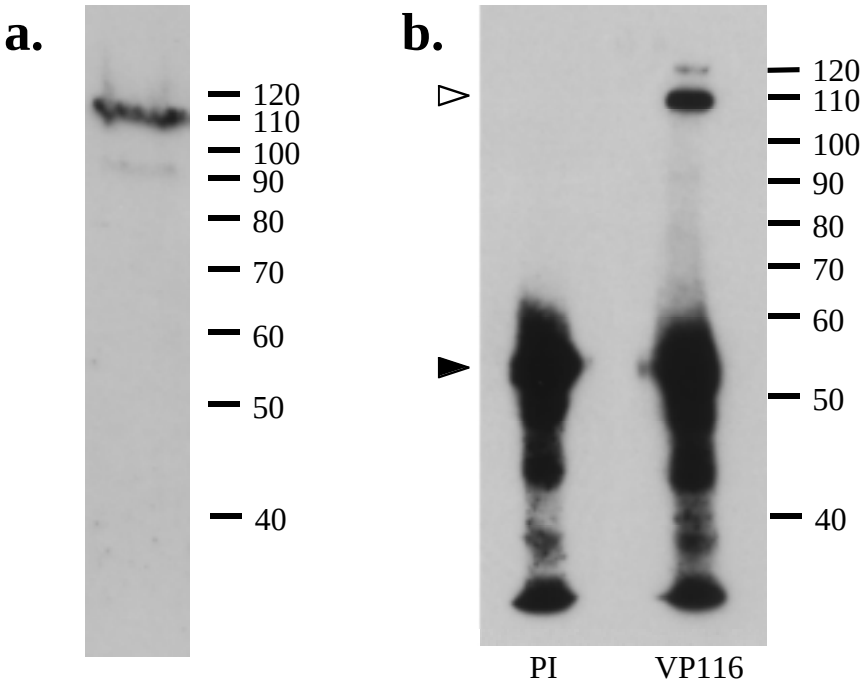

Figure 3.2. Western blot of mitotic HeLa cell lysate probed with VP116 antibodies and immunoprecipitation of HsMKLP-1 from mitotic HeLa lysates. a) Western blot of mitotic HeLa cell lysate probed with VP116 antibodies. VP116 recognizes a major protein at ~110 kDa with a minor band additionally observed at ~95 kDa. Molecular mass markers (kDa) are indicated. b) Immunoprecipitation of HsMKLP-1 from mitotic HeLa lysates using pre-immune (PI) or VP116 antibodies. Immunoprecipitates were analyzed by Western blotting using VP116 antibodies. Locations of IgG (filled arrowhead) and HsMKLP-1 (open arrowhead) are indicated.

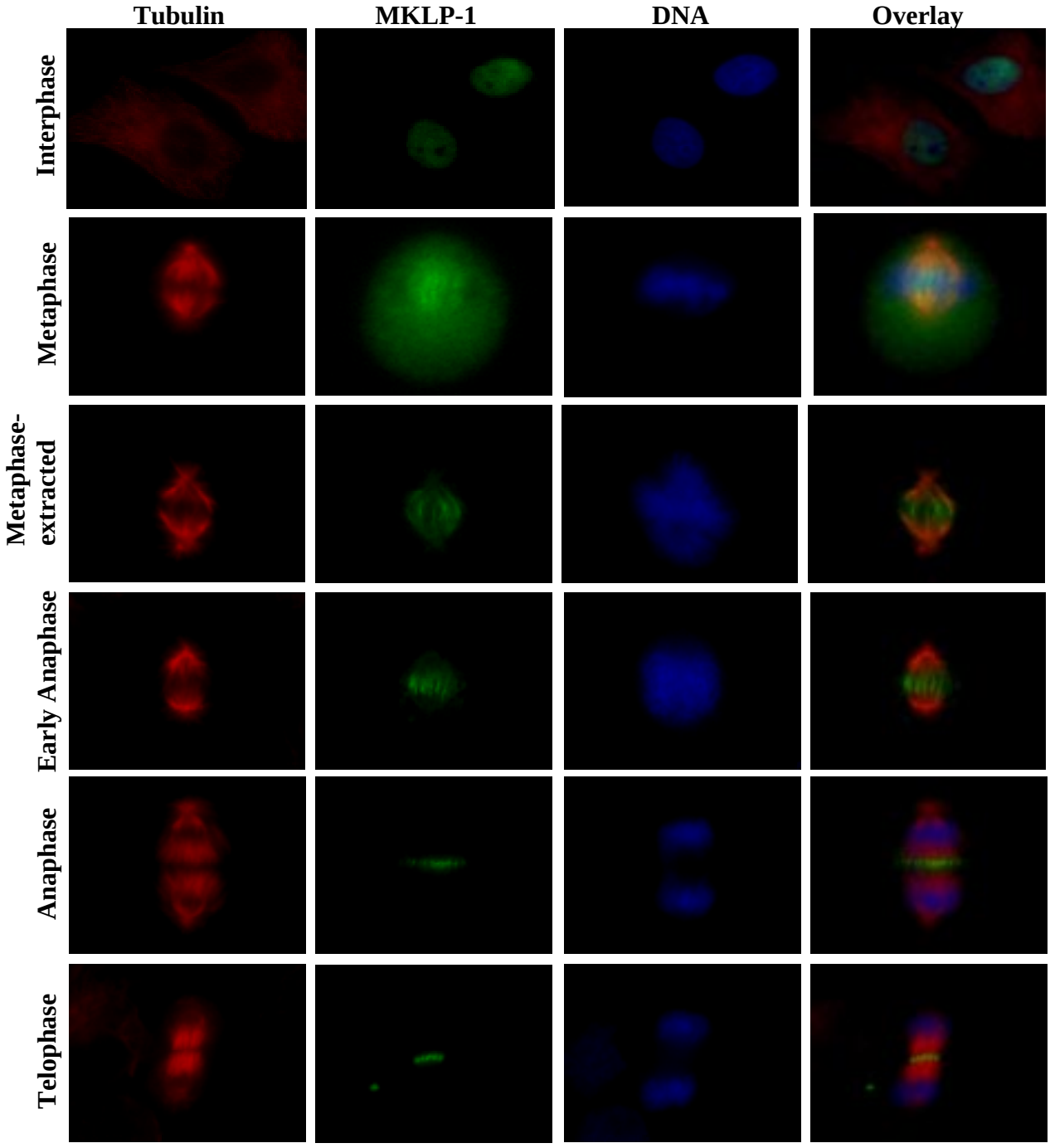
Tubulin
MKLP-1
DNA
Overlay
Interphase
Metaphase
Metaphase-extracted
Early Anaphase
Anaphase
Telophase

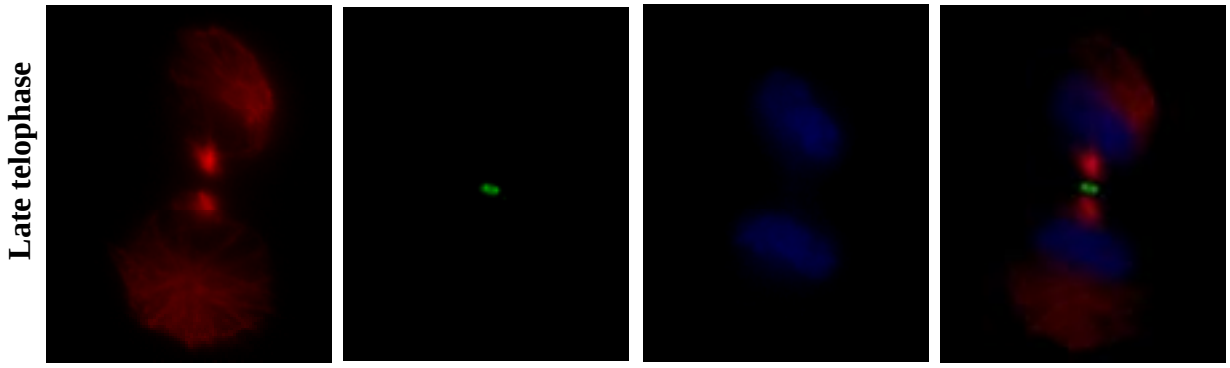

Figure 3.3. Immunolocalization of HsMKLP-1 in HeLa cells. HeLa cells were stained with VP116, a monoclonal antibody to α-tubulin, and DAPI to visualize the DNA. Representative images of cells at the indicated stages of the cell cycle are shown. Metaphase extracted cells (third row) were extracted prior to fixation to remove the cytoplasmic pool of HsMKLP-1 in order to better observe spindle localization.

anaphase), VP116 staining was concentrated at the spindle interzone where it formed a discrete band during late anaphase (Fig. 3.3, anaphase). In telophase, VP116 staining was localized to the midbody with no cytoplasmic staining evident (Fig. 3.3, telophase, late telophase). No staining was observed under these conditions when preimmune antibodies were used in place of VP116.

Fractionation and partial purification of HsMKLP-1 from HeLa cells

As suggested by the localization of HsMKLP-1 to interphase nuclei, HsMKLP-1 fractionated in a manner consistent with nuclear localization in HeLa cells (Fig. 3.4). HeLa cells were lysed in hypotonic buffer (Fig. 3.4, Lys) and isolated nuclei were treated with NP-40/deoxycholate to remove the outer membrane and associated proteins (Fig. 3.4, S1). Stripped nuclei were then lysed using a combination of salt and both ionic and non-ionic detergents and fractionated to produce a nuclear extract (Fig. 3.4, S3). Western blotting indicates that HsMKLP-1 fractionates solely with the nuclear extract (S3). No protein was detectable in the cytoplasmic fraction (S1), detergent-extracted fraction of nuclei (S2), or final pellet after nuclear lysis (P).

In order to evaluate purification strategies for native HsMKLP-1, the fractionation of HsMKLP-1 in clarified mitotic extracts was examined using ion-exchange and gel filtration chromatography. During the course of each chromatographic step, HsMKLP-1 was followed by immunoblot using VP116 antibodies. Mitotic HeLa cells were chosen as starting material for purification because HsMKLP-1 is suggested to be enriched in mitotic cells relative to interphase cells (Fig. 3.3 and (Ohta et al., 1996)) and because HsMKLP-1 was found to be readily soluble in extracts of mitotic HeLa cells. HsMKLP-1 bound to both S-Sepharose and Q-Sepharose, which allowed HsMKLP-1 to be fractionated away from the majority of HeLa cell proteins. However, following ion-exchange and gel filtration chromatography, HsMKLP-1 represented a minor protein component within HsMKLP-1 containing fractions only visible by immunoblot, suggesting that the abundance of HsMKLP-1 in mitotic cells is low and insufficient for purification at the current scale (starting with 10 L of HeLa cell culture).

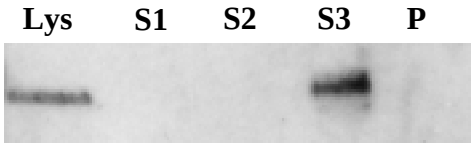

Figure 3.4. Nuclear fractionation of HsMKLP-1 in HeLa cells

HeLa cells were fractionated into cytoplasmic (S1) and nuclear fractions following hypotonic lysis (Lys). The nuclear pellet was treated with NP-40 and deoxycholate to release associated membranes and proteins and separated into supernatant (S2) and pellet fractions following centrifugation. The pellet fraction (stripped nuclei) was resuspended in buffer containing SDS, deoxycholate, Triton X-100 and NaCl and fractionated into supernatant (S3) and pellet (P) fractions following centrifugation. Fractions were analyzed by Western blotting using VP116 antibodies as described in Materials and Methods. VP116 recognized a single band at ~100 kDa and only the relevant portion of the immunoblot is shown.

Discussion:

The goal of this work was to produce MKLP-1 specific antibodies to be used as a tool for characterizing native HsMKLP-1. Of the three polyclonal antibodies generated, VP116 exhibited greater immunoreactivity against HsMKLP-1 proteins on immunoblots and was therefore chosen for additional characterization. Several factors suggest that VP116 is specific for MKLP-1 family members. First, VP116 is generated against the C-terminal tail domain of HsMKLP-1 (AA 641-856), which does not exhibit any obvious homology to proteins outside of the MKLP-1 family of KLPs. Second, VP116 did not recognize the N-terminal motor domain of HsMKLP-1, which shares significant (30-40%) homology to other KLPs, suggesting that VP116 is not likely to cross-react with other KLPs. Third, the immunolocalization pattern of VP116 in HeLa cells (Fig. 3.3) is virtually identical to the previously reported localization of MKLP-1 in PtK1 cells (Nislow et al., 1992) and similar to localization patterns of other MKLP-1 family members (Adams et al., 1998; Powers et al., 1998; Raich et al., 1998; Sellitto and Kuriyama, 1988).

VP116 recognized a single band of ~100 kDa in lysates of unsynchronized HeLa cells, which is similar to the predicted MW of HsMKLP-1 (98 kDa). In mitotic HeLa cells, VP116 recognized proteins at ~110 and 95 kDa (Fig. 3.2a). The nature of this doublet is not known, but is likely to represent alternative or post-translationally modified forms of HsMKLP-1 rather than non-specific cross-reactivity of VP116, since a doublet with similar MW (~115/100 kDa) was previously observed in immunoblots of HeLa cell fractions using a monoclonal MKLP-1 antibody (Nislow et al., 1990). In addition, the 110 and 95 kDa proteins co-fractionated in mitotic HeLa cell extracts (data not shown), which suggests they share similar biochemical properties. MKLP-1 family members have been shown to functionally interact with polo-like kinase (Adams et al., 1998; Lee et al., 1995) as well as the aurora/Ipl1p-related kinase Air2 (Severson et al., 2000), which suggests that HsMKLP-1 may be phosphorylated *in vivo*.

MKLP-1 specific antibodies will be required for characterization of native HsMKLP-1 due to the low abundance of HsMKLP-1 in HeLa cells as well as the sheer number of other KLPs present in humans. Immunoblotting of HeLa cell fractions with VP116 allowed HsMKLP-1 to be followed through fractionation and chromatography procedures designed to evaluate strategies for purification of native HsMKLP-1. Using a similar approach but on a larger scale (starting with 70 L of HeLa cell culture), DeLuca et al. (2001) have developed a purification strategy for KLPs from HeLa cells and have been able to partially purify HsMKLP-1 using VP116 antibodies to monitor fractionation. Future purification of HsMKLP-1 by these methods

will allow the motility, MT-binding, and ATPase activity of the native protein to be compared with bacterially-expressed MKLP-1 and the number of subunits to be determined.

CHAPTER 4: ATPASE AND MICROTUBULE BINDING OF THE MKLP-1 MOTOR DOMAIN

Introduction:

Kinesin-like proteins (KLPs) convert the energy from ATP hydrolysis into unidirectional movement along microtubule (MT) filaments and thereby generate force to transport cellular "cargo" such as organelles or orchestrate events during cell division. The majority of the 250+ KLPs identified to date can be classified into nine families based on their degree of sequence homology and location of the conserved motor domain within the polypeptide (N-terminal, internal, or C-terminal) (Greene et al., 1996; Kim and Endow, 2000). A model for how KLPs operate is beginning to emerge based on extensive biochemical, biophysical, and structural analyses of selected KLPs such as conventional kinesin, Ncd, and more recently, Kif1A and Eg5. Crystal structures of kinesin motor domains from members of the KHC (Kozielski et al., 1997; Kull et al., 1996; Sack et al., 1997), C-terminal (Gulick et al., 1998; Sablin et al., 1998; Sablin et al., 1996), Unc104/KIF1 (Kikkawa et al., 2000), and BimC (Turner et al., 2001) families have been solved. The degree of structural and biochemical similarity between the individual motor domains of kinesin family members suggests that all kinesins share a similar catalytic core and that unique subfamily characteristics are specified primarily by sequences outside of the catalytic core. For example, differences in the structure of the neck linker region immediately adjacent to the catalytic core of conventional kinesin and the minus-end directed Ncd direct these proteins in opposite directions along MTs and suggest why kinesin, but not Ncd, is capable of processive movement (Case et al., 1997; Endow and Waligora, 1998; Henningsen and Schliwa, 1997; Sablin et al., 1998). Structural differences between kinesin family members are likely the result of specific adaptations that functionally distinguish the different kinesin families from one another.

Since almost all of the present knowledge of how motors operate is derived from work on only four of the nine KLP families, it is still unclear how closely members of the other five families conform to the current models of KLP force generation. One of these five families, the MKLP-1 family, is distinguished by two specific features within its motor domain that differentiate it from kinesin and other KLPs, and that may be important for the function of the MKLP-1 family (Greene et al., 1996). The first distinguishing feature is the MKLP-1 neck linker sequence (HsMKLP-1 sequence: QEVEVARPVD), which is highly conserved among family members but bears little resemblance to the neck linkers of other plus-end directed KLPs (consensus: K/RxIxNxxxV/IN) (Vale and Fletterick, 1997). The second distinguishing feature of

the MKLP-1 motor domain is the presence of a conserved ~64 AA insertion (HsMKLP-1 residues 152-215) in the motor catalytic core that interrupts the sequence corresponding to Loop 6 in the kinesin motor domain structure (Kull et al., 1996). It is not obvious what effect an insertion in Loop 6 would have on MKLP-1 function, although the position, size, and degree of conservation of this insert among family members suggests that it may influence the structure, function, and/or regulation of the MKLP-1 motor domain. Together, the unique MKLP-1 neck linker sequence and Loop 6 insertion may confer novel motile properties to this family related to their roles in mitosis and cytokinesis.

MKLP-1 family members operate within anti-parallel MT arrays in the mitotic spindle (Nislow et al., 1992), where they are suggested to contribute to central spindle organization (Adams et al., 1998; Powers et al., 1998; Raich et al., 1998). Consistent with the idea that motors operating within MT arrays may have evolved distinct properties from motors involved in transport along stationary MT tracks, MKLP-1 exhibits several unique characteristics that functionally distinguish it from kinesin. Previous work suggested that MT-binding of human MKLP-1 (HsMKLP-1) and CHO1 from *C. griseus* is insensitive to ATP (Kuriyama et al., 1994; Nislow et al., 1992; Nislow et al., 1990). In particular, ATP had a modest effect on the fraction of full-length and N-terminal CHO1 proteins that pelleted with MTs (Kuriyama et al., 1994). In addition, ATP was not sufficient to release HsMKLP-1 from MTs in the absence of NaCl (Nislow et al., 1992). In a standard MT gliding assay, no motility was observed for HsMKLP-1, although HsMKLP-1 was demonstrated to bundle and slide MTs past each other at a rate of 4 μm/min (Nislow et al., 1992). Expression of the motor domain of CHO1 in insect cells also resulted in the formation of highly organized MT bundles (Sharp et al., 1996a). The ability to bundle and slide MTs may be an important feature of the MKLP-1 family related to its role in spindle organization.

In order to further define the interaction of the MKLP-1 motor domain with MTs, we have chosen to determine the MT-binding and steady state kinetic properties of recombinant monomeric and dimeric motor domain constructs of HsMKLP-1. Monomeric and dimeric HsMKLP-1 exhibited nucleotide-sensitive MT-binding and MT-stimulated ATPase activity as expected for a KLP, although the concentration of ATP required for half-maximal ATPase activity (K_{mATP}) is ~2-20 fold higher than values reported for similar kinesin and KLP constructs, suggesting that the affinity of MKLP-1 for ATP is relatively weak. Consistent with MT-binding studies of other KLPs, MT binding was greatest in the absence of nucleotide and in the presence of the ATP analog AMP-PNP, followed by ATP and ADP. Binding of the monomer and dimer

was similar in the absence of nucleotide or in the presence of AMP-PNP, although the dimer bound MTs with greater affinity than the monomer in the presence of ADP and ATP. Furthermore, in the presence of ATP, the dimer exhibited tight binding to MTs at NaCl concentrations sufficient to disrupt the binding of the monomer, suggesting the presence of additional sequences in the dimer that contribute to MT-binding. This work supports the idea that overall, the MKLP-1 motor domain operates in a similar fashion to other KLPs with respect to MT-binding and ATP hydrolysis, but that MKLP-1 exhibits enhanced MT-binding of the dimer and weaker affinity for ATP that functionally distinguishes it from other kinesin family members. Differences in the catalytic core and neck linker sequence of MKLP-1 may confer unique properties to the MKLP-1 motor domain, which relate to its role in MT organization and sliding within the MT spindle.

Materials and Methods

Preparation of HsMKLP-1 proteins

HsMKLP-1 proteins 461Δ, 524Δ, 619Δ, and Δ641 were prepared as described in Chapter 2. Protein concentrations measured by Bradford assay (Bradford, 1976) were corrected for impurities by densitometry of Coomassie-blue stained protein gels. Protein concentrations are expressed as the concentration of motor domains. Attempts to measure active site concentration by titration with the fluorescent ATP analog methylanthraniloyl-ATP (mant-ATP) (Sadhu and Taylor, 1992) or by incubation with [α-^{32}P]ATP followed by gel filtration chromatography (Gilbert and Mackey, 2000) were unsuccessful due to the low signal to noise ratio, which may reflect weak binding of ATP. Active site concentration was, therefore, estimated by saturation of MT binding.

MW determination

Monomer molecular weight was calculated directly from the protein sequence. Stokes radius (R_s) was determined by FPLC on a Superose 6 gel filtration column. The column was equilibrated and run with AB containing 200 mM NaCl and 0.02% Tween-20. Proteins of known Stokes radius (carbonic anhydrase, ovalbumin, BSA, alcohol dehydrogenase, β-amylase, catalase, apoferritin, thyroglobulin) were run as standards. Sedimentation coefficient ($s_{20,w}$) was determined by rate zonal centrifugation on 5-20% linear sucrose gradients in AB with catalase, BSA, and ovalbumin as standards. No difference in the sedimentation coefficient for 619Δ was observed for gradients run in the presence of 125 mM NaCl. The native molecular weight was calculated from: $M= (6\pi\eta N R_s s_{20,w})/(1-\upsilon\rho)$ where $\upsilon= 0.72$ cm^3/g and the frictional coefficient was calculated from: $f/f_0 = R_s/(3M\upsilon/4\pi N)^{1/3}$ (Siegel and Monty, 1966).

Microtubule binding assays

Tubulin was purified as previously described (Walker et al., 1988). MTs were polymerized from tubulin at 37˚C in the presence of GTP, stabilized with taxol, pelleted, and resuspended in AB buffer plus 10% sucrose and taxol to remove excess GTP. Reactions (50 µl final volume) containing 1 µM 461Δ or 619Δ and 2.0 µM tubulin (as taxol-stabilized MTs) were carried out in AB buffer plus 10% sucrose, 10 µM taxol (Calbiochem), and 5 mM nucleotide or 0.1 mU apyrase (Sigma). The final NaCl concentration was 25 mM (461Δ) or 75 mM (619Δ) unless otherwise indicated. In MgADP•Pi reactions, 5 mM MgADP and 15 mM sodium phosphate pH 6.9 were added and the concentration of NaCl was adjusted to compensate for the increase in ionic strength. Ionic strength was calculated from $I=0.5\sum c_i Z_i^2$, where c_i is the molar concentration and Z_i is the charge of each ionic species. To examine the effect of NaCl on 461Δ binding to MTs, reactions were performed with 2 µM 461Δ and 2.5 µM tubulin. Fractional binding of 461Δ and 619Δ to MTs was performed with 1 µM motor and reactions were supplemented with 0.1 mg/ml BSA (461Δ) or ovalbumin (619Δ) and 10-50 µM taxol. After 15 minutes at 22°C, reactions were centrifuged in a Beckman TLA-45 rotor at 40,000 rpm for 15 minutes (25°C) and supernatant and pellet fractions were run on 7.5% (619Δ) or 9% (461Δ) SDS-polyacrylamide gels and stained with Coomassie blue. Serial dilution of identical binding reactions were used as standards. The amount of motor protein in each fraction was determined by densitometry of scanned SDS-polyacrylamide gels using an AlphaImager 2000 gel documentation system. The amount of 461Δ in the pellet fraction of MT-binding reactions could not be accurately quantified at high tubulin concentrations due to its similarity in molecular mass to tubulin, therefore the amount of 461Δ in the pellet fraction was determined by subtracting the amount of 461Δ in the supernatant fraction from the total concentration of 461Δ. The calculated fraction of motor protein in the pellet was plotted relative to tubulin concentration and data were fit to either a hyperbola or the quadratic equation (Mackey and Gilbert, 2000) to obtain values for K_d and fractional binding.

Determination of ATPase activity

For determination of K_{mATP} and $K_{0.5MT}$, steady state ATPase assays were performed in AB buffer supplemented with 20 µM taxol using a coupled pyruvate kinase-lactate dehydrogenase assay as previously described (Deavours et al., 1998) with 0.01-6 mM MgATP and 0.1-15 µM (tubulin concentration) taxol-stabilized, GTP-depleted MTs prepared as described above. For determination of K_{mATP} the tubulin concentration was 2.5 µM. For the determination of $K_{0.5MT}$ the

concentration of MgATP was 5 mM. In reactions with less than 1 mM MgATP, NaCl was added to 50 mM; at higher MgATP concentrations the amount of NaCl added was adjusted to compensate for the increase of ionic strength with increasing MgATP concentrations. Ionic strength was calculated as described above taking into consideration the concentrations of Mg^{2+}, SO_4^{2-}, and ATP. To determine the effect of ionic strength on $K_{0.5MT}$, reactions were supplemented with 65 mM NaCl. To obtain values for K_{mATP} and $K_{0.5MT}$, data were fit to rectangular hyperbolae using Kaleidograph. The basal ATPase rate was measured at 25°C in AB buffer using 5'-γ-^{32}P ATP as previously described (Deavours et al., 1998).

Results:

Expression, purification, and characterization of N-terminal constructs of HsMKLP-1

In order to identify structural and functional domains of HsMKLP-1, N-terminal constructs extending to AA 461, 524, and 619 of HsMKLP-1 were expressed in *E. coli* as C-terminal fusions to thioredoxin (Fig. 4.1a). All of these constructs encompass the putative catalytic core of HsMKLP-1 (AA 1-422) that shares homology with the core motor domain of kinesin as well as sequences adjacent to the catalytic core. In addition, the longest construct (Trx-619Δ) contains sequences having a high probability of forming coiled-coils (see Fig. 4.1 legend). The expressed proteins also contained a 6 histidine tag which allowed the proteins to be purified from induced cell lysates using metal-affinity chromatography. To avoid potential interference of the N-terminal 127 AA tag with the activity of the motor domain of HsMKLP-1, the thioredoxin tag was removed by thrombin digestion and the proteins were further purified by ion-exchange chromatography. Figure 4.1b shows a Coomassie-blue stained gel of the purified N-terminal proteins hereafter designated as 461Δ, 524Δ, and 619Δ.

Sucrose density gradient centrifugation and gel filtration chromatography were used to determine the native molecular mass of the N-terminal constructs (Table 4.1). The ratio of the native molecular mass with that predicted based on the amino acid composition of each construct indicate that 461Δ and 524Δ exist as monomers. In comparison, the calculated molecular mass of 619Δ is 3-fold greater (221,173) than the predicted molecular mass (74,359). Although this suggests that 619Δ exists as a higher order oligomer, previous characterization of HsMKLP-1 and CHO1 demonstrate that these proteins exist as dimers (Kuriyama et al., 1994), and preliminary cross-linking experiments with 619Δ (data not shown) support the assignment of 619Δ as a dimer. The region from AA 524-619, which mediates dimerization of 619Δ, spans the region identified from PAIRCOIL analysis as having a high propensity of forming coiled coils (AA 537-617) (Berger et al., 1995). In addition, a C-terminal construct of HsMKLP-1 (AA 641-

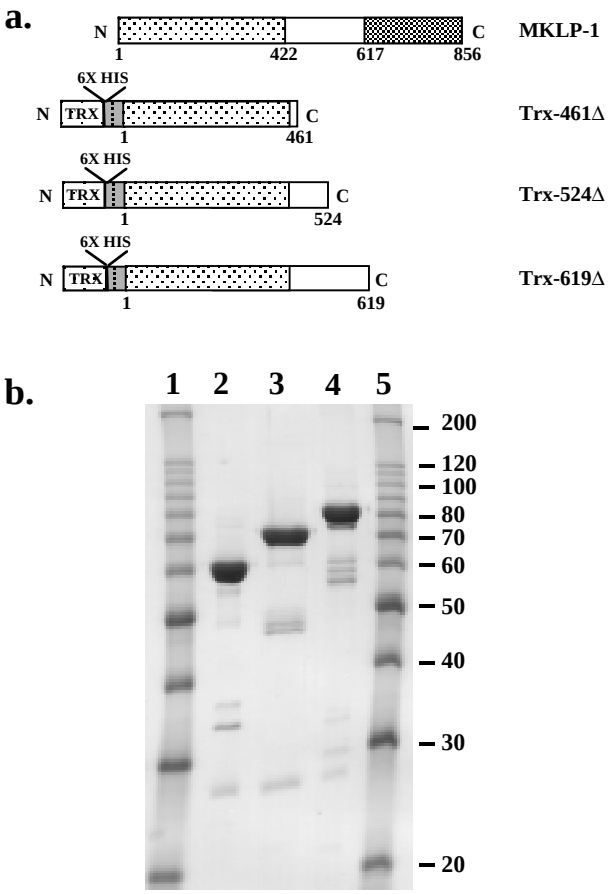

Figure 4.1. Full-length HsMKLP-1 and HsMKLP-1 constructs expressed in bacterial cells. a.) Schematic representation of HsMKLP-1 and HsMKLP-1 constructs. The motor domain of HsMKLP-1 which shares sequence similarity to the motor domain of kinesin is shown as a stippled box. The stalk domain, which includes sequences predicted to form coiled coils by the program PAIRCOILS (Berger et al., 1995) (http://nightingale.lcs.mit.edu/cgi-bin/score) (AA's 537-617) is in white. The 239 AA tail domain is shown in gray. Constructs encoding HsMKLP-1 AA 1-461 (Trx-461Δ), 1-524 (Trx-524Δ), and 1-619 (Trx-619Δ) were expressed as C-terminal fusions to thioredoxin (TRX) and a 56 residue linker containing a 6-Histidine (6X HIS) tag. The thrombin protease cleavage site is 30 AA N-terminal to the start codon of HsMKLP-1 and is indicated by the dashed line. b.) Coomassie Blue-stained gel of HsMKLP-1 proteins purified from bacterial cells. 461Δ (lane 2), 524Δ (lane 3), and 619Δ (lane 4) were purified from bacterial cells by metal affinity chromatography, digested with thrombin to remove the N-terminal 127 AA tag, and further purified using ion-exchange chromatography. Several lower molecular mass bands generated by thrombin cleavage consistently co-purified with each protein and were

estimated to represent 25-30% of protein preparations based on densitometry of Coomassie-blue stained protein gels. The sizes of molecular mass markers (lanes 1 and 5) are indicated. The calculated molecular mass of HsMKLP-1 proteins based on their amino acid sequence are 55,752 (461Δ), 64,586 (524Δ), and 74,359 (619Δ).

Table 4.1. Physical properties of HsMKLP-1 proteins[1]

	461Δ	524Δ	619Δ	Δ641
Monomer molecular mass[2]:	55,752	64,586	74,359	24,502
Stokes Radius (Å):	38.51	44.79	75.74	44.68
$S_{20,w}$:	3.7	4.1	7.1	1.29
Calculated molecular mass:	57,970	75,529	221,173	23,706
Frictional Coefficient:	1.5	1.6	1.9	2.4
Oligomerization:	monomer	monomer	dimer	monomer

[1]Stokes radii were determined by gel filtration chromatography and sedimentation coefficients were determined by rate zonal centrifugation. The native molecular mass and frictional coefficient were calculated as described in Materials and Methods (Siegel and Monty, 1966).
[2]Monomer molecular mass was determined from the protein sequence and includes any AA's remaining after removal of the thioredoxin fusion partner from Trx-461Δ, Trx-524Δ, and Trx-619Δ.

856) is monomeric (Table 4.1), which suggests that coiled coil sequences do not extend into the C-terminal tail domain of HsMKLP-1. The calculated frictional coefficients increase with increasing length of the N-terminal constructs and indicate that 461Δ, 524Δ, and 619Δ have an extended conformation as has been observed for kinesin and other KLPs.

MT-binding activity of the HsMKLP-1 monomer and dimer

To examine the binding of the motor domain of HsMKLP-1 to MTs and to compare the binding of monomeric and dimeric species of HsMKLP-1, the binding of 461Δ and 619Δ to MTs was tested under different nucleotide conditions (Fig. 4.2). Although both 461Δ and 524Δ were demonstrated to be monomeric, we chose to characterize 461Δ because it more closely represented an individual motor domain of HsMKLP-1 based on homology with the kinesin motor domain (Fig. 4.1a). In the absence of MTs, 619Δ tended to aggregate at NaCl concentrations less than 75 mM and 619Δ binding reactions were therefore performed in 75 mM NaCl. The solubility of 461Δ was not affected by NaCl in the range of 0-500 mM; however, because MT binding was markedly reduced at 75 mM NaCl, 461Δ binding reactions were performed at 25 mM NaCl. Under these conditions, no observable pelleting of 461Δ and minimal pelleting of 619Δ was observed in the absence of MTs (Fig. 4.2) and solubility was not affected by any of the nucleotide conditions tested (not shown). While the majority of 619Δ pelleted with MTs in all nucleotide conditions tested, the majority of 461Δ was not bound to MTs in MgATP, MgADP, and MgADP•Pi. Relative to reactions with MgATP, binding of 461Δ to MTs was increased in the presence of a non-hydrolyzable analog of ATP (MgAMP-PNP) and in reactions in which all di- and tri- nucleotide phosphate was depleted with the enzyme apyrase (APY). The fraction of 461Δ that cosedimented with MTs under these conditions was increased both at higher motor concentrations and lower NaCl concentrations (Fig. 4.3a).

The fraction of 619Δ pelleting with MTs in the presence of MgATP, MgADP, and MgADP•Pi was not qualitatively different from the amount of 619Δ pelleting under conditions known to induce tight binding of KLPs to MTs (MgAMP-PNP and no nucleotide). To a lesser extent, the binding of 461Δ to MTs also did not appear solely dependent on MgATP (compare Fig. 4.2a ATP and AMP-PNP reactions). To understand better the relative contributions of nucleotide and ionic interactions to MT-binding, binding reactions were performed over a range of NaCl concentrations in the presence of MgATP or MgAMP-PNP (Fig. 4.3). MT-binding of both 461Δ and 619Δ was sensitive to ionic strength; as NaCl concentrations were increased the amount of motor pelleting with MTs decreased. Compared to the dimer, the MT-binding of 461Δ was more sensitive to NaCl; while ~125 mM NaCl was sufficient to disrupt the binding of

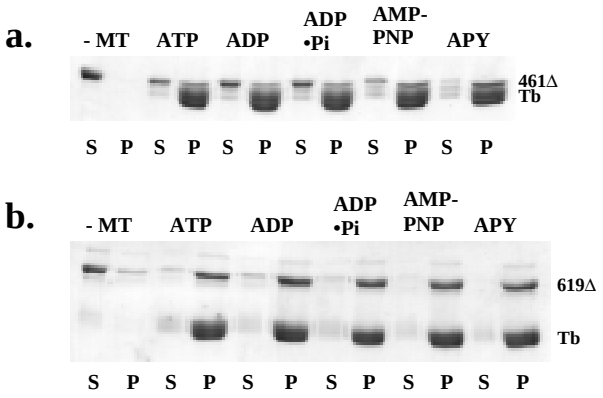

Figure 4.2. Effect of nucleotide on the MT binding properties of 461Δ and 619Δ
461Δ (a) or 619Δ (b) and taxol-stabilized MTs (2 μM tubulin) were incubated with 5 mM MgATP (ATP), MgADP (ADP), MgAMP-PNP (AMP-PNP) or 0.1 mU apyrase (APY). ADP•Pi reactions were supplemented with 5 mM MgADP and 15 mM sodium phosphate. Motor concentration was 1 μM. Reactions were centrifuged and the resulting supernatants (S) and pellets (P) from each as well as for motor alone (-MTs) were analyzed by SDS-PAGE and Coomassie blue staining. Locations of 461Δ, 619Δ and tubulin (Tb) are indicated.

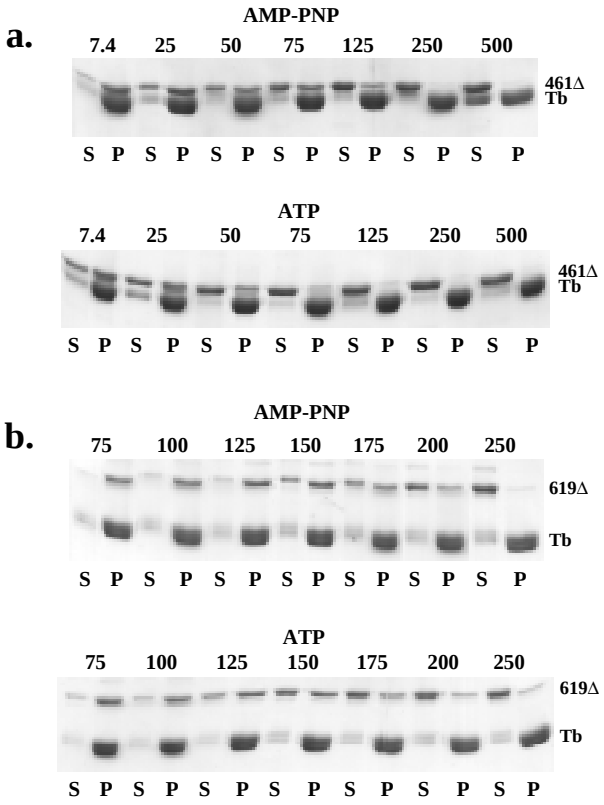

Figure 4.3. Effect of NaCl on the MT binding properties of 461Δ and 619Δ in the presence of MgATP and MgAMP-PNP

MT binding reactions with 461Δ (a) or 619Δ (b) were performed as described in Figure 4.2 with 5 mM MgAMP-PNP (top panels) or MgATP (lower panels) and 7.4-500 mM (461Δ) or 75-250 mM (619Δ) NaCl. In (a) the concentration of 461Δ and tubulin was 2 μM and 2.5 μM, respectively. In (b) the concentration of 619Δ and tubulin was 1 μM and 2 μM, respectively.

461Δ to MTs, ~200 mM NaCl was necessary to inhibit the MT binding of 619Δ. At each NaCl concentration, the fraction of motor pelleting in the presence of MgAMP-PNP was greater than the fraction pelleting in the presence of MgATP (compare Fig. 4.3a 75 mM reactions and Fig. 4.3b 125 mM reactions), suggesting that the MT-binding of 461Δ and 619Δ is at least partially sensitive to MgATP. Conditions sufficient to disrupt the majority of 461Δ binding to MTs (MgAMP-PNP + 125 mM NaCl, MgATP + 75 mM NaCl) did not affect the binding of 619Δ to MTs.

To further define the interaction between the MKLP-1 motor domain and MTs, the binding of 461Δ and 619Δ to MTs was quantified under four nucleotide conditions (MgADP, MgATP, MgAMP-PNP, and no nucleotide), which are representative of nucleotide intermediates in the ATPase cycle (Fig. 4.4 and 4.5, Tables 4.2 and 4.3). The binding of 461Δ and 619Δ to MTs was performed using a fixed concentration of motor (1 μM) with tubulin concentrations ranging from 0.05-50 μM (Fig. 4.4 and 4.5). In this assay, the binding of 461Δ and 619Δ to MTs approached 100% in all nucleotide conditions tested (fractional binding 0.92-1.07) suggesting that the proteins were fully active and stable (Tables 4.2 and 4.3). Binding of 619Δ was relatively tight under all nucleotide conditions with K_d values less than or close to 1 μM (Table 4.3). Binding was tightest in the absence of nucleotide followed by MgAMP-PNP, MgATP, and MgADP. The binding of 461Δ to MTs was weaker than 619Δ in the presence of MgATP and MgADP, however as observed for the dimer, the magnitude of 461Δ binding was greatest in the absence of nucleotide and with MgAMP-PNP followed by MgADP and MgATP. The binding of 461Δ to MTs was decreased ~2-fold in the presence of 50 mM NaCl as compared to binding at 25 mM NaCl (Fig. 4.4, Table 4.2). In the absence of NaCl, K_d values for 461Δ were less than or close to 1 μM in all nucleotide conditions and 461Δ binding stoichiometry approached one motor domain per tubulin dimer (data not shown).

MT-stimulated ATPase activity of the MKLP-1 monomer and dimer

To establish whether the motor domain of HsMKLP-1 is able to hydrolyze ATP, the steady state ATPase activity of 461Δ and 619Δ was determined as a function of MgATP and MT concentration (Fig. 4.6). 461Δ exhibited a low basal rate of ATP hydrolysis (0.02 s^{-1}) that was stimulated 1000–fold in the presence of MTs to a maximal rate of 20 s^{-1} (Table 4.4). The maximal rate of hydrolysis by the dimer was almost 3 times slower (7 s^{-1}), consistent with slower rates of ATP hydrolysis for kinesin dimers as compared to monomers (Huang et al., 1994; Jiang et al., 1997; Moyer et al., 1996). Tubulin was effective at stimulating the ATPase activity of 461Δ and 619Δ ($K_{0.5MT}$ was calculated to be 0.26 ± 0.02 μM and 0.39 ± 0.04 μM, respectively).

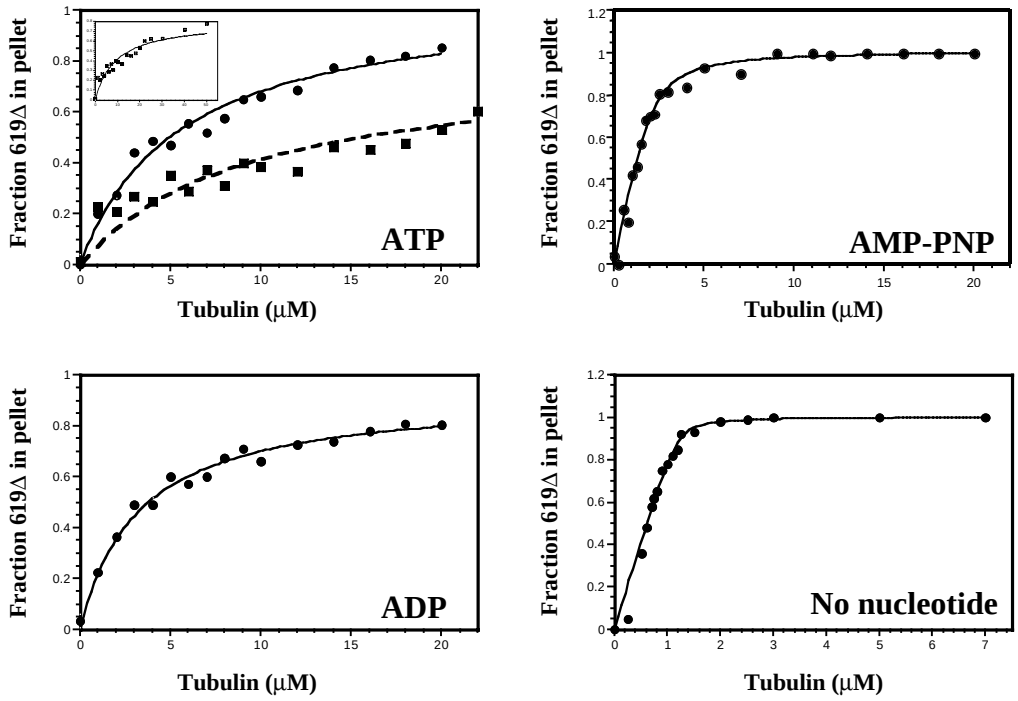

Figure 4.4. Binding isotherms for 461Δ in the presence of MgATP, MgADP, MgAMP-PNP or no nucleotide

MT-binding reactions were performed as described in Figure 4.2 with tubulin concentrations ranging from 0.25-50.0 μM. The concentration of 461Δ in the supernatant (unbound) fraction from MT-binding reactions was quantified from grayscale images of SDS-PAGE gels. The fraction of 461Δ in the pellet fraction (obtained by subtracting the amount of 461Δ in the supernatant fraction from the total concentration of 461Δ) was plotted relative to the tubulin concentration in each reaction and best fit to either a rectangular hyperbola (ATP and ADP) or the quadratic equation (no nucleotide, AMP-PNP) in order to obtain values for K_d and fractional binding (Table 4.2). Binding in the presence of MgATP was performed at 25 mM (circles) and 50 mM (squares) NaCl. For comparison, only the curve from 0-22 μM tubulin is shown for data collected at 50 mM NaCl, and the entire curve is shown in the inset.

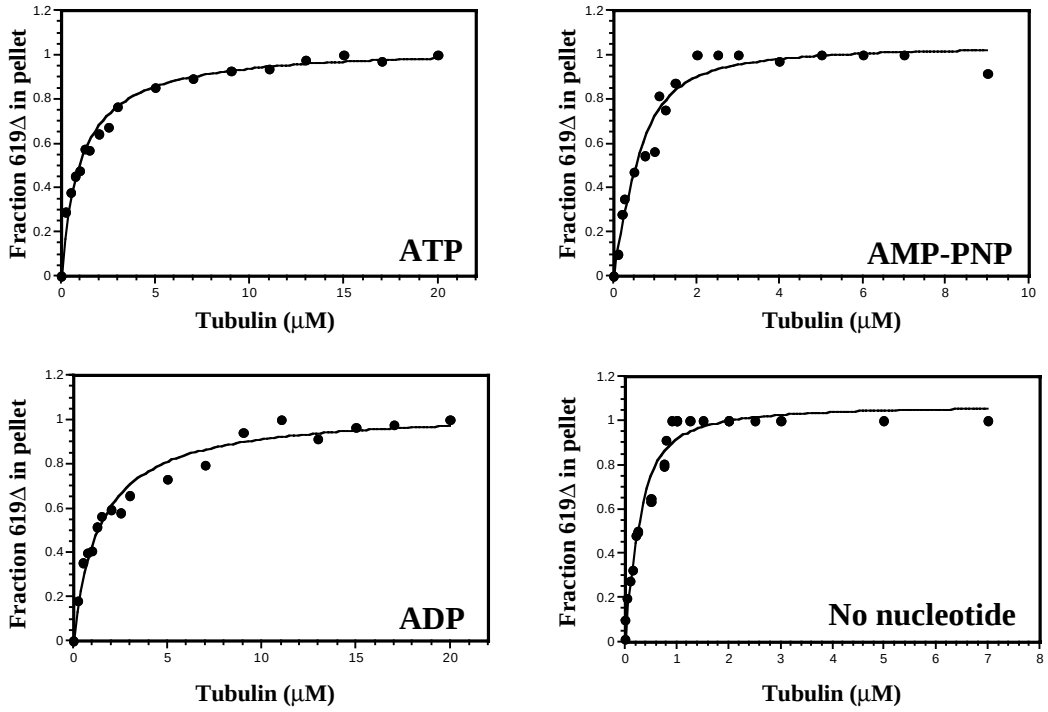

Figure 4.5. Binding isotherms for 619Δ in the presence of MgATP, MgADP, MgAMP-PNP or no nucleotide

MT-binding reactions with 619Δ (1 μM) were performed as described in Figure 4.4 with tubulin concentrations ranging from 0.05-20.0 μM. The concentration of 619Δ in the supernatant (unbound) and pellet (bound) fractions from MT-binding reactions was quantified from grayscale images of SDS-PAGE gels and the fraction of 619Δ in the pellet fraction was plotted as a function of tubulin concentration and best fit to either a rectangular hyperbola (ATP and ADP) or the quadratic equation (no nucleotide, AMP-PNP) in order to obtain values for K_d and fractional binding (Table 4.3).

Table 4.2. Effect of nucleotide on the affinity and fractional binding of 461Δ to MTs[1]

	NaCl (mM)	K_d (μM)	Fractional binding
no nucleotide[2]	25	0.02 ± 0.02	1.00 ± 0.02
MgAMP-PNP (5 mM)	25	0.27 ± 0.12	1.01 ± 0.02
MgADP (5 mM)	25	3.25 ± 0.36	0.92 ± 0.03
MgATP (5 mM)	25	5.52 ± 0.62	1.05 ± 0.04
MgATP (5 mM)	50	9.22 ± 1.87	0.80 ± .06

[1]The concentration of 461Δ in the supernatant (unbound) fraction from MT-binding reactions were fit to either a rectangular hyperbola (MgATP and MgADP) or the quadratic equation (no nucleotide, MgAMP-PNP) in order to obtain values for K_d and fractional binding. Reactions were performed with the indicated nucleotide and NaCl concentrations under constant 461Δ concentration (1.0 μM) with tubulin concentrations ranging from 0.25-50.0 μM. [2]Reactions performed in the absence of nucleotide were supplemented with 0.1 mU apyrase.

Table 4.3. Effect of nucleotide on the affinity and fractional binding of 619Δ to MTs[1]

	K_d (μM)	Fractional binding
no nucleotide	0.13 ± 0.05	1.07 ± 0.04
MgAMP-PNP (5 mM)	0.23 ± 0.14	1.05 ± 0.05
MgADP (5 mM)	1.44 ± 0.15	1.04 ± 0.03
MgATP (5 mM)	1.06 ± 0.08	1.04 ± 0.02

[1]The concentration of 619Δ in the supernatant (unbound) and pellet (bound) fractions from MT-binding reactions was fit to either a rectangular hyperbola (MgATP and MgADP) or the quadratic equation (no nucleotide, MgAMP-PNP) in order to obtain values for K_d and fractional binding. Reactions were performed in 75 mM NaCl under constant 619Δ concentration (1 μM) with tubulin concentrations ranging from 0.05-20.0 μM. Reactions were supplemented with the indicated nucleotide concentrations or 0.1 mU apyrase (no nucleotide).

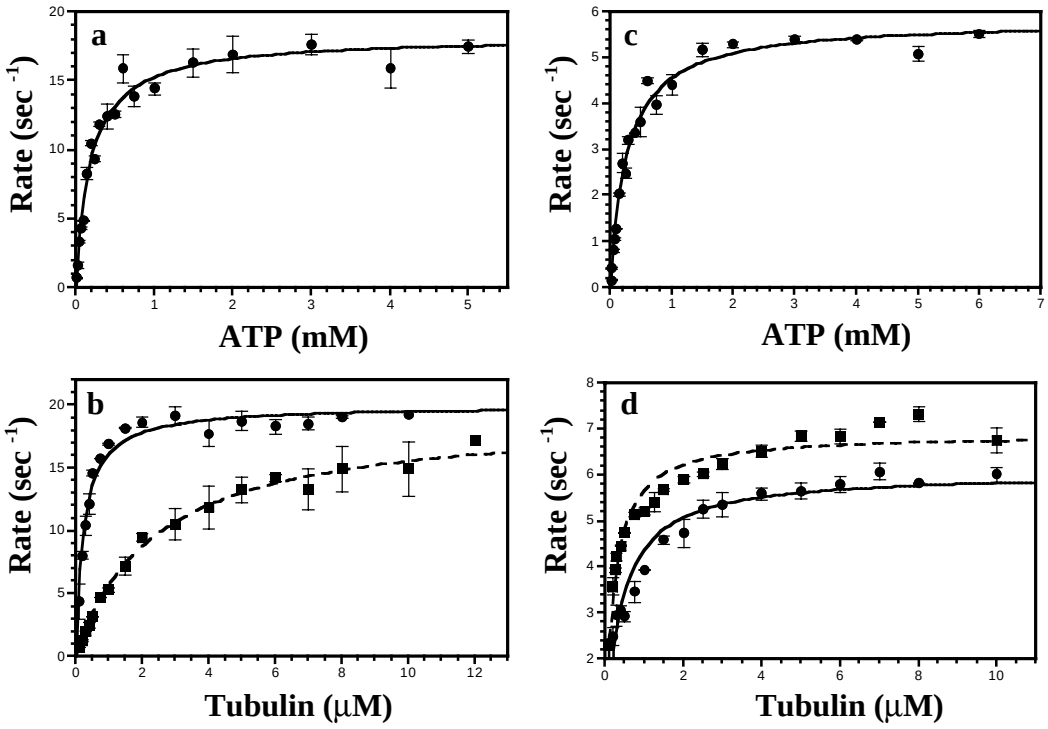

Figure 4.6. MT-stimulated ATPase rate of 461Δ and 619Δ

MT-stimulated ATPase activity of 461Δ (a, b) and 619Δ (c, d) were determined as a function of MgATP concentration (a, c) and tubulin concentration (b, d) using a coupled pyruvate kinase-lactate dehydrogenase assay. The final concentration of motor was 0.1 μM. For determination of K_{mATP} the tubulin concentration was 2.5 μM. For the determination of $K_{0.5MT}$ the concentration of MgATP was 5 mM. In (b) and (d) rates were measured in the presence of 0 mM (circles) and 65 mM (squares) NaCl. Rates were plotted as a function of MgATP or tubulin concentration and fit to rectangular hyperbolae in order to obtain values for k_{cat}, K_{mATP}, and $K_{0.5MT}$ (Table 4.4).

Table 4.4. Steady state rate constants of 461Δ and 619Δ[1]

	461Δ	619Δ
k_{cat}[2]	20.0 ± 0.29 s^{-1}	6.9 ± 0.09 s^{-1}
K_{mATP}	190 ± 20 μM	280 ± 20 μM
$K_{0.5MT}$	0.26 ± 0.02 μM	0.39 ± 0.04 μM
$K_{0.5MT}$ (65 mM)	2.41 ± 0.25 μM	0.22 ± 0.02 μM

[1]Steady state rates of ATP hydrolysis were determined using a pyruvate kinase-lactate dehydrogenase coupled assay as described in Fig. 4.6. [2]The maximal turnover rate, (k_{cat}) represents the maximal rate measured in the presence of 5 mM MgATP.

Assays performed at 65 mM NaCl resulted in a 10-fold increase in the value of $K_{0.5MT}$ for 461Δ (2.41 ± 0.25 μM) while the value of $K_{0.5MT}$ for the dimer was slightly decreased (0.22 ± 0.02 μM). This is consistent with the observation that the MT-binding of 461Δ but not 619Δ is sensitive to NaCl concentrations around 65 mM (Fig. 4.3). An increase in $K_{0.5MT}$ with increasing ionic strength has been documented for both kinesin and Ncd (Foster et al., 1998; Lockhart and A., 1994; Ma and Taylor, 1995b; Pechnatnikova and Taylor, 1997), although a decrease in $K_{0.5MT}$ at higher ionic strength was measured for a reported dimeric construct of Eg5 (Lockhart and Cross, 1996). The K_{mATP} for both 461Δ and 619Δ (0.19 ± 0.02 mM and 0.28 ± 0.02 mM, respectively) are much larger than values reported for other KLPs which suggests that a higher concentration of MgATP is required to maximally stimulate the ATPase activity of HsMKLP-1.

Discussion:

Previous work on HsMKLP-1 has demonstrated that the MT-binding properties of HsMKLP-1 are similar, yet distinguishable from those of kinesin. We have extended this characterization of HsMKLP-1 using purified recombinant N-terminal constructs of HsMKLP-1. HsMKLP-1 constructs extending to AA 524 are monomeric while a construct extending to AA 619 is dimeric (Table 4.1), suggesting that HsMKLP-1 remains monomeric for ~60% of its length. This is in contrast to members of the KHC and C-terminal kinesin families which are monomeric for only 25-30% of their total length. In addition, a C-terminal construct of HsMKLP-1 extending from AA 641-856 is monomeric as well, suggesting that sequences important in mediating dimerization span the region from 524-641, which is in close agreement to the coiled-coil domain predicted by PAIRCOIL analysis (AA 537-617). This region is much smaller than coiled-coil regions identified for other dimeric kinesin-like proteins (typically in the range from ~150-600 AA), but is expected to be sufficient for dimerization based on work with truncated kinesin proteins (Jiang et al., 1997).

Both monomeric (461Δ) and dimeric (619Δ) N-terminal constructs of HsMKLP-1 bound MTs in a MT-pelleting assay with greater binding observed in the absence of nucleotide or with MgAMP-PNP as compared to binding in the presence of MgATP, MgADP, and MgADP•Pi (Fig. 4.2, Tables 4.2 and 4.3). This is consistent with equilibrium binding studies of conventional kinesin, Ncd, and Eg5 constructs which demonstrate that ADP and ADP•Pi states are weak-binding and no nucleotide and ATP states are strong-binding (Crevel et al., 1996; Foster et al., 1998; Lockhart and Cross, 1996; Rosenfeld et al., 1996). In reactions containing 75 mM NaCl, 619Δ bound MTs tightly in all nucleotide conditions tested (K_d values less than or close to 1 μM), and although the binding of the monomer was not measured in the presence of 75

mM NaCl, the affinity of 461Δ for MTs at this ionic strength is expected to be low based on MT pelleting assays performed at 75 mM NaCl (Fig. 4.3a), the observed two-fold decrease in binding affinity in the presence of 50 mM NaCl versus 25 mM NaCl (Table 4.2), and the ~10-fold increase in $K_{0.5MT}$ at 65 mM NaCl (Table 4.4). Tight binding of 619Δ to MTs in the presence of MgATP may be explained by additional motor-MT interactions that serve to augment MT binding or by an uncoupling of MT-binding from ATP hydrolysis. Alternatively, tight binding of 619Δ may reflect continuous attachment of the dimer to the MT during processive movement, in which at least one motor domain of the dimer remains bound to the MT at any given time.

The observation that the binding of 619Δ to MTs is more dependent upon ionic than nucleotide-dependent contributions (Fig. 4.3) is consistent with previous work on the MT-binding properties of MKLP-1 family members. Similar to 619Δ, a baculovirus-expressed N-terminal construct of CHO1 cosedimented with MTs in both the presence and absence of ATP (Kuriyama et al., 1994). In addition, in the absence of NaCl, ATP was not sufficient to release native HsMKLP-1 from MTs, although HsMKLP-1 could be extracted from MTs in the presence of ATP + 100 mM NaCl or with 300 mM NaCl in the absence of ATP (Nislow et al., 1992). The majority of 619Δ remained bound to MTs at 100 mM NaCl in the presence of MgATP, although MgATP facilitated release of 619Δ from MTs at NaCl concentrations above 125 mM. Differences in ionic sensitivity of HsMKLP-1 and 619Δ are most likely due to the lower ionic strength buffer used for MT-binding of 619Δ. In the absence of MgATP, 200 mM NaCl was sufficient to disrupt binding of 619Δ to MTs (Fig. 4.3b). In addition, the MT-stimulated ATPase activity of 619Δ (V_{max}= 6 s^{-1}) is sufficient to account for the previously reported rate of MT-sliding by HsMKLP-1 (4 μm/min) (Nislow et al., 1992), and consistent with this previous report, no motility was observed for coverslip-adsorbed 461Δ, 619Δ, or thioredoxin-tagged full-length HsMKLP-1, although the proteins did bind MTs (data not shown). Relative to KHC and other plus-end directed KLPs, the divergent sequence of the MKLP-1 neck linker suggests that MKLP-1's mechanism of movement may differ from that proposed for plus-end directed KLPs.

In comparison to similar KLP constructs, a high concentration of MgATP was required for half-maximal ATPase activity. The K_{mATP} for the monomer and dimer were 190 and 280 μM, respectively, compared to ~25-100 uM for monomeric constructs of kinesin and Ncd (Mackey and Gilbert, 2000; Moyer et al., 1996; Pechnatnikova and Taylor, 1997), and 13-62 μM for dimeric constructs of kinesin, Ncd, and Eg5 (Foster et al., 1998; Gilbert et al., 1995; Lockhart and Cross, 1996; Pechatnikova and Taylor, 1999), suggesting that the affinity of HsMKLP-1 for ATP is weak. Weak ATP binding is not related to altered interactions with MTs since MTs

effectively stimulated the ATPase activity of both 461Δ and 619Δ ($K_{0.5MT}$ ~0.3-0.4 μM). Kinesin has been demonstrated to undergo an isomerization after ATP binding, which is suggested to correspond to conformational changes of the neck linker that serve to "lock" ATP in the nucleotide binding site (Rice et al., 1999; Schnitzer et al., 2000). The unique sequence of the MKLP-1 neck linker suggests that MKLP-1 force production may be different from other N-terminal KLPs, and may account for the weak binding of ATP. Unique features of the MKLP-1 motor domain may reflect specialization for organizing and sliding MTs within the mitotic spindle. A model for MKLP-1's mechanism of force generation awaits further characterization of the neck linker and structural determination of the MKLP-1 motor domain.

CHAPTER 5: IDENTIFICATION OF NUCLEAR LOCALIZATION DETERMINANTS OF THE MITOTIC KINESIN-LIKE PROTEIN-1

(Portions published as: Deavours, B.E. and Walker, R.A. (1999) *Biochem. Biophys. Res. Comm.* 260: 605-608.)

Introduction

Microtubules (MTs) and kinesin-like proteins (KLPs) orchestrate many of the dynamic processes that occur within cells during cell division. Specifically, KLPs have been shown to contribute to the assembly and maintenance of the mitotic spindle, chromosome attachment to the spindle, separation of sister chromatids during anaphase, regulation of spindle MT dynamics, and cytokinesis. Because the activity of mitotic KLPs is limited to a discrete phase of the cell cycle (M-phase), the activity of these proteins must be tightly regulated both temporally with respect to the phase of the cell cycle and spatially within the cell. Additionally, the activity of some mitotic KLPs may be further restricted to a discrete phase of mitosis. Mechanisms of regulation that may serve to limit the activity of mitotic KLPs to M-phase include restricting the availability of the protein by 1) limiting its synthesis to just prior to the onset of M phase or 2) sequestering the protein in an intracellular compartment during interphase. Additional levels of regulation include modifying the activity of the KLP by M-phase specific post-translational modifications such as phosphorylation or interaction with regulatory proteins. Multiple mechanisms of regulation may exist for each KLP, thereby enhancing the level of control over motor activity.

Of the five kinesin families that contain mitotic KLPs, members of four of these families (MKLP-1, Chromokinesin, C-terminal, and MCAK/KIF 2) localize to interphase nuclei. A functional role for KLPs in the nucleus has not been established, and it is generally assumed that nuclear localization serves as a mechanism to regulate the activity of mitotic KLPs by controlling their association with MTs. In order to test this hypothesis, I chose to identify sequences directing nuclear localization of HsMKLP-1 as part of an effort to define factors contributing to the regulation of mitotic KLPs. HsMKLP-1 is a member of the MKLP-1 family of KLPs whose members have been shown to be essential for mitosis in mammalian cells (Nislow et al., 1990) and cytokinesis in *C. elegans* and *D. melanogaster* (Adams et al., 1998; Powers et al., 1998; Raich et al., 1998). HsMKLP-1 is localized to interphase nuclei in mammalian cells and becomes associated with the mitotic spindle following nuclear envelope breakdown during prometaphase (Chapter 3) (Nislow et al., 1992). During anaphase, HsMKLP-1 localizes to the mitotic spindle interzone where it is incorporated into the midbody during telophase. Because

the activity of MKLP-1 subfamily members does not appear to be necessary until the later stages of mitosis and/or cytokinesis (Adams et al., 1998; Nislow et al., Powers et al., 1998; Raich et al., 1998), sequestration of HsMKLP-1 in the nucleus may serve to regulate its activity in interphase cells by limiting its interaction with MTs. This would prevent inappropriate interaction of HsMKLP-1 with MTs and ensure that HsMKLP-1 is available soon after nuclear envelope breakdown. MKLP-1 subfamily members have been shown to bind and bundle MTs *in vivo* (Kuriyama et al., 1994) and *in vitro* (Nislow et al., 1992) and if nuclear localization serves to prevent HsMKLP-1 from prematurely interacting with MTs, then mislocalization of HsMKLP-1 in the interphase cytoplasm should lead to a disruption of the interphase MT array. Since this array is essential for the spatial distribution of organelles and membrane-associated transport, disruption of this structure would conceivably have severe consequences for the cell.

Materials and Methods

GFP fusion plasmid construction

Xho I, Hind III, and Pst I fragments from p32a-MKLP-1 (Chapter 2) encoding HsMKLP-1 AA 460-856, 534-856, and 714-856 were cloned into the pC1-S65T mammalian expression vector (Clontech) as C-terminal fusions to the S65T mutant of GFP, thereby creating pC1S65T-Δ460, pC1S65T-Δ534, and pC1S65T-Δ714, respectively. cDNA encoding AAs 1-461 of HsMKLP-1 was amplified from p32-461Δ (Chapter 2) using Pfu polymerase (Stratagene) and the following primers:

5'-GACGACGACTCCGGAGCCATGGTGTCAGCG-3' (460 forward)

5'-CAATGGTTCATTTCAAGCTTAACCTCGAGGCTG-3' (460 reverse), which contain restriction enzyme sites for BspE I (underline) and Xho I (dashed underline). The PCR product was digested with BspE I and Xho I and ligated into appropriately digested pC1S65T, creating pC1S65T-461Δ. cDNA encoding AAs 641-856 of HsMKLP-I was amplified from p32a-Δ641 (Chapter 2) using Pfu polymerase, T7 terminator primer, and the following primer which contains a restriction enzyme site for Bsp EI (underlined):

5'-GACGACGACTCCGGAGCCATGGAGAAT-3' (641 forward).

The PCR product was digested and ligated into pC1S65T as described above for pC1S65T-461Δ to create pC1S65T-Δ641. To disrupt putative NLS 4 of HsMKLP-1 (from AA 799-806, see Fig. 5.1a), amino acids ^{804}Lys and ^{805}Arg were mutated to Thr and Ser, respectively, by PCR using the following primer, which spans AA 801-810 of HsMKLP-1:

5'-TACTGTGGAAGATCTA**GA**A**TGT**TCGACTACC-3' (810 reverse).

The mutation (mutated nucleotides are shown in bold) is adjacent to a Bgl II restriction enzyme site of HsMKLP-1 (dotted underline) and is encompassed within a 375 bp Bgl II fragment of the

HsMKLP-1 cDNA sequence. Mutation of these nucleotides created a unique Xba I site (double underline). A 533 bp fragment amplified from p32a-Δ641 using the 810 reverse and 641 forward primers was digested with Bgl II and ligated to replace the 375 bp BgII fragment from pC1S65T-Δ641 to create pS65T-Δ641$^{\Delta 4}$. Plasmids were screened for the mutation by Xba I restriction digestion and mutations were confirmed by sequencing. The Pst I fragment from pS65T-Δ641$^{\Delta 4}$ was ligated into appropriately digested pC1S65T to create pC1S65T-Δ701$^{\Delta 4}$. Full-length HsMKLP-1 was cloned into pC1S65T by ligating the 1545 bp Xho I fragment from pC1S65T-Δ460 into Xho I-digested pC1S65T-461Δ, to create pC1S65T-MKLP. The disrupted NLS was incorporated into pC1S65T-MKLP (pC1S65T-MKLP$^{\Delta 4}$) by replacement of the 791 bp Pst I fragment with the Pst I fragment from pS65T-Δ641$^{\Delta 4}$.

Myc-tagged plasmid construction

cDNA encoding full-length HsMKLP-1, HsMKLP-1 AA 1-510, AA 511-856, and AA 724-856 were amplified from p32a-MKLP-1 (Chapter 2) using Pfu polymerase and the following primers, which contain restriction enzyme sites for Kpn I (underline), Eco RI (thick underline), Bam HI (dotted underline), or Sma I (dashed):

5'-GACGGTACC**GCCA**CCATGGTGTCAGCGAGAA-3' (0 forward),

5'-AAGGGTACC**G**C**C**A**C**CATG**G**AAACTGAAACAGTCATGCAG-3' (724 forward),

5'-CGACAGAATTCACGA**GCC**A**CC**ATG**G**TTGATGAGTTT-3' (511 forward),

5'-CTCATCGGATCCCATTTGTCGTAAGTTATGTCG-3' (510 reverse),

5'-GTCAGTCCCGGGCTTTTTGCGCTTGGGTTG-3' (856 reverse).

Several nucleotides around the methionine start codon (double underline) in the forward primers were optimized (bold) to reflect the consensus Kozak sequence for vertebrate mRNAs (GCCACCATGG). PCR products from reactions with 0 forward/510 reverse, 511 forward/856 reverse, 724 forward/856 reverse, and 0 forward/856 reverse reactions were digested with Kpn I/Bam HI (510Δ, Δ724), Eco RI/Sma I (Δ511), or Kpn I/Sma I (full-length), and cloned into Kpn I/Bam HI-digested (510Δ, Δ724), Eco RI/Eco RV-digested (Δ511), or Kpn I/Eco RV-digested (full-length) pcDNA3.1/Myc-His(+)B vector (Invitrogen) to create pcDNA3.1-510Δ, pcDNA3.1-Δ511, pcDNA3.1-Δ724, and pcDNA3.1-MKLP, respectively. Initial cloning of the HsMKLP-1 cDNA into pET32a (Chapter 2) resulted in a Lys to Val change in the second amino acid of HsMKLP-1 and to verify that this amino acid change did not affect the localization of HsMKLP-1, PCR was used to change the second amino acid of pcDNA3.1-510Δ and pcDNA3.1-MKLP-1 to Lys. pcDNA3.1-510Δ was amplified using the 510 reverse primer and the following primer, which spans the translational start codon of HsMKLP-1 (double underline):

5'-CTTGGTACCGCCACCATG**AA**GTCAGCGAGAGCTAAG-3' (0 forward^{Lys}). The mutated amino acids are shown in bold and the Kpn I site is underlined. The PCR product was digested with Kpn I/Hpa I and ligated into Kpn I/Hpa I-digested pcDNA3.1-510Δ and pcDNA3.1-MKLP to create pcDNA3.1-510Δ^{Lys} and pcDNA3.1-MKLP^{Lys}. cDNA encoding HsMKLP-1 AA 1-723 was amplified from pcDNA3.1-MKLP^{Lys} as described above using the 856 reverse primer and the following primer:
5'-TGTTTCGGATCCCATGTTAGAGGCGGGCTTATG-3' (723 reverse). The PCR product was digested with Kpn I/Bam HI and ligated into Kpn I/Bam HI-digested pcDNA3.1/Myc-His(+)B vector to create pcDNA3.1-723Δ. Mutation of putative NLS 4 (described above) was incorporated into full-length HsMKLP-1 by replacing the 1072 bp Eco RV fragment of pcDNA3.1-MKLP^{Lys} with the Eco RV fragment from pC1S65T-MKLP$^{\Delta 4}$ to create pcDNA3.1-MKLP$^{\Delta 4}$. The Eco RV fragment from pC1S65T-MKLP$^{\Delta 4}$ was also used to replace the 1072 bp Eco RV fragment from p32a-MKLP-1 to create p32a-MKLP$^{\Delta 4}$. To incorporate the NLS 4 mutation in Δ724, p32a-MKLP$^{\Delta 4}$ was amplified using the 724 forward and 856 reverse primers and the PCR product was digested with Kpn I/Sma I and ligated into Kpn I/Eco RV-digested pcDNA3.1/Myc-His(+)B vector to create pcDNA3.1-Δ724$^{\Delta 4}$. In order to determine the contribution of the C-terminal 26 AA's of HsMKLP-1 (which includes putative NLS 5, Fig. 5.3a) to nuclear localization of HsMKLP-1, the 2519 bp fragment released from digestion of pcDNA3.1-MKLP^{Lys} with Kpn I/Bam HI was ligated into Kpn I/Bam HI-digested pcDNA3.1/Myc-His(+)B vector to create pcDNA3.1-MKLP$^{\Delta 5}$. The 350 bp fragment released from digestion of pcDNA3.1-Δ724 with Kpn I/Bam HI was ligated into Kpn I/Bam HI-digested pcDNA3.1/Myc-His(+)B vector to create pcDNA3.1-Δ724$^{\Delta 5}$, which also lacks sequences encoding the C-terminal 26 AA's of HsMKLP-1. Sequences encoding the C-terminal 26 AA's of Δ724$^{\Delta 4}$ were removed by digesting the PCR product amplified from p32a-MKLP$^{\Delta 4}$ with 724 forward and 856 reverse primers with Kpn I/Bam HI and ligating this fragment into Kpn I/Bam HI-digested pcDNA3.1/Myc-His(+)B vector to create pcDNA3.1-Δ724$^{\Delta 4,5}$.

Transient transfection and immunofluorescence

HeLa cells grown to subconfluence on coverslips were transiently transfected with plasmid DNA using calcium phosphate as described (Sambrook et al., 1989) and typically observed 16-30 hours after transfection. Cells expressing GFP-fusions were either processed for immunofluorescence or observed live after Hoescht staining (100 ng/ml Hoescht 33342 for 30 minutes at 37°C) to visualize the DNA. For immunofluorescence, cells expressing GFP and myc-tagged proteins were fixed in 3.7% formaldehyde in PBS for 10 minutes at room temperature, permeabilized with either 0.5% Triton-X 100 in PBS for 10 minutes at room

temperature (GFP-fusions) or 100% acetone for 30 s at -20°C (myc-tagged proteins). Acetone permeabilization was found to reduce non-specific staining observed in control cells stained with the c-myc antibody. For colocalization of myc-tagged proteins and MTs, cells were fixed in methanol (-20˚C, 10 minutes) to better preserve MT structure. Cells were processed for immunofluorescence essentially as described (Chapter 3). Briefly, cells were blocked in 10% BSA in PBS for 10 minutes and incubated with a polyclonal anti-His antibody (1:200, Clontech) or monoclonal c-myc antibody (1:500, Sigma) for 1 hour. Coverslips were extensively washed in PBS supplemented with 0.1% Tween-20 and incubated with Oregon Green conjugated anti-rabbit secondary antibodies (10 μg/ml, Molecular Probes) plus 1 μg/ml DAPI for 30 minutes. Coverslips were washed as before, mounted on glass slides, and observed using a Nikon Microphot SA microscope equipped with an appropriate multipass dichroic mirror/barrier filter and filter-wheel mounted excitation filters. For colocalization of myc-tagged proteins and MTs, cells were first incubated with a monoclonal anti-tubulin antibody (DM1α 1:500, Sigma), followed by Texas Red conjugated anti-mouse secondary antibodies (8 μg/ml, Molecular Probes) plus 1 μg/ml DAPI. Cells were then incubated with a FITC-conjugated monoclonal c-myc antibody (1:200, Covance).

Results:

Nuclear localization of HsMKLP-1 in HeLa cells (Chapter 3 and (Nislow et al., 1992)) suggested that HsMKLP-1 has a functional nuclear localization sequence (NLS). HsMKLP-1 was previously reported to contain an NLS in its extreme N-terminus (Nislow et al., 1992). However, my previous work on the subcellular fractionation of N- and C-terminal HsMKLP-1 proteins expressed in insect cells suggested that nuclear localization determinants resided in the C-terminus of the protein (Chapter 2). Using the PSORT II program (Kenta Nakai, http://psort.nibb.ac.jp:8800/helpwww2.html), five NLS's (labeled 1-5 in Fig. 5.1 a) were identified in the AA sequence of HsMKLP-1. Of these, three reside in the C-terminal tail domain (Fig. 5.1 a). To establish whether NLS's reside in the N- or C-terminus of HsMKLP-1, HsMKLP-1 AA 1-461 and 460-856, which roughly correspond to the N- and C-termini of HsMKLP-1, respectively, were expressed in HeLa cells as fusions to the S65T mutant of GFP (Fig. 5.1 b, Fig. 5.2). Localization of S65T (Fig. 5.2 a, b) and the N-terminal half of HsMKLP-1 (S65T-461Δ, Fig. 5.2 e, f) appeared to be both cytoplasmic and nuclear. The C-terminal half of HsMKLP-1 (S65T-Δ460) colocalized with nuclei (Fig. 5.2 g, h) as did a full-length MKLP-S65T fusion (S65T-MKLP, Fig. 5.2 c, d). This suggested that nuclear localization determinants reside within the C-terminal half of HsMKLP-1 and that the putative NLS's 1 (^{285}KKRR^{288}) and 2

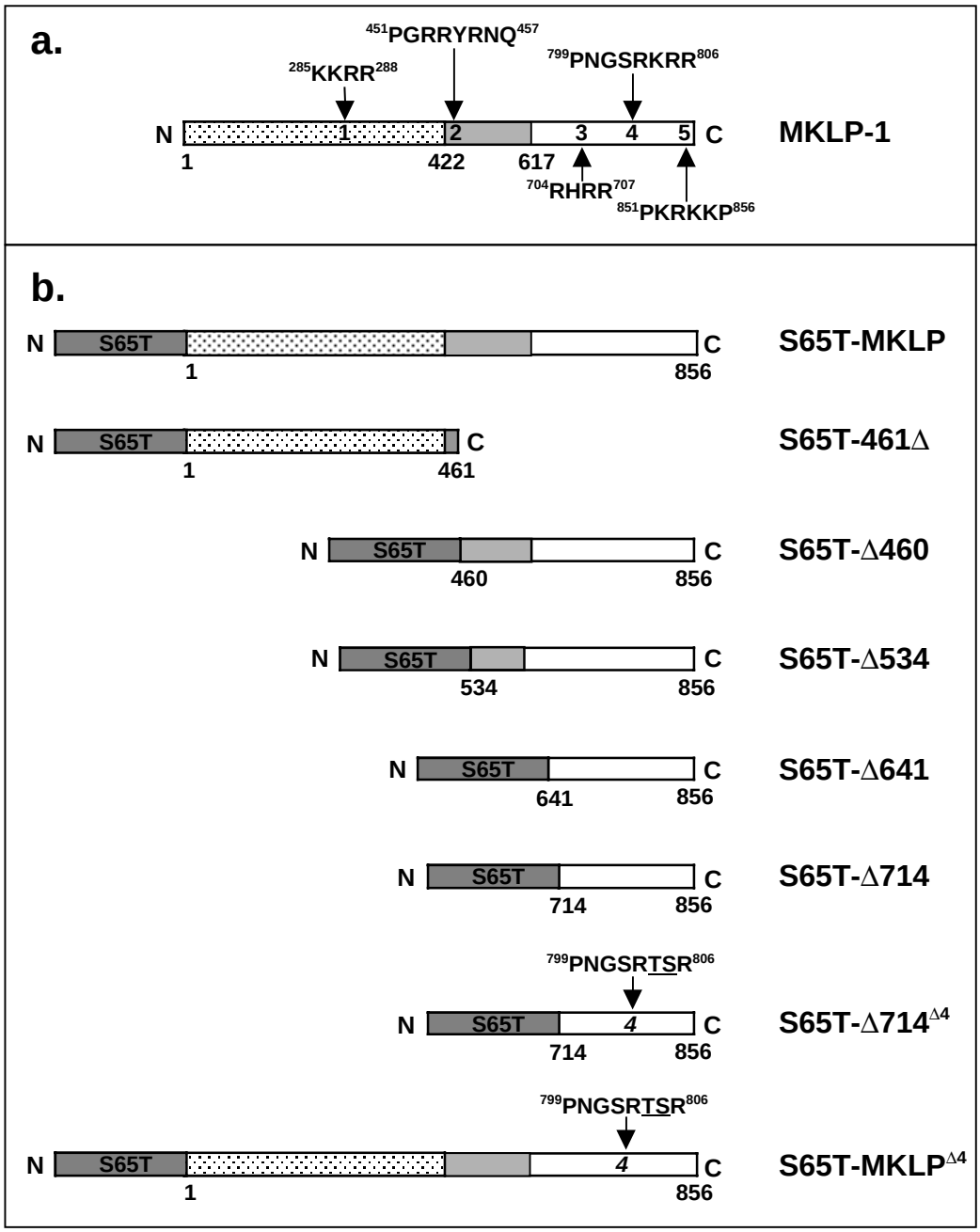

Figure 5.1. Schematic diagram of the HsMKLP-1 coding sequence and GFP constructs a.) Linear HsMKLP-1 AA sequence with putative nuclear localization sequences (NLS) identified using the PSORT II program (Kenta Nakai, http://psort.nibb.ac.jp:8800/helpwww2.html). The NLS sequences are labeled 1-5, with the respective sequence shown above or below the number. The motor domain of HsMKLP-1 is shown as a stippled box. The stalk domain of HsMKLP-1, which includes sequences predicted to form coiled-coils (AA 537-617) is shown in gray and the C-terminal tail domain is shown in

white. b.) Schematic of GFP constructs expressed in HeLa cells. S65T-MKLP encodes full-length HsMKLP-1, whereas constructs S65T-461Δ, S65T-Δ460, S65T-Δ534, S65T-Δ641, and S65T-Δ714 encode AA 1-461, 460-856, 534-856, 641-856, and 714-856 of HsMKLP-1. Lys^{804} and Arg^{805} of putative NLS 4 (^{796}PNGSRKRR^{804}) were mutated to Thr and Ser, respectively, in constructs S65T-$\Delta714^{\Delta4}$ and S65T-$MKLP^{\Delta4}$ (italicized 4). All constructs were expressed as C-terminal fusions to the S65T mutant of the green fluorescent protein.

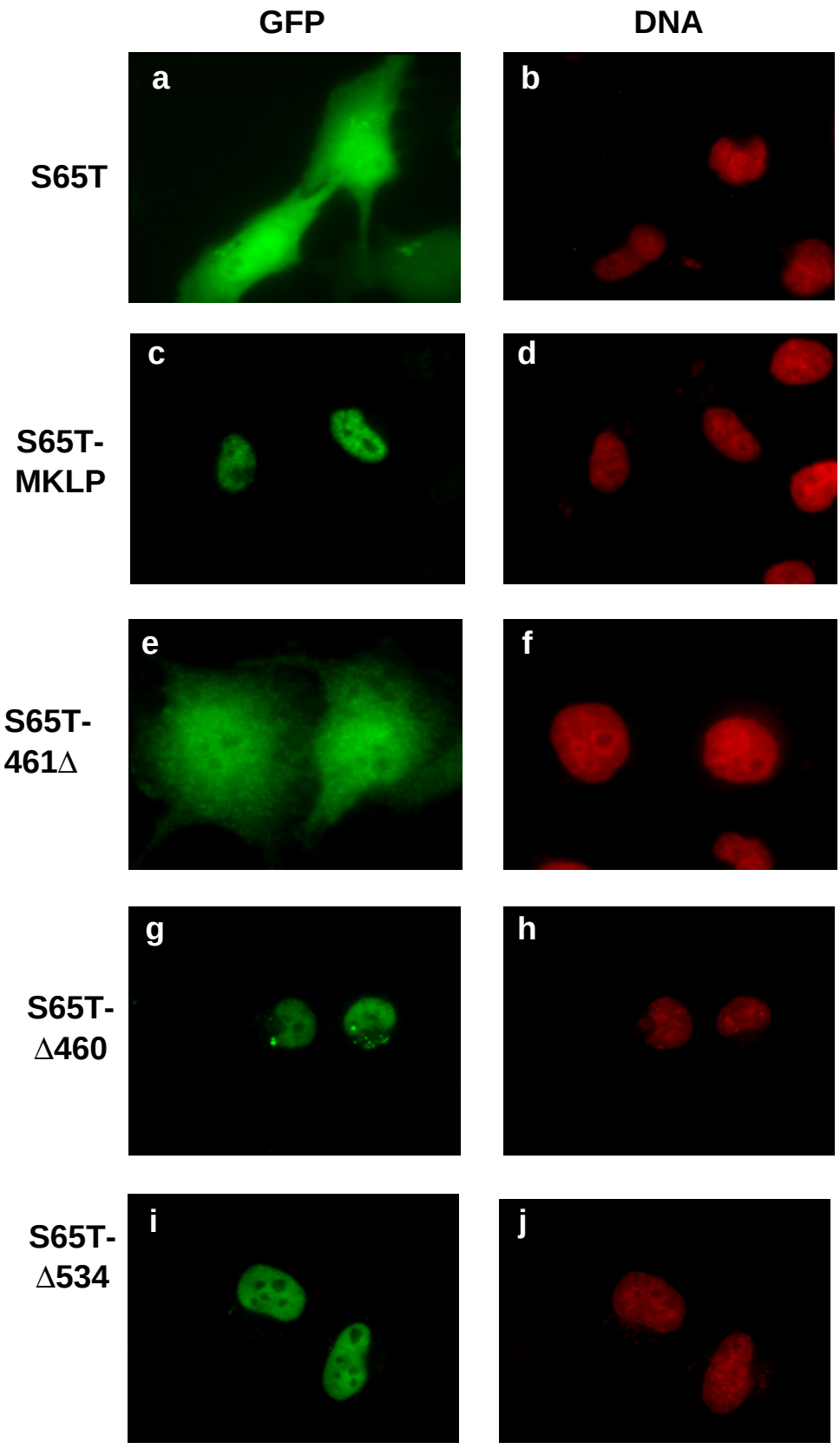
GFP
DNA
a
b
S65T
c
d
S65T-
MKLP
e
f
S65T-
461Δ
g
h
S65T-
Δ460
i
j
S65T-
Δ534

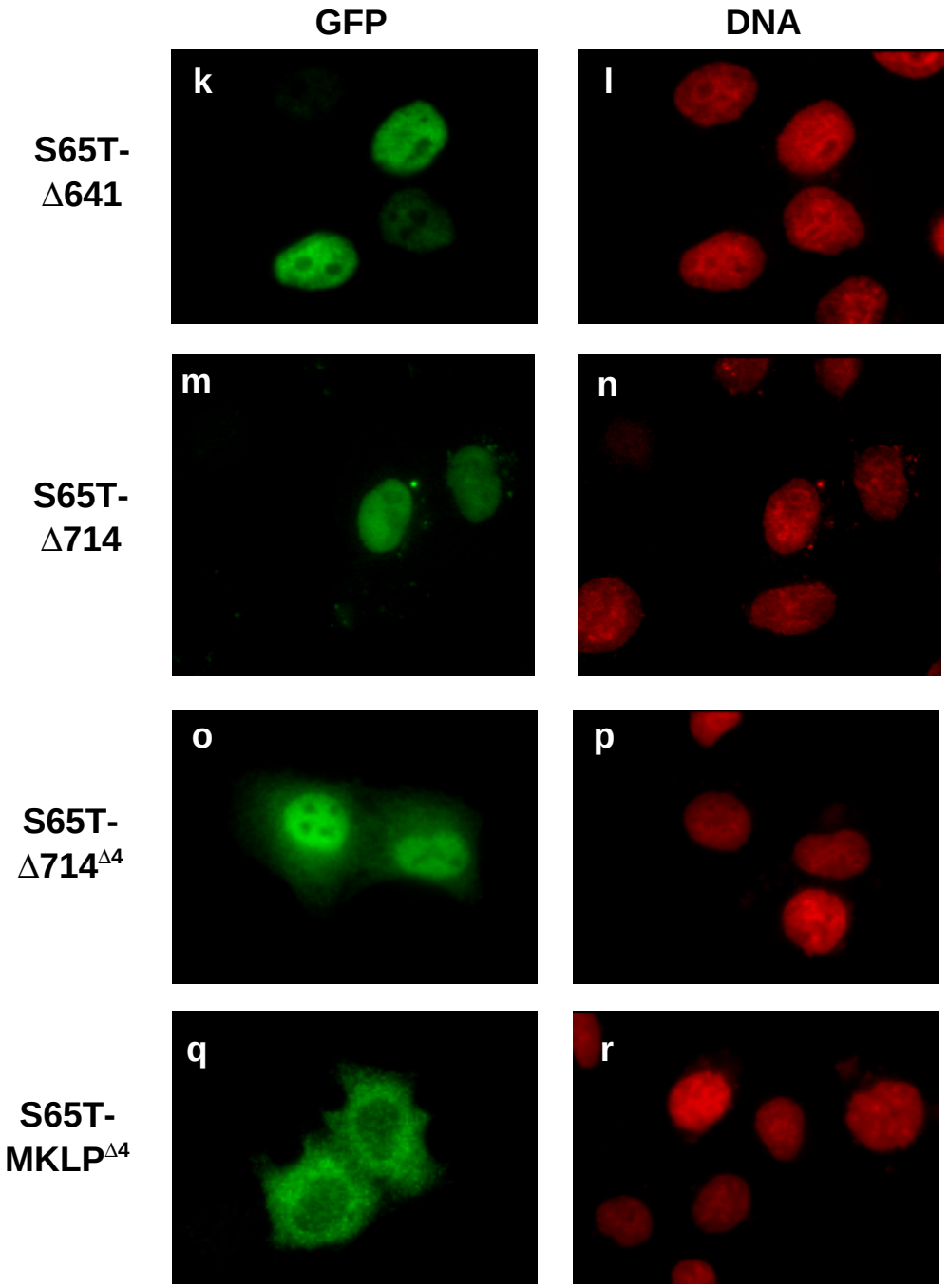

Figure 5.2. Localization of GFP-HsMKLP-1 fusions in transfected HeLa cells.
Paired images of GFP fluorescence (left) and DNA (right) of HeLa cells expressing the S65T mutant of GFP (a, b) and S65T fused to full-length (S65T-MKLP, c, d) or N- and C-terminal domains of HsMKLP-1: S65T-461Δ (e, f), S65T-Δ460 (g, h), S65T-Δ534 (i, j), S65T-Δ641 (k, l) and S65T-Δ714 (m, n). The NLS ^{796}PNGSR**KR**R^{804} was mutated to ^{796}PNGSR**TS**R^{804} in constructs S65T-Δ714^{Δ4} (o, p) and S65T-MKLP^{Δ4} (q, r). The width of each image = 100 μm.

(^{451}PGRRYRNQ^{457}) do not direct nuclear localization (Fig. 5.1 a). Three additional C-terminal HsMKLP-1 constructs (S65T-Δ534, S65T-Δ641, and S65T-Δ714, Fig. 5.1 b), all of which contain putative NLS's 4 and 5, were also found to colocalize with nuclei (Fig. 5.2 i-n).

During the course of these experiments, Dr. Richard McIntosh's lab reported that mutation of putative NLS 4 (^{796}PNGSR**KR**R^{804}) to ^{796}PNGSR**TS**R^{804} abolished nuclear localization of HsMKLP-1 (Gryka and McIntosh, 1998). This work was presented in a poster session at the American Society for Cell Biology Meeting and has not been formally published. In order to confirm the role of NLS 4 in directing HsMKLP-1 localization, AA's Lys^{804} and Arg^{805} were mutated to Thr^{804} and Ser^{805}, respectively, as reported (Fig. 5.1 b). Mutation of these two amino acids is predicted to disrupt the cluster of positively charged amino acids necessary for nuclear import by this NLS. Mutation of Lys^{804} and Arg^{805} abolished nuclear localization of full-length HsMKLP-1 fused to S65T (S65T-MKLP$^{\Delta 4}$, Fig. 5.2 q, r), but partially disrupted nuclear localization of S65T-Δ714 (S65T-Δ714$^{\Delta 4}$, Fig. 5.2 o, p).

Suprisingly, no colocalization of motor with cytoplasmic MTs was observed in cells expressing S65T-461Δ (Fig. 5.2 e) or S65T-MKLP$^{\Delta 4}$ (Fig. 5.2 q). Both of these constructs contained the N-terminal motor domain of HsMKLP-1 (AA 1-432), which has been demonstrated to bind MTs *in vitro* (Chapter 4). In addition, both native HsMKLP-1 (Nislow et al., 1992) and CHO1 expressed in insect cells (Kuriyama et al., 1994) have been shown to bind MTs *in vitro*. In order to determine if the N-terminal S65T tag interfered with the MT-binding of the HsMKLP-1 motor domain, HsMKLP-1 proteins were additionally expressed as N-terminal fusions to the 10 AA c-myc epitope as well as a 6 AA His tag (Fig. 5.3). The relative size of the myc/His-tag (extending no more than 47 AA past the C-terminal AA of HsMKLP-1 proteins) as well as its position at the C-terminus rather than the N-terminus of the protein is less likely to interfere with MT-binding of the HsMKLP-1 motor domain. Furthermore, expression of HsMKLP-1 proteins as myc/His-fusions allowed us to confirm that the localization of S65T-MKLP-1 proteins was not altered due to fusion to the much larger S65T tag.

Full-length HsMKLP-1 (MKLP$^{myc/His}$) and N- and C-terminal halves of HsMKLP-1 encompassing AA 1-510 (510Δ$^{myc/His}$) and AA 511-856 (Δ511$^{myc/His}$) as well as AA 1-723 (723Δ$^{myc/His}$) and AA 724-856 (Δ724$^{myc/His}$) were expressed as N-terminal fusions to the myc epitope and localized in HeLa cells relative to nuclei (Fig. 5.3 b, 5.4 a-j). Full-length HsMKLP-1 (MKLP$^{myc/His}$, Fig. 5.4 a, b) and both C-terminal MKLP-1 constructs (Δ511$^{myc/His}$, Δ724$^{myc/His}$, Fig. 5.4 e, f and i, j, respectively) colocalized with nuclei, consistent with results for full-length

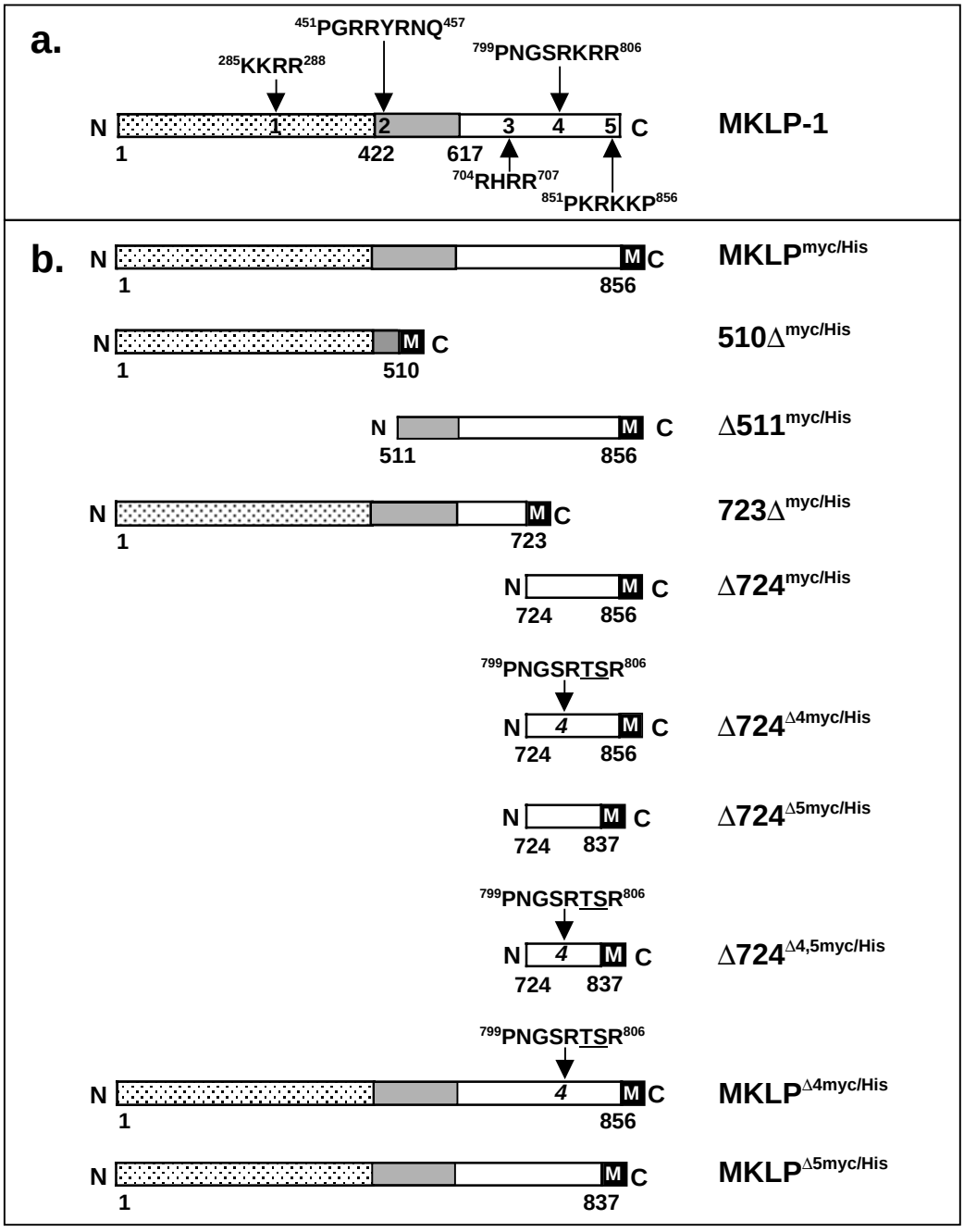

Figure 5.3. Schematic diagram of the HsMKLP-1 coding sequence and myc-tagged constructs a.) For comparison, the linear HsMKLP-1 AA sequence with putative nuclear localization sequences 1-5 from Fig. 5.2 a is shown. b.) Schematic of myc-tagged constructs expressed in HeLa cells. MKLP$^{myc/His}$ encodes full-length HsMKLP-1, whereas constructs 510Δ$^{myc/His}$, Δ511$^{myc/His}$, 723Δ$^{myc/His}$, Δ724$^{myc/His}$, encode AA 1-510, 511-856, 1-723, 724-856, of HsMKLP-1. Lys^{804} and Arg^{805} of putative NLS 4 (^{796}PNGSRKRR^{804}) were mutated to Thr and Ser,

respectively, in constructs $\Delta 724^{\Delta 4myc/His}$ and $MKLP^{\Delta 4myc/His}$ (italicized 4). The C-terminal 26 AA's of HsMKLP-1 (including putative NLS 5) were removed in constructs $\Delta 724^{\Delta 5myc/His}$, $\Delta 724^{\Delta 4,5myc/His}$, and $MKLP^{\Delta 5myc/His}$. All constructs were expressed as N-terminal fusions to a 16-26 AA linker followed by the 10 AA myc-epitope, 5 AA linker, and 6 AA His-tag (black box).

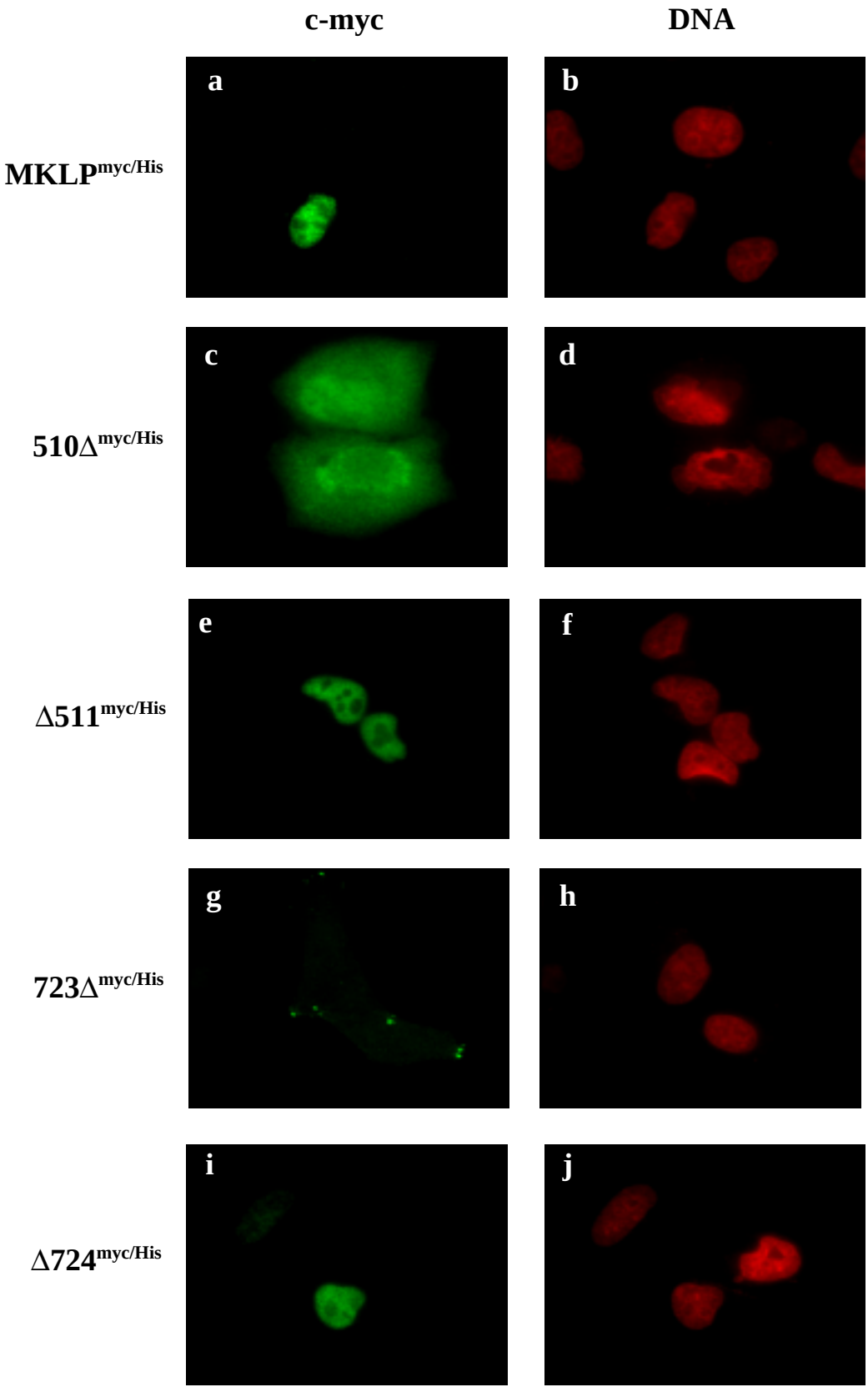
c-myc
DNA
a
b
MKLP^myc/His
c
d
510Δ^myc/His
e
f
Δ511^myc/His
g
h
723Δ^myc/His
i
j
Δ724^myc/His

Figure 5.4. Localization of HsMKLP-1-myc fusions in transfected HeLa cells.
Paired images of myc fluorescence (left) and DAPI staining of DNA (right) of HeLa cells expressing myc-tagged full-length HsMKLP-1 ($MKLP^{myc/His}$, a, b) or N- and C-terminal domains of HsMKLP-1: $510\Delta^{myc/His}$ (c, d), $\Delta511^{myc/His}$ (e, f), $723\Delta^{myc/His}$ (g, h), $\Delta724^{myc/His}$ (i, j). The width of each image = 100 μm.

and C-terminal S65T-MKLP constructs. Localization of 510Δ$^{myc/His}$, which encodes the MKLP-1 motor domain, was diffusely cytoplasmic with some concentration in nuclei (Fig. 5.4 c, d). In contrast, 723Δ$^{myc/His}$ did not localize to nuclei and was instead localized to very discrete foci at the cell periphery (Fig. 5.4 g, h). In highly-expressing cells, 723Δ$^{myc/His}$ localization was observed along discrete fibers at the cell periphery. These fibers were reminiscent of MTs or MT bundles and experiments designed to evaluate the localization of 723Δ$^{myc/His}$ to MTs are discussed below.

Mutation of Lys^{804} and Arg^{805} within NLS 4 to Thr^{804} and Ser^{805} was sufficient to disrupt the nuclear localization of full-length HsMKLP-1 fused to S65T (S65T-MKLP$^{\Delta 4}$, Fig. 5.2 q, r) and to verify these results for myc-tagged HsMKLP-1, full-length HsMKLP-1 with mutated NLS 4 (MKLP$^{\Delta 4myc/His}$) was expressed in HeLa cells as a fusion to the myc epitope (Fig. 5.5 g, h). As expected, mutation of NLS 4 was sufficient to disrupt nuclear localization of full-length HsMKLP-1, although different patterns of localization were observed for MKLP$^{\Delta 4myc/His}$ (Fig. 5.5 g, h) and S65T-MKLP$^{\Delta 4}$ (Fig. 5.2 c, d). Whereas S65T-MKLP$^{\Delta 4}$ localization was diffusely cytoplasmic, MKLP$^{\Delta 4myc/His}$ localization was concentrated at discrete foci at the cell periphery, identical to the localization of 723Δ$^{myc/His}$ (Fig. 5.4 g, h). Removal of putative NLS 5 (MKLP$^{\Delta 5myc/His}$) was also sufficient to disrupt nuclear localization of HsMKLP-1 (Fig. 5.5 i, j), suggesting that both NLS 4 and 5 are required for nuclear uptake. The localization of MKLP$^{\Delta 5myc/His}$ was identical to that of 723Δ$^{myc/His}$ and MKLP$^{\Delta 4myc/His}$, with localization concentrated in foci at the cell periphery (Fig. 5.5 i, j).

Consistent with the localization of S65T-Δ714$^{\Delta 4}$ (Fig. 5.2 o, p), mutation of NLS 4 did not completely disrupt nuclear localization of AA 724-856 of HsMKLP-1 (Δ724$^{\Delta 4myc/His}$, Fig. 5.5 a, b). In addition, removal of NLS 5 from Δ724$^{myc/His}$ (724$^{\Delta 5myc/His}$, Fig. 5.5 c, d) or Δ724$^{\Delta 4myc/His}$ (724$^{\Delta 4,5myc/His}$, Fig. 5.5 e, f) also did not completely abolish nuclear localization. All three of these constructs were localized diffusely to the cytoplasm as well as to nuclei.

HsMKLP-1 has been demonstrated to bind MTs *in vitro* and the localization of 723Δ$^{myc/His}$, MKLP$^{\Delta 4myc/His}$, and MKLP$^{\Delta 5myc/His}$ to discrete foci at the cell periphery suggested that these proteins might localize to MTs *in vivo*. In order to determine whether 723Δ$^{myc/His}$, MKLP$^{\Delta 4myc/His}$, and MKLP$^{\Delta 5myc/His}$ colocalized with MTs, HeLa cells were double labeled with antibodies against the c-myc epitope and tubulin (Fig. 5.6). In each case, localization of HsMKLP-1 proteins appeared continuous with MTs, although it did not completely overlap with tubulin staining. Furthermore, no gross alteration of the interphase MT array was observed in

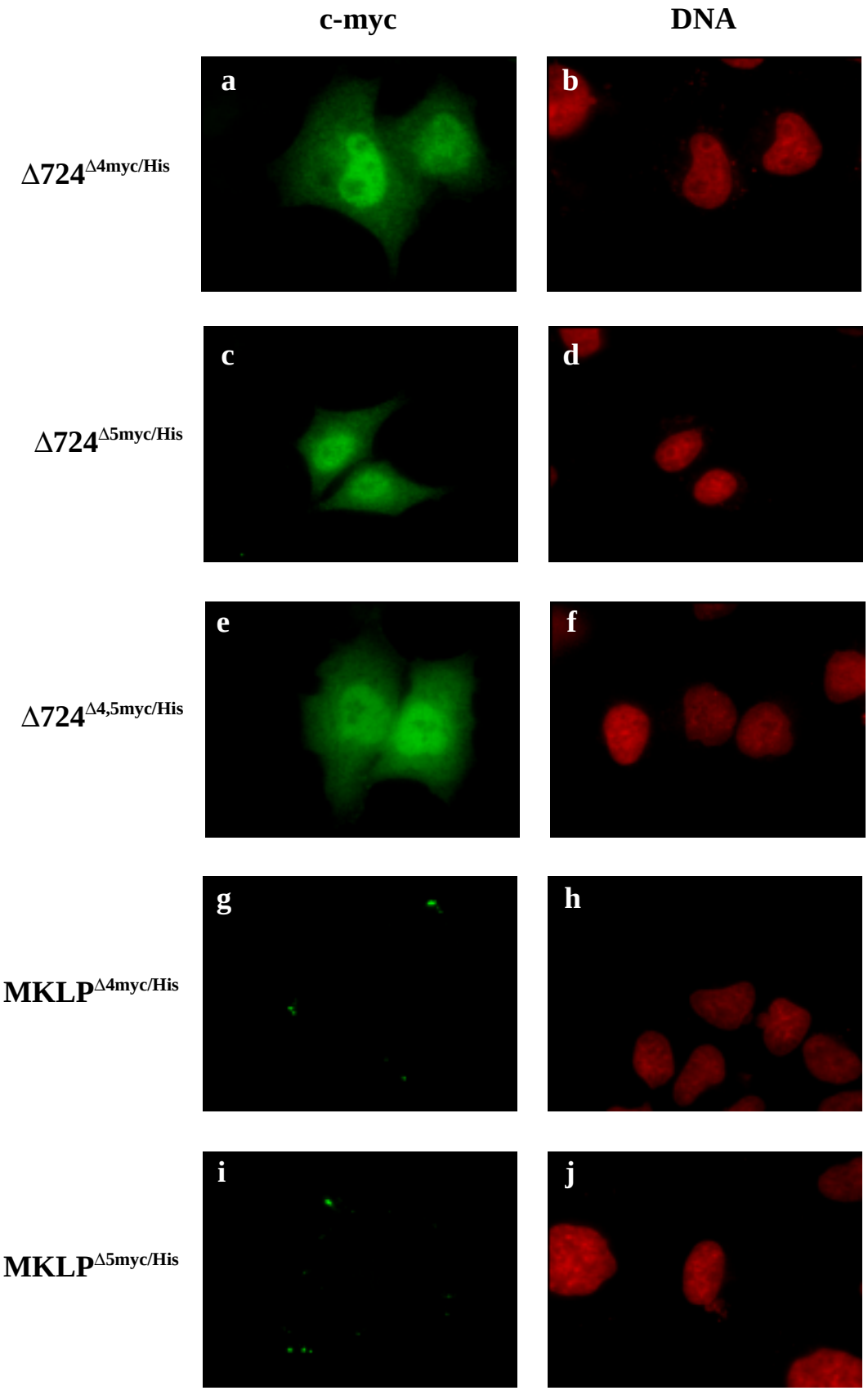
c-myc
DNA
a
b
Δ724Δ4myc/His
c
d
Δ724Δ5myc/His
e
f
Δ724Δ4,5myc/His
g
h
MKLPΔ4myc/His
i
j
MKLPΔ5myc/His

Figure 5.5. Localization of HsMKLP-1-myc NLS mutants in transfected HeLa cells. Paired images of myc fluorescence (left) and Hoescht staining (right) of HeLa cells expressing myc-tagged HsMKLP-1 constructs. Putative NLS 4 (^{796}PNGSR**KR**R^{804}) was mutated to ^{796}PNGSR**TS**R^{804} in HsMKLP-1 constructs $\Delta724^{\Delta4myc/His}$ (a, b) and $MKLP^{\Delta4myc/His}$ (g, h), while the C-terminal 26 AA's of HsMKLP-1 (which includes putative NLS 5) were removed in constructs $\Delta724^{\Delta5myc/His}$ (c, d) and $MKLP^{\Delta5myc/His}$ (i, j). $\Delta724^{\Delta4,5myc/His}$ (e, f) was created by removing the C-terminal 26 AA's of $\Delta724^{\Delta4}$. The width of each image = 100 μm.

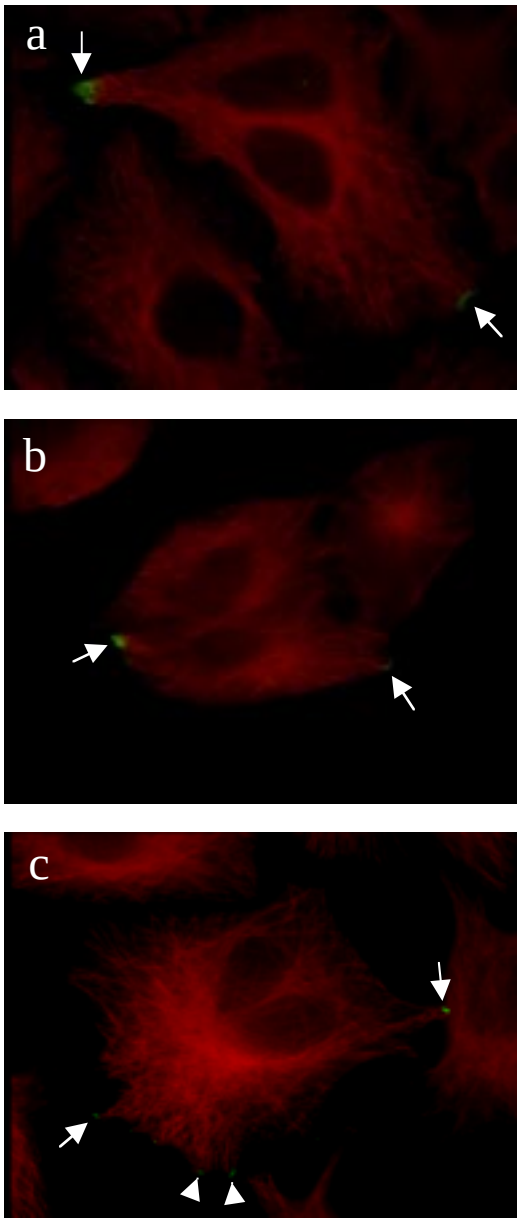

Figure 5.6. Colocalization of HsMKLP-1-myc fusions and microtubules in transfected HeLa cells

Images of myc fluorescence (green) and tubulin staining (red) of HeLa cells expressing $723\Delta^{myc/His}$ (a), $MKLP^{\Delta 4myc/His}$ (b), and $MKLP^{\Delta 5myc/His}$ (c). Arrows indicate myc localization.

cells expressing 723Δ$^{myc/His}$, MKLP$^{\Delta 4myc/His}$, or MKLP$^{\Delta 5myc/His}$. The localization of S65T and myc-tagged proteins is summarized in Table 5.1.

Discussion:

The goal of this work was to identify sequences directing nuclear import of HsMKLP-1 in order to address the role of nuclear localization in regulating the activity of HsMKLP-1 during interphase. Full-length HsMKLP-1 fused to either S65T (Fig. 5.2 c, d) or the myc-epitope (Fig. 5.4 a, b) localized to nuclei, which demonstrates that the HsMKLP-1 motor subunit is capable of specifying nuclear localization. HsMKLP-1 AA 724-856 colocalized with nuclei (Δ724$^{myc/His}$, Fig. 5.4 i, j) whereas AA 1-723 did not (723Δ$^{myc/His}$, Fig. 5.4 g, h), indicating that sequences directing nuclear localization of HsMKLP-1 are localized to the C-terminal tail domain and that putative NLS's 1-3 (Fig. 5.1 a), identified from sequence analysis of the HsMKLP-1 AA sequence, are not functional. Within the C-terminal tail domain, mutation of NLS 4 (MKLP$^{\Delta 4myc/His}$, Fig. 5.5 g, h) or removal of NLS 5 of HsMKLP-1 (MKLP$^{\Delta 5myc/His}$, Fig. 5.5 i, j) were sufficient to abolish nuclear localization of full-length HsMKLP-1, which suggests that both of these sequences may contribute to a functional NLS *in vivo*. In addition to NLS 5, AA's 830-850 were removed from MKLP$^{\Delta 5myc/His}$ and it remains possible that sequences other than NLS 5 are important for nuclear localization.

Although mutation of NLS 4 and 5 abolished nuclear localization of full-length HsMKLP-1, these mutations individually or together were not sufficient to disrupt nuclear localization of the C-terminal 132 AA of HsMKLP-1 (Δ724$^{\Delta 4myc/His}$, Δ724$^{\Delta 5myc/His}$, Δ724$^{\Delta 4,5myc/His}$, Fig. 5.5 a-f). All of these C-terminal constructs exhibited nuclear localization as well as diffuse localization to the cytoplasm. Δ724$^{\Delta 4myc/His}$, Δ724$^{\Delta 5myc/His}$, Δ724$^{\Delta 4,5myc/His}$ are predicted to be <20 kDa in size, which suggests that their small size (<60 kDa) may permit them to diffuse through nuclear pore complexes (Gorlich, 1998). Passive diffusion of small proteins into the nucleus may also explain why S65T (27 kDa) and 510Δ$^{myc/His}$ (<60 kDa) localization is nuclear as well as cytoplasmic (Fig. 5.2 a, b; Fig. 5.4 c, d). The observation that 723Δ$^{myc/His}$, which includes AA 1-510 of HsMKLP-1, does not localize to nuclei (Fig. 5.4 g, h) further suggests that 510Δ$^{myc/His}$ does not have a functional NLS. Because HsMKLP-1 is present in HeLa cells (Chapter 3), it is also possible that these proteins are transported into the nucleus by forming a complex with native HsMKLP-1.

Table 5.1 Summary of localization of S65T and myc-tagged HsMKLP-1 proteins

	S65T	myc
Full length constructs:		
MKLP-1	nuclear	nuclear
MKLP$^{\Delta 4}$	cytoplasmic	MTs (periphery)
MKLP$^{\Delta 5}$	ND	MTs (periphery)
N-terminal constructs:		
510Δ	cytoplasmic[1]	cytoplasmic + nuclear
723Δ	ND	MTs (periphery)
C-terminal constructs:		
Δ511	nuclear[2]	nuclear
Δ641	nuclear	ND
Δ724	nuclear[3]	nuclear
Δ724$^{\Delta 4}$	cytoplasmic + nuclear[4]	cytoplasmic + nuclear
Δ724$^{\Delta 5}$	ND	cytoplasmic + nuclear
Δ724$^{\Delta 4,5}$	ND	cytoplasmic + nuclear

Represents results for: [1]S65T-461Δ, [2]S65T-Δ534, [3]S65T-Δ714, [4]S65T-Δ724$^{\Delta 4}$. ND= not determined.

Disruption of nuclear localization determinants in C-terminal constructs of HsMKLP-1 ($\Delta724^{\Delta4myc/His}$, $\Delta724^{\Delta5myc/His}$, $\Delta724^{\Delta4,5myc/His}$, Fig. 5.5 a-f) also allowed us to address whether the tail domain of HsMKLP-1 binds MTs *in vivo*. HsMKLP-1 has been demonstrated to bundle and slide MTs *in vitro* (Nislow et al., 1992) and was previously suggested to contain a MT-binding site in the tail domain (Sharp et al., 2000). The diffuse cytoplasmic localization of $\Delta724^{\Delta4myc/His}$, $\Delta724^{\Delta5myc/His}$, $\Delta724^{\Delta4,5myc/His}$ is not consistent with MT localization, which suggests that the HsMKLP-1 tail domain does not contain a functional MT-binding site.

Although the constructs differed slightly, HsMKLP-1 proteins fused to the C-terminus of S65T (Fig. 5.2) or expressed as N-terminal fusions to the myc epitope (Figs. 5.4, 5.5) exhibited similar patterns of localization in HeLa cells with the exception of S65T-$MKLP^{\Delta4}$ and $MKLP^{\Delta4myc/His}$ (Table 5.1). Localization of S65T-$MKLP^{\Delta4}$ (Fig. 5.2 q, r) was cytoplasmic, whereas $MKLP\Delta4^{myc/His}$ was localized to discrete foci at the cell periphery (Fig. 5.5 g, h), which was continuous with MT localization (Fig. 5.6). S65T fused to the N-terminus of HsMKLP-1 may sterically prevent association of the HsMKLP-1 motor domain with MTs, or may alter the folding of the HsMKLP-1 motor domain so that it no longer binds MTs.

The localization of $723\Delta^{myc/His}$, $MKLP^{\Delta4myc/His}$, and $MKLP^{\Delta5myc/His}$ is consistent with these proteins localizing to MT plus ends at the cell periphery (Fig. 5.4 g, h; Fig. 5.5 g-j; Fig. 5.6). All of these constructs encompass the N-terminal motor domain of HsMKLP-1 (AA 1-422), which binds MTs *in vitro* (Chapter 4) and may serve to target these proteins to MTs *in vivo*. HsMKLP-1 has been demonstrated to be a plus-end directed motor (Nislow et al., 1992), and one model to account for the localization of $723\Delta^{myc/His}$, $MKLP^{\Delta4myc/His}$, and $MKLP^{\Delta5myc/His}$ is that these proteins move toward the plus ends of interphase MTs where they accumulate. However, $510\Delta^{myc/His}$, which also encompasses the motor domain of HsMKLP-1 did not localize to MTs (Fig. 5.4 c, d). Based on work with bacterially-expressed HsMKLP-1 proteins (Chapter 4), $510\Delta^{myc/His}$ is predicted to be monomeric, whereas $723\Delta^{myc/His}$, $MKLP^{\Delta4myc/His}$, and $MKLP^{\Delta5myc/His}$ are expected to be dimeric because they include sequences required for dimerization of HsMKLP-1 proteins (AA 524-641, Chapter 4). *In vitro*, a monomeric HsMKLP-1 motor domain construct exhibited reduced affinity for MTs in comparison to a dimeric HsMKLP-1 motor domain construct (Chapter 4), which suggests that differences in the affinity of monomeric and dimeric N-terminal HsMKLP-1 proteins for MTs may account for differences in MT-binding *in vivo*. Furthermore, although the monomeric HsMKLP-1 motor domain binds MTs *in vitro*, two motor domains may be required for MT-binding *in vivo*, as suggested by the MT localization of monomeric and dimeric constructs of HsEg5 *in vivo* (Blangy et al., 1998).

In the absence of a functional NLS, localization of HsMKLP-1 to interphase MTs suggests that nuclear localization serves to limit HsMKLP-1's interaction with MTs, although it is not clear what effect expression of HsMKLP-1 in the interphase cytoplasm has on cells. Because HsMKLP-1 bundles MTs *in vitro*, expression of HsMKLP-1 in the interphase cytosol could conceivably lead to bundling and disorganization of the interphase MT array. However, no gross disruption of the interphase MT array was observed in cells expressing $723\Delta^{myc/His}$, $MKLP^{\Delta 4myc/His}$, and $MKLP^{\Delta 5myc/His}$, suggesting that expression of HsMKLP-1 in the cytoplasm does not interfere with the general organization of the interphase MT array. However, this does not exclude the possibility that cytoplasmic HsMKLP-1 may exert a more subtle effect on cells. For example, by binding to MT plus ends HsMKLP-1 may affect MT dynamics *in vivo*. In these experiments cells were routinely observed 24-27 hours after transfection and it is possible that more dramatic effects may be seen in cells harvested at later timepoints.

Nuclear localization may be just one mechanism of regulating the activity of mitotic KLPs during interphase. The notion that KLPs may be subject to multiple mechanisms of regulation is illustrated by HsEg5, a member of the *bim C* family that is involved in the separation of centrosomes and anaphase B spindle pole separation. Mechanisms suggested to contribute to HsEg5 regulation *in vivo* include cell-cycle dependent protein accumulation (which limits protein accumulation to M-phase) (Sawin and Mitchison, 1995), phosphorylation by two mitotic protein kinases (Blangy et al., 1995; Giet et al., 1999; Sawin and Mitchison, 1995), and control over the oligomeric state of the protein (Blangy et al., 1998). Members of the MKLP-1 family have been shown to interact with 2 mitotic protein kinases (Adams et al., 1998; Lee et al., 1995; Severson et al., 2000), which suggests that HsMKLP-1 may also be subject to complex regulation *in vivo*.

CHAPTER 6: CA^{2+}/CALMODULIN REGULATION OF THE *ARABIDOPSIS* KINESIN-LIKE CALMODULIN BINDING PROTEIN

(Published as: Deavours, B.E., Reddy, A.S.N., and Walker, R.A. (1998) *Cell Motil. & Cytoskel.* 40: 408-416.)

Introduction:

Secondary messengers such as calcium transduce external cues to a cell's operating machinery that in turn enables a cell to sense and coordinate responses to various stimuli. Calcium can exert its effects directly on target proteins or indirectly through the action of calcium binding proteins such as calmodulin. Calmodulin does not possess an intrinsic enzymatic activity, but functions by binding and regulating the activity of a wide range of cellular enzymes (Roberts and Harmon, 1992). Together calcium and calmodulin are critical components of signal transduction pathways in plants, although the targets of calcium and calmodulin in plants have not been well defined (Pooviah and Reddy, 1993).

The kinesin family of MT-dependent motor proteins share sequence similarity to kinesin within the motor domain; these proteins are implicated in many dynamic processes including vesicle transport, organelle positioning and mitosis (for review see (Moore and Endow, 1996)). Although several motor proteins have been identified in higher plants, the roles and functions of these motors have not been as well characterized as they have been in other cell types). Polypeptides from tobacco (Asada et al., 1997; Asada and Shibaoka, 1994; Cai et al., 1993) and *Arabidopsis* (Mitsui et al., 1994) have been shown to possess properties characteristic of kinesins. Immunofluorescence and synchronization studies suggest that several of these kinesins may have roles in mitosis (Asada et al., 1997; Bowser and Reddy, 1997; Liu et al., 1996; Liu and Palevitz, 1996; Mitsui et al., 1996).

KCBP (kinesin-like calmodulin binding protein) was identified from *Arabidopsis* based on its ability to bind to calmodulin in a calcium-dependent manner (Reddy et al., 1996b). This motor is unique among MT-dependent motor proteins in that it has a calmodulin-binding site located adjacent to its motor domain. This site is localized to a 23 AA sequence in the very C-terminus of the motor and exhibits a predicted structure similar to calmodulin-binding domains of other proteins (Reddy et al., 1996b). KCBP falls into a distinct group within the C-terminal subfamily of kinesins (Reddy et al., 1997) and has been reported to be a minus-end directed motor (Song et al., 1997). The KCBP protein is expressed in all cells of *Arabidopsis* with the highest expression in flowers and has since been identified from potato and tobacco (Reddy et

al., 1996a; Reddy et al., 1996b; Wang et al., 1996). Immunofluorescence experiments have localized KCBP to the preprophase band, mitotic spindle, and phragmoplast in both dividing *Arabidopsis* and tobacco cells, suggesting possible involvement of KCBP in mitosis (Bowser and Reddy, 1997). Interestingly, *Arabidopsis* plants lacking a functional KCBP gene appear to develop normally with the only observed defect in trichome morphogenesis (Oppenheimer et al., 1997).

The presence of the calmodulin-binding site suggests a direct role for Ca^{2+}/calmodulin in the regulation of KCBP. In support of this hypothesis, addition of Ca^{2+}/calmodulin to MT-gliding assays abolished motility suggesting that Ca^{2+}/calmodulin interferes with the binding of KCBP to MTs (Song et al., 1997). However, these motility assays were performed using clarified bacterial lysates in which the relative amounts of motor and Ca^{2+}/calmodulin were not known. In order to further define the regulation of KCBP by Ca^{2+}/calmodulin and begin to elucidate the role this motor plays in plant cells, we have characterized the effects of Ca^{2+}/calmodulin on the MT-binding and ATPase activity of KCBP.

Materials and Methods:

Expression and purification of Trx-KCBP

A DNA sequence encoding residues 821-1261 of the KCBP motor was removed from pGEX-3-KCBP (Song et al., 1997) by digestion with EcoRI and inserted into pET-32b (Novagen). The KCBP sequence was expressed as a fusion protein containing thioredoxin (109 residues), a 56 residue linker containing a 6 histidine tag, and 441 residues encoded by KCBP including the calmodulin binding domain. BL21 (DE3) pLys cells containing the pET-32bKCBP construct were grown at 37°C until A_{550}=0.6. Protein expression was induced with 0.25 mM IPTG and proceeded at 22°C for 4 hours. Cells were pelleted, washed once with AB (20 mM PIPES, pH 6.9, 1 mM $MgSO_4$, 1 mM EGTA) and frozen at -70°C. Cell pellets were thawed and resuspended in lysis buffer (20 mM Tris-HCl, pH 8.0, 100 mM NaCl, 0.5 mM β-mercaptoethanol, 0.5 mM MgATP, 1 mM PMSF) plus 10 mM $MgCl_2$ and 40 μg/ml DNase I. Cell lysates were centrifuged at 20,000 xg for 15 minutes and the resulting supernatant was centrifuged at 100,000 xg for 15 minutes. The high speed supernatant was incubated with Talon metal affinity resin (Clontech) according to the manufacturer's protocol. After extensive washing with lysis buffer, bound protein was eluted from the column with lysis buffer plus 100 mM imidazole. For ATPase assays and quantitative MT-binding reactions, Trx-KCBP was subjected to additional purification using S-sepharose (Walker, 1995). Eluates were combined

and dialyzed against EGTA-free AB containing 1 mM DTT and 0.1 mM MgATP and stored at -70°C.

MW determination

Monomer molecular weight was determined from the protein sequence. Stokes radius (R_s) was determined by gel filtration chromatography on Sephacryl S-200. The column was equilibrated and run with AB containing 0.2 M NaCl and 0.02% Tween-20. Proteins of known Stokes radius (catalase, alcohol dehydrogenase, BSA, ovalbumin, MC6 (Chandra et al., 1993), carbonic anhydrase and cytochrome C) were run as standards. Sedimentation coefficient ($s_{20,w}$) was determined by rate zonal centrifugation on 5-20% linear sucrose gradients with catalase, BSA and ovalbumin as standards. The native molecular weight was calculated from: $M= (6\pi\eta N R_s s_{20,w})/(1-\upsilon\rho)$ where $\upsilon= 0.72$ cm^3/g. The frictional coefficient was calculated from: $f/f_0 = R_s/(3M\upsilon/4\pi N)^{1/3}$ (Siegel and Monty, 1966).

Microtubule binding assays

All motor concentrations are expressed as monomer concentration. Tubulin was purified as previously described (Walker et al., 1988). Reactions (100 µl final volume) containing 5 µM Trx-KCBP and 5 µM tubulin (as taxol-stabilized MTs) were carried out in AB buffer plus 50 mM NaCl, 20 µM taxol (Calbiochem), and nucleotide or apyrase (Sigma). Calcium (as $CaCl_2$) and calmodulin were included in reactions as indicated. The free calcium concentration was estimated by the method of Fabiato (1979) taking into account pH, [EGTA], [Mg^{2+}] and [ATP]. For determination of binding stoichiometry and K_d, reactions were performed in 50 µl EGTA-free AB buffer supplemented with 0.1 mg/ml ovalbumin and 5 mM MgAMP-PNP. After 20 minutes at 22°C, reactions were centrifuged in a Beckman TLA-45 rotor at 34,000 rpm for 15 minutes (25°C) and supernatant and pellet fractions were analyzed via SDS-PAGE. For quantification of Trx-KCBP, supernatant and pellet fractions were run on 7.5% SDS-polyacrylamide gels as previously described (Moore et al., 1996). The amount of motor protein in each fraction was determined by measuring the Coomassie blue staining of Trx-KCBP bands relative to known amounts of Trx-KCBP (Huang and Hackney, 1994). Quantification of Trx-KCBP binding to MTs as a function of calcium concentration (Fig. 6.3b) was determined by densitometry of SDS-polyacrylamide gels as previously described (Moore et al., 1996).

Determination of ATPase activity

For determination of K_{mATP} and $K_{0.5MT}$, steady state ATPase assays were performed using a coupled pyruvate kinase-lactate dehydrogenase assay as previously described (Moore et al.,

1996). Reactions (500 µl) were performed at 25°C with 100 nM Trx-KCBP, 0.01-2 mM MgATP, and 0.1-7.5 µM (tubulin concentration) taxol-stabilized, GTP-depleted microtubules. Basal and MT-stimulated ATPase rates were measured at 25°C in EGTA-free AB ± 20 µM taxol using 5'-γ-^{32}P ATP as previously described (Chandra and Endow, 1993). For ATPase assays, high purity calmodulin (Calbiochem) was dialyzed against water.

Results:

Expression, purification and characterization of Trx-KCBP

A portion of the stalk and the entire motor domain of KCBP was expressed as a fusion with thioredoxin (Fig. 6.1). This portion of the KCBP motor includes the putative ATP and MT-binding domains as well as the calmodulin-binding site. The expressed protein, termed Trx-KCBP, also contained a 6 histidine tag which allowed the protein to be purified from induced cell lysates using a metal-affinity resin. Sucrose density gradient centrifugation and gel filtration chromatography were used to determine the native MW of Trx-KCBP. The Stoke's radius, $s_{20,w}$ and frictional coefficient were determined to be 4.8 nm, 8.15 and 1.15, respectively. The calculated MW of ~162,000 is approximately twice that predicted based on the amino acid sequence of Trx-KCBP (68,081), indicating that Trx-KCBP exists predominantly as a dimer.

The calmodulin binding of Trx-KCBP was examined using a fluorescent analog of calmodulin that previously has been used to study the interactions of calmodulin and calmodulin-binding proteins (Bertrand et al., 1994; Fischer et al., 1996; Vorherr et al., 1990). In the presence of 100 µM free calcium, dansyl calmodulin bound Trx-KCBP with a stoichiometry of calmodulin:Trx-KCBP motor domain of 1:1 (data not shown). The presence of MTs did not alter the ability of dansyl calmodulin to bind Trx-KCBP, and no binding of dansyl calmodulin to Trx-KCBP was detected in the presence of 1 mM EGTA. The 1:1 ratio observed for calmodulin binding to Trx-KCBP differed from that reported for the binding of calmodulin to a synthetic KCBP calmodulin-binding domain peptide (calmodulin:peptide stoichiometry = 1:2 (Reddy et al., 1996b)); this difference likely reflects the distance between the two calmodulin-binding domains in the Trx-KCBP dimer which prevents simultaneous binding.

A centrifugation assay was used to examine the binding of purified Trx-KCBP to MTs (Fig. 6.2a). Blot overlay assays in which KCBP with and without thioredoxin were used to examine the binding of KCBP to tubulin have previously demonstrated that thioredoxin did not interfere with motor-tubulin interactions (Narasimhulu et al., 1997). Trx-KCBP did not pellet in the absence of MTs and, as expected for a motor protein, bound MTs in an ATP/GTP-dependent

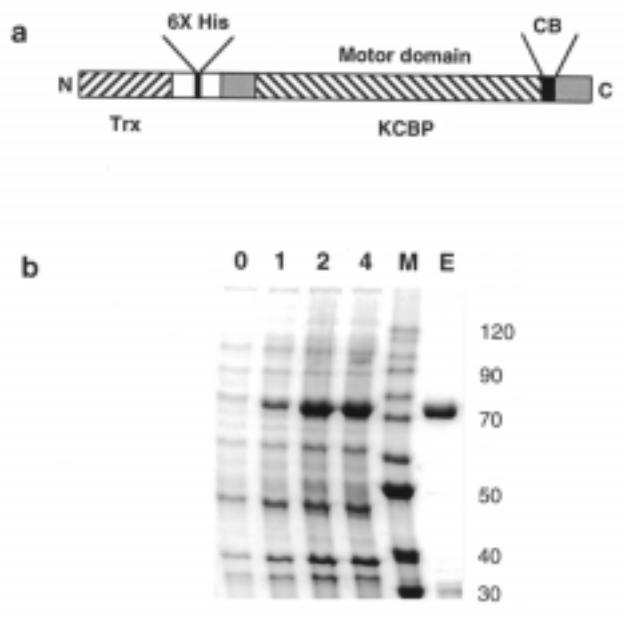

Figure 6.1. Expression of Trx-KCBP in bacterial cells.

a.) Schematic representation of Trx-KCBP. The KCBP sequence was expressed as a fusion protein containing thioredoxin (Trx), a 56 residue linker containing a 6 histidine tag (6X HIS), and 441 residues encoded by KCBP including the proposed motor domain and calmodulin binding (CB) site. b.) Expression and purification of Trx-KCBP in *E. coli*. Protein expression was induced by IPTG and samples withdrawn at 0, 1, 2, and 4 hours following induction were analyzed by SDS-PAGE to monitor Trx-KCBP expression. Trx-KCBP was purified by metal-affinity chromatography and the eluate from the column is shown (E). The calculated MW of Trx-KCBP based on AA sequence is 68,101. Locations of molecular weight markers (M) are indicated.

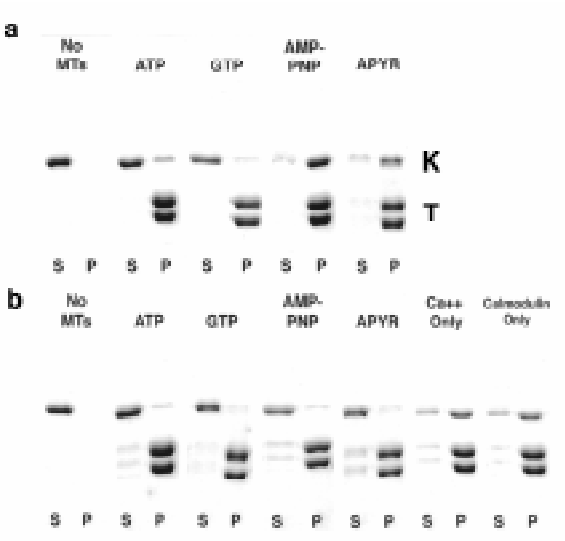

Figure 6.2. Effect of Ca^{2+}/calmodulin on the MT binding properties of Trx-KCBP a.) Trx-KCBP (5 μM) and MTs (5 μM tubulin) were incubated with 5 mM MgATP, MgGTP, MgAMP-PNP or 1 U apyrase (APYR). Samples were centrifuged and the resulting supernatants (S) and pellets (P) from each, as well as for Trx-KCBP alone (no MTs) were analyzed by SDS-PAGE and Coomassie Blue staining. b.) Reactions as above were supplemented with $CaCl_2$ (780 μM free calcium) and either 5 μM (No MTs and MgATP) or 15 μM (MgGTP, MgAMP-PNP and Apyrase) bovine brain calmodulin. Additional MgAMP-PNP reactions were prepared that included calcium only or 15 μM calmodulin only. Locations of Trx-KCBP (K) and tubulin (T) are indicated.

manner. In the presence of hydrolyzable nucleotide (MgATP or MgGTP), Trx-KCBP dissociated from MTs and was found predominantly in the supernatant. In comparison, under conditions that promote tight binding of MT motors to MTs, such as MgAMP-PNP or depletion of hydrolyzable nucleotide (apyrase), Trx-KCBP was found in the MT pellet.

Effects of Ca^{2+}/calmodulin on the microtubule binding properties of Trx-KCBP

To determine the qualitative effects of Ca^{2+}/calmodulin on Trx-KCBP binding to MTs, excess calcium (free [calcium] = 780 μM) and calmodulin (15 μM) were added to reactions of 5 μM Trx-KCBP and MTs under various nucleotide conditions (Fig. 6.2b). In the absence of MTs, Ca^{2+}/calmodulin did not alter the amount of Trx-KCBP that pelleted, indicating that Ca^{2+}/calmodulin had no effect on the solubility of Trx-KCBP. In the presence of MTs and either MgATP or MgGTP, there was no apparent change in the relative amounts of Trx-KCBP found in the supernatant and pellet fractions as compared to reactions without Ca^{2+}/calmodulin (Fig. 6.2a vs 6.2b). However, in the presence of Ca^{2+}/calmodulin and either MgAMP-PNP or 1 U apyrase, there was a shift of Trx-KCBP from the pellet fraction to the supernatant fraction (Fig. 6.2b), indicating that Ca^{2+}/calmodulin inhibited KCBP binding to MTs under conditions that normally induce tight interaction. Calcium or calmodulin alone did not affect Trx-KCBP binding to MTs in the presence of MgAMP-PNP.

The degree of Ca^{2+}/calmodulin-induced dissociation of Trx-KCBP was dependent on the concentration of calmodulin and calcium present (Fig. 6.3). In the presence of MgAMP-PNP and saturating calcium levels (> 1 mM free calcium), calmodulin at a 1:1 ratio to Trx-KCBP reduced the amount of Trx-KCBP bound to MTs by nearly 60% while 2:1 and 4:1 ratios of calmodulin to Trx-KCBP reduced motor binding by ~85% and 97%, respectively (Fig. 6.3a). At a 4:1 ratio of calmodulin to Trx-KCBP, 100 μM free calcium was sufficient to decrease the amount of Trx-KCBP bound to MTs by nearly 90% (Fig. 6.3b).

Further experiments were conducted to determine if Ca^{2+}/calmodulin could dissociate pre-formed MgAMP-PNP-induced Trx-KCBP/MT complexes (Fig. 6.4). As expected, resuspension of pelleted rigor complexes with 5 mM MgATP caused release of Trx-KCBP from MTs while resuspension of rigor complexes with MgAMP-PNP (5 mM) maintained the rigor complex. Resuspension with MgAMP-PNP and calcium, or MgAMP-PNP and calmodulin, also maintained the rigor complex. However, addition of both calcium and calmodulin caused Trx-KCBP to dissociate from MTs even in the presence of MgAMP-PNP. The extent of KCBP dissociation was dependent on the concentration of calmodulin with greater dissociation

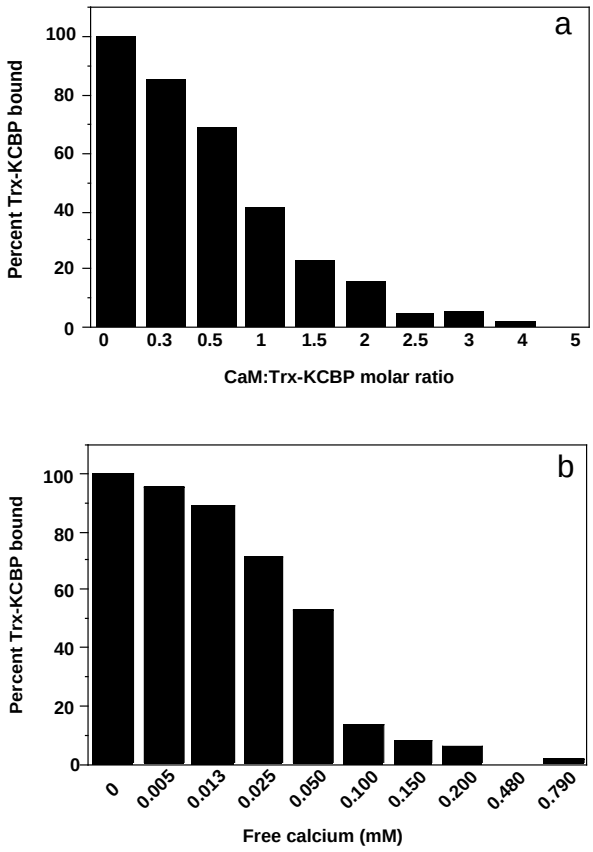

Figure 6.3. Trx-KCBP binding to MTs as a function of calcium and calmodulin concentration. a.) Trx-KCBP (5 μM) and MTs (5 μM tubulin) were incubated with 5 mM MgAMP-PNP, $CaCl_2$ (free calcium concentration is 1.125 mM) and calmodulin concentrations ranging from 0-25 μM calmodulin. Reactions (100 μl final volume) were carried out in EGTA-free AB plus 50 mM NaCl and 20 μM taxol. b.) Reactions were supplemented with 20 μM calmodulin (4:1 ratio of calmodulin:Trx-KCBP) and $CaCl_2$ to yield free calcium concentrations from 0-0.790 mM. Reactions were processed and the amount of Trx-KCBP in the supernatant and pellet fractions of Coomassie stained SDS-polyacrylamide gels was quantified as detailed in Materials and Methods. The amount of Trx-KCBP bound at 0 μM calmodulin and 0 mM free calcium was set at 100% and a small correction was applied for Trx-KCBP pelleting in the absence of MTs (<10%).

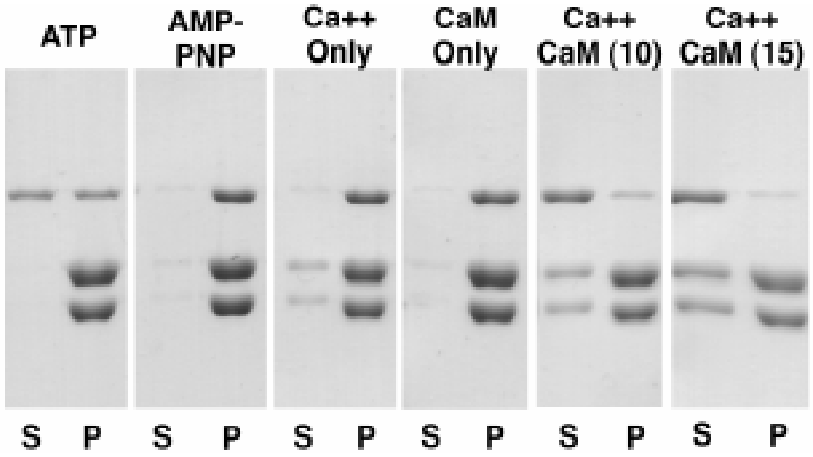

Figure 6.4. Ca^{2+}/calmodulin-induced dissociation of Trx-KCBP bound to MTs. Reactions containing 5 mM MgAMP-PNP were prepared and centrifuged as described in Fig. 6.2a. The resulting pellets were resuspended in 100 µl AB buffer containing MgATP (ATP), MgAMP-PNP (AMP-PNP) and MgAMP-PNP with calcium (CA), 15 µM calmodulin (CAM), calcium and 10 µM calmodulin (CA CAM 10), or calcium and 15 µM calmodulin (CA CAM 15). Under these conditions the free calcium concentration is estimated to be 780 µM. Samples were centrifuged and the resulting supernatants (S) and pellets (P) from each are shown.

associated with a higher (15 vs. 10 μM) concentration of calmodulin. Interestingly, Ca^{2+}/calmodulin (even with MgAMP-PNP present) was more effective than MgATP at releasing Trx-KCBP from MTs.

To define further the Ca^{2+}/calmodulin-induced inhibition of Trx-KCBP binding to MTs, the stoichiometry and affinity of Trx-KCBP binding to MTs was quantified by measuring Trx-KCBP in supernatant and pellet fractions of MT-binding reactions. Although the calcium and calmodulin concentrations used in Fig. 6.2 clearly demonstrated the dramatic inhibitory effect of Ca^{2+}/calmodulin on Trx-KCBP binding to MTs, the complete loss of binding did not permit analysis of binding stoichiometry and affinity. Therefore conditions (100 μM free calcium, 1:1 calmodulin:Trx-KCBP molar ratio) under which some interaction between motor and MTs still occurred were used. Trx-KCBP alone exhibited a stoichiometry of binding to MTs of 1.5:1 motor domain:tubulin dimer and a K_d of 0.065 ± 0.038 μM (Table 6.1). Addition of either calcium alone or calmodulin at a 1:1 molar ratio to Trx-KCBP did not alter the stoichiometry or lower the affinity of Trx-KCBP for MTs. In comparison, calcium and calmodulin together reduced the apparent stoichiometry of Trx-KCBP to tubulin dimer to 0.5:1 and the affinity of Trx-KCBP for MTs about 3-fold.

Effects of Ca^{2+}/calmodulin on the ATPase activity of Trx-KCBP

To investigate the effect of Ca^{2+}/calmodulin on the enzymatic activity of Trx-KCBP, we initially used a coupled pyruvate kinase-lactate dehydrogenase enzyme assay to measure MT-stimulated ATPase activity (Moore et al., 1996). Based on this method, the K_{mATP} and $K_{0.5MT}$ of Trx-KCBP in the absence of calcium and calmodulin were calculated to be 0.030 ± 0.0035 mM and 0.65 ± 0.075 μM, respectively (Fig. 6.5). Because Ca^{2+}/calmodulin was found to interfere with the coupled enzyme assay, 5'-γ-^{32}P ATP was used to measure ATPase activity in the presence of Ca^{2+}/calmodulin. Trx-KCBP exhibited a low basal ATPase rate (0.06 s^{-1}) that was stimulated ~25-fold in the presence of MTs (to 1.5 s^{-1}) (Table 6.2). Calcium alone (free [calcium] = 100 μM), and calmodulin at a 1:1 or 2:1 ratio to Trx-KCBP in either the presence or absence of calcium, did not affect the basal ATPase activity of Trx-KCBP. However, these same calmodulin concentrations in combination with calcium reduced the MT-stimulated rate of ATP hydrolysis of Trx-KCBP by 27% (to 1.1 s^{-1}) at a 1:1 calmodulin:Trx-KCBP ratio and by 47% (to 0.8 s^{-1}) at a 2:1 ratio. In comparison, calcium alone, or calmodulin at a 1:1 or 2:1 ratio did not inhibit the MT-stimulated ATP hydrolysis rate of Trx-KCBP (Table 6.2), and Ca^{2+}/calmodulin had no effect on the MT-stimulated ATPase activity of MC6 (Chandra et al., 1993), a well characterized motor domain construct of Ncd (data not shown).

Table 6.1. Effect of Ca^{2+}/calmodulin on the affinity and stoichiometry of Trx-KCBP binding to MTs[1]

	K_d (μM)	Stoichiometry
KCBP	0.065 ± 0.038	1.5:1
Calcium	0.064 ± 0.043	1.5:1
CaM	0.035 ± 0.029	1.5:1
Ca^{2+}/CaM	0.190 ± 0.057	0.5:1

[1]The concentration of Trx-KCBP in the supernatant (unbound) and pellet (bound) fractions from MT-binding experiments were used to fit a rectangular hyperbolae in order to obtain values for K_d and stoichiometry. A calmodulin:Trx-KCBP ratio of 1:1 and/or 100 μM free calcium were added to the appropriate reactions. Reactions were performed under constant MT concentration (2.0 μM) with Trx-KCBP concentrations ranging from 0.5-7.0 μM. Stoichiometry is expressed as the ratio of Trx-KCBP motor domain:tubulin dimer. Corrections were applied to account for Trx-KCBP pelleting in the absence of MTs (< 10%) and for tubulin that did not pellet (20%).

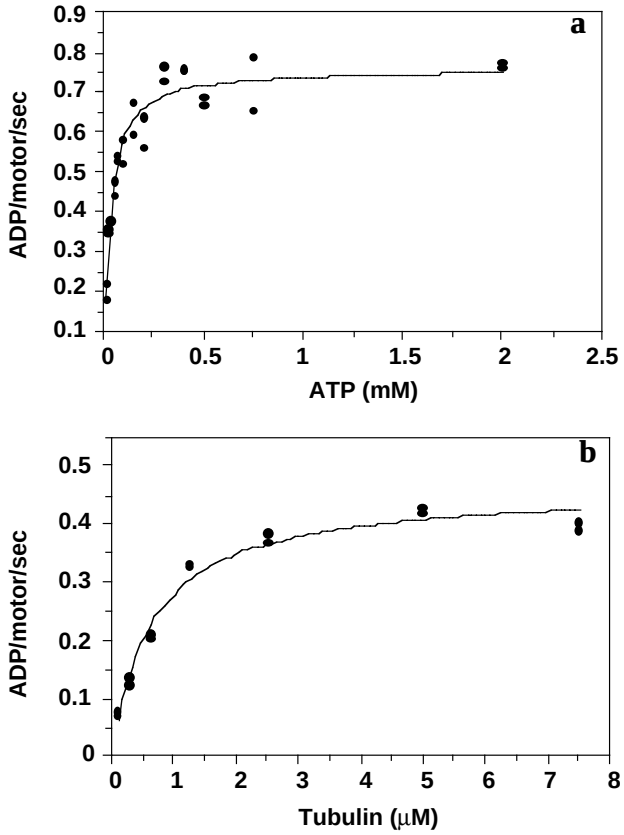

Figure 6.5. MT-stimulated ATPase rate of Trx-KCBP

The MT-stimulated ATPase rates of Trx-KCBP as a function of ATP concentration (a) and tubulin concentration (b) were determined using a couple pyruvate kinase-lactate dehydrogenase assay. For determination of K_{mATP} the tubulin concentration was 2.5 μM. For the determination of $K_{0.5MT}$ the concentration of MgATP was 1 mM. K_{mATP} and $K_{0.5MT}$ were calculated to be 0.030 ± 0.0035 mM and 0.65 ± 0.075 μM, respectively.

Table 6.2. Effect of Ca^{2+}/calmodulin on the ATPase activity of Trx-KCBP

	-MTs (s^{-1})	+MTs (s^{-1})
KCBP	0.07 ± 0.01 (9)	1.50 ± 0.06 (3)
+ 100 μM Ca^{2+}	0.07 ± 0.01 (5)	1.57 ± 0.02 (2)
+ 1X CaM	0.07 ± 0.01 (6)	1.28 ± 0.07 (3)
+ 100 μM Ca/1X CaM	0.10 ± 0.03 (6)	1.09 ± 0.02 (2)
+ 2X CaM	0.07 ± 0.01 (4)	1.41 ± 0.03 (2)
+ 100 μM Ca/2X CaM	0.07 ± 0.01 (3)	0.80 ± 0.02 (2)

ATPase rates were measured using 5'-γ-^{32}P ATP in reactions containing 4 mM MgATP and ± 10 μM taxol-stabilized GTP-depleted MTs as previously described (Chandra et al., 1993). Rates are expressed as k_{cat} (± standard error). Number of experiments are given in parentheses. Calmodulin:Trx-KCBP ratios of 1:1 (1X) or 2:1 (2X) and/or 100 μM free calcium were added to the appropriate reactions.

Discussion:

Consistent with previous motility studies (Song et al., 1997), Trx-KCBP exhibited the nucleotide sensitive MT binding and MT-stimulated ATPase activity characteristic of a MT-dependent motor protein. Ca^{2+}/calmodulin was found to inhibit the MT binding and MT-stimulated ATPase activity of Trx-KCBP in a concentration dependent manner. Excess Ca^{2+}/calmodulin eliminated MT binding in the presence of MgAMP-PNP as measured by standard pelleting assays (Figs. 6.2b, 6.3). However, lower Ca^{2+}/calmodulin (1:1 calmodulin:Trx-KCBP) levels resulted in sufficient Trx-KCBP binding to allow measurement of affinity and stoichiometry. Under these conditions, ~40% of Trx-KCBP remained bound to MTs in a pelleting assay (Fig. 6.3), the affinity of Trx-KCBP for MTs was decreased nearly 3-fold, and the apparent binding stoichiometry was reduced to a similar extent (Table 6.1). In comparison, calcium and equimolar calmodulin reduced the MT-stimulated ATPase activity by almost 30% (Table 6.2). The slightly different extents of Ca^{2+}/calmodulin inhibition observed in the MT-binding and ATPase assays may reflect the conditions of each assay (e.g., different nucleotides, simple binding vs. enzymatic activity coupled to conformational change). Calcium alone (free concentration of 100 μM) or calmodulin alone at 1:1 or 2:1 molar ratios to Trx-KCBP did not affect Trx-KCBP's MT binding, basal ATPase or MT-stimulated ATPase activities. Taken together, these data suggest that Ca^{2+}/calmodulin regulates Trx-KCBP activity by regulating its association with tubulin subunits.

Since each Trx-KCBP dimer contains 2 calmodulin binding sites (one per motor domain), three different complexes of calmodulin:Trx-KCBP may exist (0:2, 1:2 and 2:2 calmodulin:Trx-KCBP motor domain) and each may differ in MT binding properties. Experiments with dansyl calmodulin demonstrated that at 100 μM free calcium and 1:1 calmodulin:Trx-KCBP, ~70% of Trx-KCBP had calmodulin bound while at >1.5:1 calmodulin:Trx-KCBP, >95% of Trx-KCBP had calmodulin bound (data not shown). Thus, at excess Ca^{2+}/calmodulin (Figs 6.2b and 6.3), essentially all Trx-KCBP dimers have 2 calmodulin molecules bound, suggesting that this complex (2:2) has an extremely low affinity for MTs and may be considered "inactive". However, interpretation of the calcium and equimolar calmodulin results is more complicated since the results likely reflect contributions from a population of calmodulin:Trx-KCBP complexes in which the relative proportions of the three possible complexes is not known. For example, it is not clear whether one versus 2 calmodulin molecules bound would have the same effect on Trx-KCBP binding to MTs in the pelleting assay. Future analysis of KCBP monomer constructs should provide insight into this issue.

The observed inhibition by Ca^{2+}/calmodulin is consistent with a model in which Ca^{2+}/calmodulin regulates KCBP activity *in vivo* by affecting the motor's association with MTs. Based on the results, Ca^{2+}/calmodulin would promote KCBP dissociation from MTs by lowering motor affinity for MTs and would thereby inhibit KCBP-based motility in response to increases in cytosolic calcium. Stimuli such as temperature, light, mechanical stimulation and certain plant hormones have been reported to increase the cytosolic concentration of calcium (Bush, 1993). Transient increases in cytosolic calcium also have been reported in dividing plant cells and may serve to govern the metaphase to anaphase transition (Hepler, 1987; Hepler, 1992). KCBP has been localized to the preprophase band, mitotic spindle and phragmoplast in dividing *Arabidopsis* cells and may be involved in stabilizing these structures *in vivo* (Bowser and Reddy, 1997). If capable of crosslinking adjacent MTs or components of the spindle matrix, KCBP could by virtue of its minus-end directed motility generate forces that serve to stabilize the mitotic spindle. Furthermore, KCBP may be involved in the formation of a bipolar spindle in a manner similar to Ncd in oocytes (Matthies et al., 1996). An influx of calcium and its association with calmodulin at the onset of anaphase would inhibit KCBP and reduce opposition to forces pushing the spindle poles apart during anaphase B. Because localization of KCBP persists following anaphase B, KCBP could remain attached to spindle MTs by a second MT-binding site in an inactivated state. Following a return to normal cytosolic calcium levels KCBP could be reactivated and contribute to phragmoplast formation and stabilization.

KCBP, which may be ubiquitous in plants, is the only reported example of a MT motor heavy chain with a calmodulin-binding site. Calmodulin or calmodulin-like proteins have been identified as light chain subunits of certain myosins (Wolenski, 1995) and at least one axonemal dynein (King and Patelking, 1995). The question of whether calmodulin or a calmodulin-like protein acts as a light chain of KCBP awaits purification of the native motor. Calmodulin has also been reported to bind certain kinesin light chain isoforms (Matthies et al., 1993), but the role of calmodulin in regulation of kinesin and axonemal dynein is still not clear. For both kinesin (Matthies et al., 1993) and axonemal dynein (King and Patelking, 1995), calmodulin is present at the tail of the protein rather than at the motor-containing head domain as in the case of KCBP (and certain myosins such as brush border myosin I (see (Wolenski, 1995) for review)). However, despite the physically similar locations of the calmodulin-binding sites on KCBP and brush border myosin I, the effect of calcium on calmodulin binding is distinctly different (although the ultimate effect on motility is the same). In the case of brush border myosin I, calcium binding to calmodulin results in release of calmodulin from the motor and a

corresponding decrease in motility, whereas for KCBP, calcium binding to calmodulin promotes binding of calmodulin to the motor which in turn inhibits MT-based motility.

CHAPTER 7: CONCLUSIONS

As discussed in Chapter 1, kinesin and KLPs have been the subject of active research since the discovery of conventional kinesin in 1985 because of their fundamental roles in cellular organization, motility, and cell division. The research outlined here has contributed to our understanding of how two KLPs, the *Homo sapiens* mitotic kinesin-like protein-1 (HsMKLP-1) and the *Arabidopsis thaliana* kinesin-like calmodulin-binding protein (KCBP), interact with MTs and may be regulated by the cell *in vivo*. Although this work is focused on only 2 KLPs, several of the conclusions outlined here can be broadly applied to other members of the kinesin superfamily.

One of the primary goals of the present study was to characterize the structural and functional domains of HsMKLP-1 in order to define factors that contribute to HsMKLP-1 function, and the function of the MKLP-1 family in general, within the mitotic spindle. This work relied on the development of a heterologous protein expression system for expressing and purifying HsMKLP-1 proteins that would provide sufficient quantities of protein for characterization (Chapter 2). Expression of HsMKLP-1 proteins was initially tested in a standard T7 promoter based bacterial-expression strain (BL21(DE3)pLys). Poor expression in this strain was most likely due to differences in codon use between bacterial and human proteins, since HsMKLP-1 proteins were successfully expressed in a mammalian-codon optimized bacterial expression strain (BL21-CodonPlus-RIL), engineered to express additional copies of tRNAs recognizing arginine, isoleucine, and leucine codons that have been shown to limit the translation of proteins derived from AT-rich genomes. HsMKLP-1 proteins were also successfully expressed in insect cells using the baculovirus-expression system, which further suggests that poor expression of HsMKLP-1 in bacteria stems from differences in codon use.

The development of a heterologous protein expression system for expressing and purifying HsMKLP-1 proteins facilitated the generation of HsMKLP-1 specific antibodies (Chapter 3) and allowed a detailed characterization of the HsMKLP-1 motor domain (Chapter 4). This system is predicted to serve as a useful tool for future characterization of HsMKLP-1 proteins. Furthermore, the strategies for heterologous expression of HsMKLP-1 proteins outlined in the present study can be readily applied to the development of protein expression systems for other KLPs, in particular KLPs from human or mammalian sources.

As part of an effort to characterize native HsMKLP-1, baculovirus-expressed C-terminal domains of HsMKLP-1 were used to generate MKLP-1 specific antibodies (Chapter 3). These antibodies were able to recognize native HsMKLP-1 by immunoblot, immunoprecipitation, and immunofluorescence, which suggests that they will be useful for further characterization of native HsMKLP-1. In collaboration with Dr. Les Wilson's lab, these antibodies have been used to partially purify HsMKLP-1 from HeLa cells (DeLuca et al., 2001), which represents a significant step toward efforts to characterize the structural organization, MT-binding, and motility of native HsMKLP-1.

Bacterially-expressed N-terminal domains of HsMKLP-1 were used to characterize the ATPase and MT-binding properties of the HsMKLP-1 motor domain (Chapter 4) in order to determine how the MKLP-1 motor domain functionally compares to that of kinesin and Ncd. The MKLP-1 motor domain is distinguished by two specific features (~64 AA insertion, unique neck linker) that differentiate it from kinesin and other KLPs, and which may confer novel properties important for the function of the MKLP-1 family. Two key differences in the activity of the HsMKLP-1 motor domain were noted. The first was that the dimeric HsMKLP-1 motor domain bound MTs much tighter than did the monomeric motor domain in the presence of ATP and ADP, and at NaCl concentrations sufficient to disrupt the binding of the monomer. This is opposite to what is observed for monomeric and dimeric motor domains of kinesin and Ncd, in which the dimeric motor domain exhibits reduced affinity for MTs as compared to the monomer. Second, the concentration of ATP required for half-maximal ATPase activity (K_{mATP}) of HsMKLP-1 was ~2-20 fold higher than values reported for similar kinesin and KLP constructs, suggesting that HsMKLP-1 affinity for ATP is relatively weak.

This work established that the HsMKLP-1 motor domain exhibits key differences that functionally differentiate it from that of kinesin and Ncd and suggests that differences within the catalytic core and neck linker sequence of HsMKLP-1 may confer functional specificity to the HsMKLP-1 motor domain, related to its role within the mitotic spindle. This is the first detailed kinetic characterization of a member of the MKLP-1 family and will serve as a basis for future work that will address how differences in the motor domain of HsMKLP-1 relate to the function of this protein in the mitotic spindle. For example, the unique neck linker sequence of HsMKLP-1 suggests that HsMKLP-1's mechanism of force generation may be different from that of other plus-end directed KLPs and may account for the observed differences in the MT binding and ATPase activity of the HsMKLP-1 motor domain. Furthermore, the position, size, and degree of conservation of the ~64 AA insertion within the MKLP-1 motor domain suggests that it is also

important for the function of the MKLP-1 family. The development of a heterologous protein expression system for expressing and purifying large quantities of the HsMKLP-1 motor domain will also facilitate efforts to determine the crystal structure of this part of the protein, in order to understand how differences in structure contribute to its function.

The second goal of this project was to define factors that contribute to the regulation of mitotic KLPs. Although specific roles for KLPs in mitosis have been defined, very little is known about how cells regulate the activity of these proteins *in vivo*. My first objective was to identify sequences responsible for directing nuclear localization of HsMKLP-1 in order to establish the role of nuclear localization in regulating the activity of HsMKLP-1 during interphase (Chapter 5). Although this work focused solely on HsMKLP-1, the observation that members of four of the five mitotic KLP families localize to nuclei in interphase cells suggests that nuclear localization may be a general mechanism of regulation for mitotic KLPs.

Nuclear localization determinants were limited to the C-terminal 132 AA of HsMKLP-1, which includes 2 of 5 putative nuclear localization sequences (NLS) identified by sequence analysis. Mutation of one of these NLS's (^{799}PNGSRKRR^{806} to ^{799}PNGSR<u>TS</u>R^{806}) was sufficient to disrupt nuclear localization of full-length HsMKLP-1. In addition, removal of the C-terminal 26 AA's of HsMKLP-1 (which includes the remaining NLS) also abolished nuclear localization, which suggests that the NLS ^{799}PNGSRKRR^{806} and sequences at the extreme C-terminus of HsMKLP-1 are required for nuclear uptake. The importance of both of these sequences in directing nuclear import suggests that they may contribute to a functional NLS *in vivo*. HsMKLP-1 is the first KLP for which nuclear localization sequences have been identified and this work will serve as a model for the identification of nuclear localization determinants in other KLPs.

In the absence of a functional NLS, HsMKLP-1 localized to MT plus ends, suggesting that nuclear localization serves to regulate HsMKLP-1's interaction with MTs. Expression of HsMKLP-1 in the interphase cytoplasm did not result in any noticeable perturbation of the interphase MT array and future work will be needed to address what effect, if any, expression of HsMKLP-1 in the cytoplasm has on cells. Nuclear localization may be just one of several mechanisms that serves to regulate the activity of HsMKLP-1 *in vivo*, as suggested by the interaction of MKLP-1 family members with polo-like kinase (Adams et al., 1998; Lee et al., 1995) and aurora-related kinase (Severson et al., 2000).

The second objective of this project was to determine the effect of Ca^{2+}/calmodulin on the activity of the kinesin-like calmodulin-binding protein (KCBP) (Chapter 6). The calmodulin-binding site of KCBP was previously localized to a 23 AA sequence within the motor domain (Reddy et al., 1996a) and Ca^{2+}/calmodulin was found to inhibit the MT-binding and MT-stimulated ATPase activity of KCBP in a concentration-dependent manner. Ca^{2+}/calmodulin reduced the affinity and apparent stoichiometry of KCBP-binding to MTs, which is consistent with a model for Ca^{2+}/calmodulin regulating the activity of KCBP *in vivo* by regulating its association with tubulin subunits. A model for how calcium and calmodulin may regulate the activity of KCBP during mitosis was presented, and will serve to guide future experiments on the Ca^{2+}/calmodulin regulation of KCBP *in vivo*.

Although KCBP was the first calmodulin-binding KLP identified and previously suggested to be unique to plants, a calmodulin-binding KLP has since been identified in sea urchin (kinesin-C) (Rogers et al., 1999). This suggests that calcium and calmodulin regulation of KLPs is not limited to plants and may be a more widespread mechanism of regulation of KLPs. Although the effect of Ca^{2+}/calmodulin on the activity of kinesin-C has not been reported, the calmodulin binding site of kinesin-C is also located within the motor domain, which suggests that the effects of Ca^{2+}/calmodulin on the activity of kinesin-C will be similar to that of KCBP. The work presented here will serve as a model for defining the effects of Ca^{2+}/calmodulin on the activity of kinesin-C and subsequently identified calmodulin-binding KLPs.

LITERATURE CITED

Adams, R.R., A.A.M. Travares, A. Salzberg, H.J. Bellen, and D.M. Glover. 1998. *pavarotti* encodes a kinesin-like protein required to organize the central spindle and contractile ring for cytokinesis. *Genes & Dev.* 12:1483-1494.

Asada, T., R. Kuriyama, and H. Shibaoka. 1997. TKRP125, a kinesin-related protein involved in the centrosome-independent organization of the cytokinetic apparatus in tobacco BY-2 cells. *J. Cell Sci*. 110:179-189.

Asada, T., and H. Shibaoka. 1994. Isolation of polypeptides with microtubule-translocating activity from phragmoplasts of tobacco BY-2 cells. *J. Cell Sci*. 107:2249- 2257.

Barton, N.R., and L.S.B. Goldstein. 1996. Going mobile: Microtubule motors and chromosome segregation. *Proc. Natl. Acad. Sci. USA.* 93:1735-1742.

Berger, B., D. Wilson, E. Wolf, T. Tonchev, M. Milla, and P. Kim. 1995. Predicting coiled coils by use of pairwise residue correlation. *Proc. Natl. Acad. Sci.* 92:8259-8263.

Bertrand, B., S. Wakabayashi, T. Ikeda, J. Pouyssegur, and M. Shigekawa. 1994. The Na+/H+ exchanger isoform 1 (NHE1) is a novel member of the calmodulin-binding proteins. *J. Biol. Chem*. 269:13703-13709.

Blangy, A., P. Chaussepied, and E.A. Nigg. 1998. Rigor-type mutation in the kinesin-related protein HsEg5 changes its subcellular localization and induces microtubule binding. *Cell Motil. Cytoskel.* 40:174-182.

Blangy, A., H.A. Lane, P. D'Herin, M. Harper, M. Kress, and E.A. Nigg. 1995. Phosphorylation by p34cdc2 regulates spindle association of human Eg5, a kinesin-related motor essential for bipolar spindle formation in vivo. *Cell*. 83:1159-1169.

Boleti, H., E. Karsenti, and I. Vernos. 1996. Xklp2, a novel Xenopus centrosomal kinesin-like protein required for centrosome separation during mitosis. *Cell*. 84:49-59.

Bowser, J., and A.S.N. Reddy. 1997. Localization of a kinesin-like calmodulin-binding protein in dividing cells of Arabidopsis and tobacco. *Plant J.* 12:1429-1437.

Bradford, M. 1976. A rapid and sensitive method for the quantitation of microgram quantities of protein utilizing the principle of protein-dye binding. *Anal. Biochem.* 72:248-254.

Brinkley, W.B.R. 1997. Microtubules: A brief historical perspective. *J. Struct. Biol.* 118:84-86.

Bush, D.S. 1993. Regulation of cytosolic calcium in plants. *Plant Physiol.* 103:7-13.

Cai, G., A. Bartalesi, C. Delcasino, A. Moscatelli, A. Tiezzi, and M. Cresti. 1993. The kinesin-immunoreactive homologue from Nicotiana tabacum pollen tubes: Biochemical properties and subcellular localization. *Planta*. 191:496-506.

Case, R.B., D.W. Pierce, N. Hom-Booher, C.L. Hart, and R.D. Vale. 1997. The directional preference of kinesin motors is specified by an element outside of the motor catalytic domain. *Cell*. 90:959-966.

Chandra, R., and S.A. Endow. 1993. Expression of microtubule motor proteins in bacteria for characterization in in vitro motility assays. *In* Motility assays for motor proteins. Vol. 39. J.M. Scholey, editor. Academic Press, Inc., San Diego. 115-127.

Chandra, R., E.D. Salmon, H.P. Erickson, A. Lockhart, and S.A. Endow. 1993. Structural and functional domains of the Drosophila ncd microtubule motor protein. *J. Biol. Chem*. 268:9005-9013.

Cole, D.G., S.W. Chinn, K.P. Wedaman, K. Hall, T. Vuong, and J.R. Scholey. 1993. Novel heterotrimeric kinesin-related protein purified from sea urchin eggs. *Nature*. 366:268-270.

Cole, D.G., W.M. Saxton, K. Sheehan, and J.M. Scholey. 1994. A slow homotetrameric kinesin related motor protein purified from Drosophila embryos. *J. Biol. Chem*. 269:22913-22916.

Crevel, I.M.-T.C., A. Lockhart, and R.A Cross. 1996. Weak and strong states of kinesin and ncd. *J. Mol. Biol.* 257:66-76.

De Cuevas, M., T. Tao, and L.S. Goldstein. 1992. Evidence that the stalk of Drosophila kinesin heavy chain is an alpha-helical coiled coil. *J. Cell Biol*. 116:957-965.

Deavours, B.E., A.S.N. Reddy, and R.A. Walker. 1998. Ca2+/calmodulin regulation of the Arabidopsis kinesin-like calmodulin-binding protein. *Cell Motil. Cytoskel.* 40:408-416.

DeLuca, J.G., C.N. Newton, R.H. Himes, M.A. Jordan, and L. Wilson. 2001. Purification and characterization of native conventional kinesin, HSET, and CENP-E from mitotic HeLa cells. *J. Biol. Chem.* 276:28014-28021.

Downing, K.H. and E. Nogales. 1998. Tubulin and microtubule structure. *Curr. Opin. Cell Biol*. 10:16-22.

Echeverii, C.J., B.M. Paschal, K.T. Vaughan, and R.B. Vallee. 1996. Molecular characterization of the 50-kD subunit of dynactin reveals function for the complex in chromosome alignment and spindle organization during mitosis. *J. Cell Biol*. 132:617- 633.

Endow, S.A. 1993. Chromosome distribution, molecular motors and the claret protein. *Trends Gen*. 9:52-55.

Endow, S.A., and K.W. Waligora. 1998. Determinants of kinesin motor polarity. *Science*. 281:1200-1202.

Fabiato, F. 1979. Calculator programs for computing the composition of the solutions containing multiple metals and ligands used for experiments in skinned muscle cells. *J. Physiol. Paris*. 75:463-505.

Fan, J., A.D. Griffiths, A. Lockhart, R.A. Cross, and L.A. Amos. 1996. Microtubule minus ends can be labeled with a phage display antibody specific to alpha-tubulin. *J. Mol. Biol.* 259:325-330.

Fischer, R., Y. Wei, J. Anagli, and M.W. Berchtold. 1996. Calmodulin binds to and inhibits GTP binding of the ras-like GTPase Kir/Gem. *J. Biol. Chem*. 271:25067-25070.

Foster, K., and S. Gilbert. 2000. Kinetic studies of dimeric Ncd: evidence that Ncd is not processive. *Biochem.* 39:1784-1791.

Foster, K.A., J.J. Correia, and S.P. Gilbert. 1998. Equilibrium binding studies of non-claret disjunctional protein (Ncd) reveal cooperative interactions between the motor domains. *J. Biol. Chem.* 273:35307-35318.

Foster, K.A., A.T. Mackey, and S.P. Gilbert. 2001. A mechanistic model for Ncd directionality. *J. Biol. Chem.* 276:19259-19266.

Giet, R., R. Uzbekow, F. Cubizolles, K. Le Guellec, and C. Prigent. 1999. The Xenopus laevis aurora-related protein kinase pEg2 associates with and phosphorylates the kinesin-related protein XlEg5. *J. Biol. Chem.* 274:15005-15013.

Gilbert, S.P., and K.A. Johnson. 1993. Expression, purification, and characterization of the Drosophila kinesin motor domain produced in Escherichia coli. *Biochem*. 32:4677-4684.

Gilbert, S.P., and A.T. Mackey. 2000. Kinetics: A tool to study molecular motors. *Methods*. 22:337-354.

Gilbert, S.P., M.L. Moyer, and K.A. Johnson. 1998. Alternating site mechanism of the kinesin Atpase. *Biochem.* 37:792-799.

Gilbert, S.P., M.R. Webb, M. Brune, and K.A. Johnson. 1995. Pathway of processive ATP hydrolysis by kinesin. *Nature*. 373:671-676.

Gilroy, S. 1996. Signal transduction in barley aleurone protoplasts is calcium dependent and independent. *Plant Cell*. 8:2193- 2209.

Gorlich, D. 1998. Transport into and out of the cell nucleus. *EMBO J*. 17:2721-2727.

Greene, E.A., S. Henikoff, and S.A. Endow. 1996. The kinesin homepage. *www.blocks.fhcrc.org/~kinesin/*.

Gryka, M.A., and J.R. McIntosh. 1998. Overexpression of deletion mutants of MKLP-1 results in defective cytokinesis. *Mol. Biol. Cell*. 9S:392a.

Gulick, A.M., H. Song, S.A. Endow, and I. Rayment. 1998. X-ray crystal structure of the yeast Kar3 motor domain complexed with Mg.ADP to 2.3 A resolution. *Biochem*. 37:1769-1776.

Hackney, D.D. 1988. Kinesin ATPase: rate-limiting ADP release. *Proc. Natl. Acad. Sci. USA*. 85:6314-6318.

Hackney, D.D., J.D. Levitt, and D.D. Wagner. 1991. Characterization of alpha 2 beta 2 and alpha 2 forms of kinesin. *Biochem. Biophys. Res. Comm*. 174:810-815.

Hall, D.H., and E.M. Hedgecock. 1991. Kinesin-related gene unc-104 is required for axonal transport of synaptic vesicles in C. elegans. *Cell*. 65:837-847.

Hancock, W.O., and J. Howard. 1999. Kinesin's processivity results from mechanical and chemical coordination between the ATP hydrolysis cycles of the two motor domains. *Proc. Natl. Aca. Sci*. 96:13147-13152.

Harrison, B.C., R.S. Marchese, S.P. Gilbert, N. Cheng, A.C. Steven, and K.A. Johnson. 1993. Decoration of the microtubule surface by one kinesin head per tubulin heterodimer. *Nature*. 362:73-75.

Hatsumi, M., and S.A. Endow. 1992. The Drosophila ncd microtubule motor protein is spindle-associated in meiotic and mitotic cells. *J. Cell Sci*. 103:1013-1020.

Henningsen, U., and M. Schliwa. 1997. Reversal in the direction of movement of a molecular motor. *Nature*. 389:93-96.

Henson, J.H., D.G. Cole, M. Terasaki, D. Rashid, and J.M. Scholey. 1995. Immunolocalization of the heterotrimeric kinesin-related protein KRP(85/95) in the mitotic apparatus of sea urchin embryos. *Dev. Biol*. 171:182-194.

Hepler, P.K. 1987. Free calcium increases during anaphase in stamen hair cells of Tradescantia. *J. Cell Biol*. 105:2137-2143.

Hepler, P.K. 1992. Calcium and mitosis. *Intl. Rev. Cytol*. 138:239-268.

Hirokawa, N., R. Sato-Yoshitake, N. Kobayashi, K.K. Pfister, G.S. Bloom, and S.T. Brady. 1991. Kinesin associates with anterogradely transported membranous organelles in vivo. *J. Cell Biol*. 114:295-302.

Holzbaur, E.L.F., and R.B. Vallee. 1994. Dyneins: molecular structure and cellular function. *Annu. Rev. Cell Biol*. 10:339- 372.

Howard, J., A.J. Hudspeth, and R.D. Vale. 1989. Movement of microtubules by single kinesin molecules. *Nature*. 342:154-158.

Huang, T.G., and D.D. Hackney. 1994. *Drosophila* kinesin minimal motor domain expressed in *Escherichia coli*: Purification and kinetic characterization. *J. Biol. Chem*. 269:16493-16501.

Huang, T.G., J. Suhan, and D.D. Hackney. 1994. Drosophila kinesin motor domain extending to amino acid position 392 is dimeric when expressed in Escherichia coli. *J. Biol. Chem*. 269:16502-16507.

Jiang, W., M.F. Stock, L. Xun, and D.D. Hackney. 1997. Influence of the kinesin neck domain on dimerization and ATPase kinetics. *J. Biol. Chem*. 272:7626-7632.

Kashina, A.S., R.J. Baskin, D.G. Cole, K.P. Wedaman, W.M. Saxton, and J.M. Scholey. 1996. A bipolar kinesin. *Nature*. 379:270-272.

Kawaguchi, K., and S. Ishiwata. 2001. Nucleotide-dependent single-to double-headed binding of kinesin. *Science*. 291:667-669.

Kikkawa, M., Y. Okada, and N. Hirokawa. 2000. 15 A resolution model of the monomeric kinesin motor, KIF1A. *Cell*. 100:241-252.

Kim, A.J., and S.A. Endow. 2000. A kinesin family tree. *J. Cell Sci*. 113:3681-3682.

King, S.M., and R.S. Patelking. 1995. Identification of a Ca2+ binding light chain within Chlamydomonas outer arm dynein. *J. Cell Sci*. 108:3757-3764.

Kozielski, F., S. Sack, A. Marx, M. Thormahlen, E. Schonbrunn, V. Biou, A. Thompson, E.M. Mandelkow, and E. Mandelkow. 1997. The crystal structure of dimeric kinesin and implications for microtubule-dependent motility. *Cell*. 91:985-994.

Kull, F.J., E.P. Sablin, R. Lau, R.J. Fletterick, and R.D. Vale. 1996. Crystal structure of the kinesin motor domain reveals a structural similarity to myosin. *Nature*. 380:550-555.

Kuriyama, R., S. Dragas-Granoic, T. Maekawa, A. Vassilev, A. Khodjakov, and H. Kobayashi. 1994. Heterogeneity and microtubule interaction of the CHO1 antigen, a mitosis specific kinesin-like protein. *J. Cell Sci*. 107:3485-3499.

Kuriyama, R., M. Kofron, R. Essner, T. Kato, S. Dragas-Granoic, C.K. Omoto, and A. Khodjakov. 1995. Characterization of a minus end-directed kinesin-like motor protein from cultured mammalian cells. *J. Cell Biol*. 129:1049-1059.

Kuznetsov, S.A., and V.I. Gelfand. 1986. Bovine brain kinesin is a microtubule-activated ATPase. *Proc. Natl. Acad. Sci. USA*. 83:8530-8534.

Kuznetsov, S.A., E.A. Vaisberg, N.A. Shanina, N.N. Magretova, V.Y. Chernyak, and V.I. Gelfand. 1988. The quaternary structure of bovine brain kinesin. *EMBO J*. 7:353-356.

Kuznetsov, S.A., Y.A. Vaisberg, S.W. Rothwell, D.B. Murphy, and V.I. Gelfand. 1989. Isolation of a 45-kDa fragment from the kinesin heavy chain with enhanced ATPase and microtubule-binding activities. *J. Biol. Chem*. 264:589-595.

LaVallie, E.R., E.A. DiBlasio, S. Kovacic, K.L. Grant, P.F. Schendel, and J.M. McCoy. 1993. A thioredoxin gene fusion expression system that circumvents inclusion body formation in the E. coli cytoplasm. *Bio/Technology*. 11:187-193.

Lee, K.S., Y.L. Yuan, R. Kuriyama, and R.L. Erikson. 1995. Plk is an M-phase-specific protein kinase and interacts with a kinesin-like protein, CHO1/MKLP-1. *Mol. Cell Biol*. 15:7143-7151.

Liao, H., G. Li, and T.J. Yen. 1994. Mitotic regulation of microtubule cross-linking activity of CENP-E kinetochore protein. *Science*. 265:394-398.

Liu, B., R.J. Cyr, and B.A. Palevitz. 1996. A kinesin-like protein, KatAp, in the cells of Arabidopsis and other plants. *Plant Cell*. 8:119-132.

Liu, B., and B.A. Palevitz. 1996. Localization of a kinesin-like protein in generative cells of tobacco. *Protoplasma*. 195:78- 89.

Lockhart, A., and R.A. Cross. 1994. Origins of reversed directionality in the ncd molecular motor. *EMBO J.* 13:751-757.

Lockhart, A., I.M.-T.C. Crevel, and R.A. Cross. 1995a. Kinesin and ncd bind through a single head to microtubules and compete for a shared MT binding site. *J. Mol. Biol*. 249:763-771.

Lockhart, A., and R.A. Cross. 1996. Kinetics and motility of the Eg5 microtubule motor. *Biochem.* 35:2365-2373.

Lockhart, A., R.A. Cross, and D.F.A. McKillop. 1995b. ADP release is the rate-limiting step of the MT activated ATPase of non-claret disjunctional and kinesin. *FEBS*. 368:531-535.

Luckow, V.A. 1991. Cloning and expression of heterologous genes in insect cells with baculovirus vectors. *In* Recombinant DNA Technology and Applications. A. Prokop, R.K. Bajpai, and C. Ho, editors. McGraw-Hill, New York. 97-152.

Ma, Y.Z., and E.W. Taylor. 1995a. Kinetic mechanism of kinesin motor domain. *Biochem*. 34:13233-13241.

Ma, Y.Z., and E.W. Taylor. 1995b. Mechanism of microtubule kinesin ATPase. *Biochem*. 34:13242-13251.

Mackey, A.T., and S.P. Gilbert. 2000. Moving a microtubule may require two heads: A kinetic investigation of monomeric Ncd. *Biochem.* 39:1346-1355.

Mandelkow, E. and E.M. Mandelkow. 1984. Microtubule structure. *Curr. Opin. Struct. Biol*. 4:171-179.

Matthies, H.J., R.J. Miller, and H.C. Palfrey. 1993. Calmodulin binding to and cAMP-dependent phosphorylation of kinesin light chains modulate kinesin ATPase activity. *J. Biol. Chem*. 268:11176-11187.

Matthies, H.J.G., H.B. McDonald, L.S.B. Goldstein, and W.E. Theurkauf. 1996. Anastral meiotic spindle morphogenesis: role of the non-claret disjunctional kinesin-like protein. *J. Cell Biol*. 134:455-464.

McIntosh, J.R., and C.M. Pfarr. 1991. Mitotic motors. *J. Cell Biol*. 115:577-585.

Miki, H., M. Setou, K. Kaneshiro, and N. Hirokawa. 2001. All kinesin superfamily protein, KIF, genes in mouse and human. *Proc. Natl. Acad. Sci.* 98:7004-7011.

Mitchison, T., and M. Kirschner. 1984. Dynamic instability of microtubule growth. *Nature*. 312:237-242.

Mitsui, H., S. Hasezawa, T. Nagata, and H. Takahashi. 1996. Cell cycle dependent accumulation of a kinesin like protein, Katb/C, in synchronized tobacco BY 2 Cells. *Plant Mol. Biol*. 30:177-181.

Mitsui, H., K. Nakatani, K. Yamaguchi-Shinozaki, K. Shinozaki, K. Nishikawa, and H. Takahashi. 1994. Sequencing and characterization of the kinesin-related genes katB and katC of Arabidopsis thaliana. *Plant Mol. Biol*. 25:865-876.

Miyamoto, C., G.E. Smith, J. Farrell-Towt, R. Chizzonite, M.D. Summers, and G. Ju. 1985. Production of human c-myc protein in insect cells infected with a baculovirus expression vector. *Mol. Cell Biol.* 5:2860-2865.

Moore, J.D., and S.A. Endow. 1996. Kinesin proteins: A phylum of motors for microtubule based motility. *Bioessays*. 18:207-219.

Moore, J.D., H. Song, and S.A. Endow. 1996. A point mutation in the microtubule binding region of the Ncd motor protein reduces motor velocity. *EMBO J*. 15:3306-3314.

Moyer, M.L., S.P. Gilbert, and K.A. Johnson. 1996. Purification and characterization of two monomeric kinesin constructs. *Biochem*. 35:6321-6329.

Moyer, M.L., S.P. Gilbert, and K.A. Johnson. 1998. Pathway of ATP hydrolysis by monomeric and dimeric kinesin. *Biochem.* 37:800-813.

Nangaku, M., R. Sato-Yoshitake, Y. Okada, Y. Noda, R. Takemura, H. Yamazaki, and N. Hirokawa. 1994. KIF1B, a novel microtubule plus end-directed monomeric motor protein for transport of mitochondria. *Cell*. 79:1209-1220.

Narasimhulu, S.B., Y. Kao, and A.S.N. Reddy. 1997. Interaction of Arabidopsis kinesin-like calmodulin-binding protein with tubulin subunits: modulation by Ca2+-calmodulin. *Plant J.* 12:1139-1149.

Nigg, E.A., A. Blangy, and H.A. Lane. 1996. Dynamic changes in nuclear architecture during mitosis: on the role of protein phosphorylation in spindle assembly and chromosome segregation. *Exp. Cell Res*. 229:174-180.

Nislow, C., V.A. Lombrillo, R. Kuriyama, and J.R. McIntosh. 1992. A plus-end-directed motor enzyme that moves antiparallel microtubules in vitro localizes to the interzone of mitotic spindles. *Nature*. 359:543-547.

Nislow, C., C. Sellitto, R. Kuriyama, and J.R. McIntosh. 1990. A monoclonal antibody to a mitotic microtubule-associated protein blocks mitotic progression. *J. Cell Biol*. 111:511-522.

Noda, Y., R. Sato-Yoshitake, S. Kondo, M. Nangaku, and N. Hirokawa. 1995. KIF2 is a new microtubule-based anterograde motor that transports membranous organelles distinct from those carried by kinesin heavy chain or KIF3A/B. *J. Cell Biol*. 129:157-167.

O'Reilly, D.R., L.K. Miller, and V.A. Luckow. 1994. Baculovirus Expression Vectors: A Laboratory Manual. Oxford University Press, New York.

Ohta, T., M. Kimble, R. Essner, M. Kofron, and R. Kuriyama. 1996. Cell cycle dependent expression of the CHO2 antigen, a minus end directed kinesin like motor in mammalian cells. *Protoplasma*. 190:131-140.

Okada, Y., and N. Hirokawa. 1999. A processive single-headed motor: kinesin superfamily protein KIF1A. *Science*. 283:1152-1157.

Okada, Y., and N. Hirokawa. 2000. Mechanism of the single-headed processivity: Diffusional anchoring between the K-loop of kinesin and the C terminus of tubulin. *Proc. Natl. Acad. Sci.* 97:640-645.

Okada, Y., H. Yamazaki, Y. Sekine-Aizawa, and N. Hirokawa. 1995. The neuron-specific kinesin superfamily protein KIF1A is a unique monomeric motor for anterograde axonal transport of synaptic vesicle precursors. *Cell*. 81:769-780.

Oppenheimer, D.G., M.A. Pollock, J. Vacik, D.B. Szymanski, B. Ericson, K. Feldmann, and M.D. Marks. 1997. Essential role of a kinesin-like protein in Arabidopsis trichome morphogenesis. *Proc. Natl. Acad. Sci.* 94:6261-6266.

Pechatnikova, E., and E.W. Taylor. 1999. Kinetics processivity and the direction of motion of Ncd. *Biophy. J.* 77:1003-1016.

Pechnatnikova, E., and E.W. Taylor. 1997. Kinetic mechanism of monomeric non-claret disjunctional protein (Ncd) ATPase. *J. Biol. Chem.* 272:30735-30740.

Pooviah, B.W., and A.S.N. Reddy. 1993. Calcium and signal transduction in plants. *Crit. Rev. Plant Sci*. 12:185-211.

Porter, M.E., and K.A. Johnson. 1989. Dynein structure and function. *Annu. Rev. Cell Biol*. 5:119-151.

Powers, J., O. Bossinger, D. Rose, S. Strome, and W. Saxton. 1998. A nematode kinesin required for cleavage furrow advancement. *Curr. Biol.* 8:1133-1136.

Raich, W.B., A.N. Moran, J.H. Rothman, and J. Hardin. 1998. Cytokinesis and midzone microtubule organization in Caenorhabditis elegans require the kinesin-like protein ZEN-4. *Mol. Biol. Cell*. 9:2037-2049.

Reddy, A.S.N., S.B. Narasimhulu, and I.S. Day. 1997. Structural organization of a gene encoding a novel calmodulin-binding kinesin-like protein from Arabidopsis. *Gene*. 204:195-200.

Reddy, A.S.N., S.B. Narasimhulu, F. Safadi, and M. Golovkin. 1996a. A plant kinesin heavy chain like protein is a calmodulin binding protein. *Plant J*. 10:9-21.

Reddy, A.S.N., F. Safadi, S.B. Narasimhulu, M. Golovkin, and X. Hu. 1996b. A novel plant calmodulin binding protein with a kinesin heavy chain motor domain. *J. Biol. Chem*. 271:7052-7060.

Rice, S., A.W. Lin, D. Safer, C.L. Hart, N. Naber, B.O. Carragher, S.M. Cain, E. Pechatnikova, E.M. Wilson-Kubalek, M. Whittaker, E. Pate, R. Cooke, E.W. Taylor, R.A. Milligan, and R.D. Vale. 1999. A structural change in the kinesin motor protein that drives motility. *Nature*. 402:778-784.

Roberts, D.M., and A.C. Harmon. 1992. Calcium-modulated proteins: targets of intracellular calcium signals in higher plants. *Annu. Rev. Plant Phys. Plant Mol. Biol*. 43:375-414.

Rogers, G.C., K.K. Chui, E.W. Lee, K.P. Wedaman, D.J. Sharp, G. Holland, R.L. Morris, and J.M. Scholey. 2000. A kinesin-related protein, KRP(180), positions prometaphase spindle poles during early sea urchin embryonic cell division. *J. Cell Biol*. 150:499-512.

Rogers, G.C., C.L. Hart, K.P. Wedaman, and J.M. Scholey. 1999. Identification of kinesin-C, a calmodulin-binding carboxy-terminal kinesin in animal (Strongylocentrotus purpuratus) cells. *J. Mol. Biol*. 294:1-8.

Romberg, L., and R.D. Vale. 1993. Chemomechanical cycle of kinesin differs from that of myosin. *Nature*. 361:168-170.

Rosenfeld, S.S., B. Rener, J. Correia, M.S. Mayo, and H.C. Cheung. 1996. Equilibrium studies of kinesin-nucleotide intermediates. *J. Biol. Chem.* 271:9473-9482.

Sablin, E.P., R.B. Case, S.C. Dai, C.L. Hart, A. Ruby, R.D. Vale, and R.J. Fletterick. 1998. Direction determination in the minus-end-directed kinesin motor ncd. *Nature*. 395:813-816.

Sablin, E.P., F.J. Kull, R. Cooke, R.D. Vale, and R.J. Fletterick. 1996. Crystal structure of the motor domain of the kinesin related motor Ncd. *Nature*. 380:555-559.

Sack, S., J. Muller, A. Marx, M. Thormahlen, E.M. Mandelkow, S.T. Brady, and E. Mandelkow. 1997. X-ray structure of motor and neck domains from rat brain kinesin. *Biochem.* 36:16155-16165.

Sadhu, A., and E.W. Taylor. 1992. A kinetic study of the kinesin ATPase. *J. Biol. Chem*. 267:11352-11359.

Sambrook, J., E.F. Fritsch, and T. Maniatis. 1989. Molecular Cloning: A Laboratory Manual. Cold Spring Harbor Lab Press, Plainview, NY.

Sawin, K.E., and T.J. Mitchison. 1995. Mutations in the kinesin-like protein Eg5 disrupting localization to the mitotic spindle. *Proc. Natl. Acad. Sci. USA*. 92:4289-4293.

Schmid, K.J., and D. Tautz. 1998. Sequence and expression of DmMKLP1, a homolog of the human MKLP1 kinesin-like protein from Drosophila melanogaster. *Dev. Genes Evol.* 208:474-476.

Schnitzer, M.J., K. Visscher, and S.M. Block. 2000. Force production by single kinesin molecules. *Nature Cell Biol.* 2:718-723.

Sellitto, C., and R. Kuriyama. 1988. Distribution of a matrix component of the midbody during the cell cycle in chinese hamster ovary cells. *J. Cell Biol*. 106:431-439.

Severson, A.F., D.R. Hamill, J.C. Carter, J. Schumacher, and B. Bowerman. 2000. The aurora-related kinase AIR-2 recruits Zen-4/CeMKLP1 to the mitotic spindle at metaphase and is required for cytokinesis. *Curr. Biol*. 10:1162-1171.

Sharp, D.J., R. Kuriyama, and P.W. Baas. 1996. Expression of a kinesin related motor protein induces Sf9 cells to form dendrite like processes with nonuniform microtubule polarity orientation. *J. Neurosci*. 16:4370-4375.

Sharp, D.J., G.C. Rogers, and J.M. Scholey. 2000. Microtubule motors in mitosis. *Nature*. 407:41-47.

Siegel, L.M., and K.J. Monty. 1966. Determination of molecular weights and frictional ratios of proteins in impure systems by use of gel filtration and density gradient centrifugation. Application to crude preparations of sulfite and hydroxylamine reductases. *Biochim. Biophys. Acta*. 112:346-362.

Song, H., M. Golovkin, A.S.N. Reddy, and S.A. Endow. 1997. In vitro motility of AtKCBP, a calmodulin-binding kinesin protein of Arabidopsis. *Proc. Natl. Acad. Sci*. 94:322- 327.

Spector, D.L., R.D. Goldman, and L.A. Leinwand. 1998. Cells: A Laboratory Manual. Cold Spring Harbor Laboratory Press.

Turner, J., R. Anderson, J. Guo, C. Beraud, R. Fletterick, and R. Sakowicz. 2001. Crystal structure of the mitotic spindle kinesin Eg5 reveals a novel conformation of the neck-linker. *J. Biol. Chem.* 276:25496-25502.

Vaisberg, E.A., M.P. Koonce, and J.R. Mcintosh. 1993. Cytoplasmic dynein plays a role in mammalian mitotic spindle formation. *J. Cell Biol*. 123:849-858.

Vale, R.D. 1996. Switches, latches, and amplifiers: common themes of G proteins and molecular motors. *J. Cell Biol*. 135:291-302.

Vale, R.D., and R.J. Fletterick. 1997. The design plan of kinesin motors. *Annu. Rev. Cell Dev. Biol*. 13:745-777.

Vale, R.D., and L.S. Goldstein. 1990. One motor, many tails: An expanding repertoire of force-generating enzymes. *Cell*. 60:883-885.

Vale, R.D., T.S. Reese, and M.P. Sheetz. 1985a. Identification of a novel force-generating protein, kinesin, involved in microtubule-based motility. *Cell*. 42:39-50.

Vale, R.D., B.J. Schnapp, T.S. Reese, and M.P. Sheetz. 1985b. Organelle, bead, and microtubule translocations promoted by soluble factors from the squid giant axon. *Cell*. 40:559-569.

Vantard, M., A. Lambert, J. De Mey, P. Picquot, and L.J. Van Eldik. 1985. Characterization and immunocytochemical distribution of calmodulin in higher plant endosperm cells: Localization in the mitotic apparatus. *J Cell Biol*. 101:488- 499.

Vernos, I., J. Raats, T. Hirano, J. Heasman, E. Karsenti, and C. Wylie. 1995. Xklp1, a chromosomal Xenopus kinesin-like protein essential for spindle organization and chromosome positioning. *Cell*. 81:117-127.

Vorherr, T., P. James, J. Krebs, A. Enyedi, J. McCormick, J.T. Penniston, and E. Carafoli. 1990. Interaction of calmodulin with the calmodulin binding domain of the plasma membrane Ca2+ pump. *Biochem.* 29:355-365.

Vos, J.W., F. Safadi, A.S.N. Reddy, and P.K. Hepler. 2000. The kinesin-like calmodulin binding protein is differently involved in cell division. *Plant Cell*. 12:979-990.

Walczak, C.E., T.J. Mitchinson, and A. Desai. 1996. XKCM1: A Xenopus kinesin-related protein that regulates microtubule dynamics during mitotic spindle assembly. *Cell*. 84:37-47.

Walczak, C.E., and T.J. Mitchison. 1996. Kinesin related proteins at mitotic spindle poles: Function and regulation. *Cell*. 85:943-946.

Walczak, C.E., S. Verma, and T.J. Mitchison. 1997. XCTK2: A kinesin-related protein that promotes mitotic spindle assembly in Xenopus laevis egg extracts. *J. Cell Biol.* 136:859-870.

Walker, R.A. 1995. Ncd and kinesin motor domains interact with both α- and β–tubulin. *Proc. Natl. Acad. Sci.* 92:5960-5964.

Walker, R.A., E.T. O'Brien, N.K. Pryer, M.F. Soboeiro, W.A. Voter, H.P. Erickson, and E.D. Salmon. 1988. Dynamic instability of individual microtubules analyzed by video light microscopy: rate constants and transition frequencies. *J. Cell Biol*. 107:1437-1448.

Wang, S.Z., and R. Alder. 1995. Chromokinesin: a DNA-binding, kinesin-like protein. *J. Cell Biol*. 128:861-868.

Wang, W., D. Takezawa, S.B. Narasimhulu, A.S.N. Reddy, and B.W. Poovaiah. 1996. A novel kinesin like protein with a calmodulin binding domain. *Plant Mol. Biol*. 31:87-100.

Wein, H., M. Foss, B. Brady, and W.Z. Cande. 1996. DSK1, a novel kinesin-related protein from the diatom Cylindrotheca fusiformis that is involved in anaphase spindle elongation. *J. Cell Biol*. 1333:595-604.

Wolenski, J.S. 1995. Regulation of calmodulin-binding myosins. *Trends Cell Biol*. 5:310-316.

Wordeman, L., and T.J. Mitchison. 1995. Identification and partial characterization of mitotic centromere-associated kinesin, a kinesin-related protein that associates with centromeres during mitosis. *J. Cell Biol*. 128:95-104.

Yamazaki, H., T. Nakata, Y. Okada, and N. Hirokawa. 1995. KIF3A/B: a heterodimeric kinesin superfamily protein that works as a microtubule plus end-directed motor for membrane organelle transport. *J. Cell Biol*. 130:1387-1399.

Yang, J.T., R.A. Laymon, and L.S. Goldstein. 1989. A three-domain structure of kinesin heavy chain revealed by DNA sequence and microtubule binding analyses. *Cell*. 56:879-889.

Yen, T.J., D.A. Compton, D. Wise, R.P. Zinkowski, B.R. Brinkley, W.C. Earnshaw, and D.W. Cleveland. 1991. CENP-E, a novel human centromere-associated protein required for progression from metaphase to anaphase. *EMBO J*. 10:1245-1254.

Yen, T.J., G. Li, B.T. Schaar, I. Szilak, and D.W. Cleveland. 1992. CENP-E is a putative kinetochore motor that accumulates just before mitosis. *Nature*. 359:536-539.

Bettina Edith Deavours
512 Warren St.
Blacksburg, VA 24060
(540) 231-4828
anon235@vt.edu

BORN: 12 October 1973 Vineland, New Jersey

ACADEMIC DEGREES:

B.S. Biology, 1995
Virginia Polytechnic Institute and State University
GPA: 3.99

Ph.D. Biology, 2001
Virginia Polytechnic Institute and State University
Dissertation: "Microtubule interactions and regulation of the Mitotic Kinesin-Like Protein-1 and Kinesin-Like Calmodulin Binding Protein"
GPA: 4.0

RESEARCH EXPERIENCE:

Ph.D. candidate (August 1996-present)
Virginia Polytechnic Institute and State University
Advisor: Dr. Richard Walker
Research included expression and purification of motor proteins from bacterial, mammalian, and insect cell based expression systems; characterization of motor protein activity by ATP hydrolysis, microtubule sedimentation, and motility assays; purification and characterization of antibodies by immunoblotting, immunoprecipitation, and immunofluorescence; and confocal and DIC microscopy. Also mentored undergraduate research projects.

Research Assistant (1996-98, 1999, 2000, 2001)
Virginia Polytechnic Institute and State University
Responsibilities included research in addition to supervision of undergraduate students and general lab maintenance.

Participated in the Physiology: Cell and Molecular Biology course at the Marine Biological Laboratory, June 14-July 26th, 1998. Completed four laboratory rotations in actin-based molecular motors, yeast genetics, signal transduction in mammalian cells, and protein structure/function.

Post-course independent researcher at the Marine Biological Laboratory, July 29th-August 12th, 1998.
Initiated kinetic analysis of a kinesin-like protein using stopped-flow techniques in collaboration with graduate student Jan Vos and Dr. Edward Taylor (University of Chicago).

Lab Specialist (May 1995-August 1996)
Virginia Polytechnic Institute and State University
Responsibilities included: cloning, expression, and purification of proteins in bacterial expression systems; training of undergraduate and graduate students in basic molecular techniques; ordering equipment and supplies; financial record-keeping; and general organization of the lab.

RESEARCH PUBLICATIONS:

B.E. Deavours and R.A. Walker (2001) ATPase and microtubule binding of the MKLP-1 motor domain. submitted to *Biochemistry.*

Y. Kao, B.E. Deavours, K.K. Phelps, R.A. Walker and A.S.N. Reddy. (2000) Bundling of microtubules by motor and tail domains of a kinesin-like calmodulin-binding protein from *Arabidopsis*: regulation by Ca^{2+}/calmodulin. *Biochem. Biophys. Res. Comm.* 267:201-207.

B.E. Deavours and R.A. Walker. (1999) Nuclear localization of C-terminal domains of the kinesin-like protein MKLP-1. *Biochem. Biophys. Res. Comm.* 260:605-608.

B.E. Deavours, A.S.N. Reddy, and R.A. Walker. (1998) Ca^{2+}/calmodulin regulation of the *Arabidopsis* kinesin-like calmodulin-binding protein. *Cell Motil. Cytoskel.* 40:408-416.

RESEARCH GRANTS:

Graduate Research Development Project
"Identification of nuclear localization determinants and the role of nuclear localization of the mitotic kinesin-like protein"
Virginia Polytechnic Institute and State University
December 2000: $500

Sigma Xi, Grant-in-aid of research
"Regulation of the mitotic kinesin-like protein-1"
May 2000: $574

Graduate Research Development Project
"Characterization of the mitotic kinesin-like protein-1"
Virginia Polytechnic Institute and State University
August 1997: $500

Sigma Xi, Grant-in-aid of research
"Analysis of the effects of calcium and calmodulin on the microtubule motor protein KCBP"
January 1997: $500

MEETING PRESENTATIONS:

B.E. Deavours and R.A. Walker. "MKLP-1 motor domain interactions with microtubules." 40th American Society for Cell Biology Annual Meeting, December 9-13, 2000.

M.L. Kerr, B.E. Deavours, and R.A. Walker. "Purification of Ncd from Drosophila S2 cells." 39th American Society for Cell Biology Annual Meeting, December 11-15, 1999.

B.E. Deavours, J.W. Vos, P.K. Hepler, E.W. Taylor, R.A. Walker. "Kinetic studies of mechanism of kinesin calmodulin binding protein." Biophysical Society Annual Meeting, February, 1999.

B.E. Deavours and R.A. Walker. "Characterization of mitotic kinesin like protein-1: analysis of C-terminal domains expressed in HeLa and insect cells." 38th American Society for Cell Biology Annual Meeting, December 12-16, 1998.

M.L. Kerr, B.E. Deavours, and R.A. Walker. "Purification of Ncd and kinesin from Drosophila S2 cells." 38th American Society for Cell Biology Annual Meeting, December 12-16, 1998.

A.S.N. Reddy, S.B. Narasimhulu, J. Bowser, Y-L. Kao, F. Safadi, M. Golovkin, H. Song, B.E. Deavours, S.A. Endow, and R.A. Walker. "A novel calmodulin-binding microtubule motor protein from plants: localization, motility properties and Ca^{2+}/calmodulin modulation." Current Topics in Plant Biochemistry, Physiology and Molecular Biology annual symposium on Signs and Roadways: Protein Traffic and the Cytoskeleton, 1997.

B.E. Deavours and R.A. Walker. "Characterization of the effects of calcium and calmodulin on the microtubule motor protein KCBP." 75th Virginia Academy of Sciences annual meeting, May, 1997.

B.E. Deavours, A.S.N. Reddy, and R.A. Walker. "The *Arabidopsis* kinesin-like calmodulin-binding protein exhibits Ca^{2+}/calmodulin-dependent binding to microtubules." 6th International Congress on Cell Biology & 36th American Society for Cell Biology Annual Meeting, December 7-11, 1996.

SEMINARS

Interdepartmental Plant Science seminar. Virginia Tech, January, 1998. "Ca^{2+}/calmodulin regulation of the *Arabidopsis* kinesin-like calmodulin-binding protein"

Botany seminar. Virginia Tech, September, 1997.
"Ca^{2+}/calmodulin regulation of the *Arabidopsis* kinesin-like calmodulin-binding protein"

TEACHING EXPERIENCE:

Graduate Teaching Assistant (August 1999-present)
Virginia Polytechnic Institute and State University
Principles of Biology Lab for Biology Majors
Responsibilities included: Pre-lab multimedia lectures and demonstrations, supervision of students during lab sessions, writing and administration of practical and written exams, and development a class website that allowed students to access class materials and to check their grades. Because this class is designated as writing intensive, I was also responsible for developing writing assignments designed to teach biology majors how to think critically and write scientific lab reports and papers.

Graduate Teaching Assistant (Aug. 1998-Dec. 1998)
Virginia Polytechnic Institute and State University
General Biology Lab
Responsibilities included: Pre-lab lectures and demonstrations, supervision of students during lab sessions, writing and administration of quizzes and written exams.

PROFESSIONAL SERVICE:

Biology Graduate Student Association, Virginia Tech:
Graduate Student Association Delegate 1999-01
Secretary, 1997-98

Biology Departmental Seminar Committee, 1997-98
Invited, organized and hosted Dr. Knut Schmidt-Nielsen who presented a seminar entitled "Physiological Insight: On Recognizing Opportunity" in March, 1998.

Botany Seminar Committee, Virginia Tech 1997-98.

PROFESSIONAL MEMBERSHIPS:

Phi Beta Kappa
American Society for Cell Biology
Virginia Academy of Science

AWARDS AND HONORS:

Virginia Polytechnic Institute and State University
Graduate Student Association Travel award in support of presenting research at the 40th Annual Meeting for the American Society for Cell Biology, December, 2000: $300.

Virginia Polytechnic Institute and State University Graduate Student Association Travel award in support of presenting research at the 38th Annual Meeting for the American Society for Cell Biology, January, 1999: $82.

Mountain Memorial Fund Scholarship award in support of participating in the Physiology: Cell and Molecular Biology course at the Marine Biological Laboratory,
June 14-July 26th, 1998.

B.E. Deavours, Jan Vos, and Edward Taylor. "Kinetic analysis of the Kinesin-like Calmodulin Binding Protein (KCBP)", Post-course independent research award funded by NASA Center for Advanced Studies in the Space Life Sciences, Marine Biological Laboratory, July 29th-August 12th, 1998.

Cunningham Fellowship, awarded May 1996. Virginia Tech, Blacksburg, VA 24060.